SYSTEM ANALYSIS OF STEEL MANUFACTURING OFF-GAS VALORIZATION

ECO-TECHNOECONOMIC-ANALYSIS OF STEEL MANUFACTURING OFF-GAS VALORIZATION

By LINGYAN DENG, B.Eng., M.Sc.

A Thesis Submitted to the School of Graduate Studies in Partial Fulfillment of the Requirements for the Degree Doctor of Philosophy

McMaster University

Ph.D. Candidate (2020) McMaster University

Chemical Engineering Hamilton, Ontario, Canada

TITLE: eco-Technoeconomic-Analysis of Steel Manufacturing Off-gas Valorization

AUTHOR: Lingyan Deng

B.Eng. (China Institute of Industrial Relations)

M.Sc. (Ajou University)

SUPERVISOR: Professor Thomas A. Adams II

NUMBER OF PAGES: xiv, 93

Lay Abstract

Steel manufacturing accounts for up to 8.8% of all anthropogenic CO_2 emissions. As a result, governments have begun to implement carbon taxes which incentivize the steel manufacturing industry to reduce its CO_2 emissions. Two major methods have been proposed to meet these goals: producing more electricity via optimized combined cycle power plants (CCPP), and converting off-gas into methanol (CBMeOH). The present research consists of an environmental and economic analysis of status quo, CCPP, and CBMeOH systems for five locations: Ontario, the USA, Finland, Mexico, and China. The economic analysis considered factors such as carbon tax, electricity price, methanol price, electricity carbon intensity, power purchasing parity, and income tax, with the results showing the CBMeOH plant to be the most profitable for all locations. The lone exception to this result was Finland, where the CCPP system was determined to be the most profitable option. The environmental analysis revealed the CBMeOH plant to be the most environmentally friendly option for Ontario, Finland, and China, while the CCPP system was deemed most environmentally friendly for locations in the USA and Mexico.

Abstract

The steel manufacturing industry is one of the largest emitters of CO_2, accounting for upwards of 8.8% of all anthropogenic CO_2 emissions. The governments are charging taxes on CO_2 emissions, which incentivize the industry to further reduce CO_2 emissions. At present, much of the CO_2, produced in the steel manufacturing process occurs as a result of coke oven and blast furnace gas by-products. As such, two major strategies have been proposed to reduce steel-manufacturing-related CO_2 emissions: producing more electricity via optimized combined cycle power plants (CCPP), and converting off-gas by-products into methanol (CBMeOH). The present research consists of an economic and environmental analysis of the status quo, CCPP, and CBMeOH systems for five locations: Ontario, the USA, Finland, Mexico, and China. The economic analysis considered factors such as carbon tax, electricity price, methanol price, electricity carbon intensity, power purchasing parity, and income tax. In the CCPP process, desulphurization is conducted using ProMax with MDEA as the solvent, while the CBMeOH process uses a membrane to separate the bulk H_2S, with organic sulfurs such as thiophene being removed via CO_2+steam reforming and middle-temperature removal. The results of the economic analysis revealed the CBMeOH plant to be the most profitable in Ontario, the USA, China, and Mexico, while the CCPP system was shown to be the most profitable in Finland. The environmental analysis was conducted using the TRACI, CML-IA, ReCiPe2016, and IMPACT2002+ tools in SimaPro V9, with the results showing the CBMeOH system to be the most environmentally option in Ontario, Finland, and China, and the CCPP system as the most environmentally friendly option in the USA and Mexico.

Research Contributions

- Used ProMax to simulate the coke oven gas (COG) desulphurization process with MDEA as the solvent. The sweetened COG was combusted to produce electricity via a combined cycle power plant (CCPP). The CCPP system was simulated in Aspen Plus and then optimized using GAMS.
- Designed, modeled, and simulated a novel system for converting COG and blast furnace gas (BFG) into methanol (CBMeOH). Proposed an innovative COG desulphurization process that satisfies the prerequisite of less than 0.1 ppmv of sulphur compounds in the syngas used for methanol synthesis.
- Used Aspen Capital Cost Estimator V10 to calculate the capital costs, operational costs, and the net present values (NPV) of the CCPP and CBMeOH systems. The NPVs of both systems were then compared at five representative locations: Ontario, the USA, Finland, Mexico, and China.
- Compared the life cycle environmental impacts of the CCPP and CBMeOH systems at each of the five representative locations.
- Yielded results showing the economic complexity of selecting an appropriate system for a given location. Specifically, the results show that the most economically profitable option will vary depending on market conditions and political decisions.
- Demonstrated that the CCPP and CBMeOH systems can reduce indirect and direct CO_2 emissions by up to 3% and 4%, respectively, and that the CBMeOH process offers a potential CO_2 storage method.
- Estimated the CCPP capital investment with high accuracy compared to a real plant built in Ontario. This is a rare validation of techno-economic analysis methodologies.
- Proposed advanced CBMeOH systems. The idea of integrating different technologies and choosing among utilities for big system is a good reference for future studies and could be

applied in other industries. For example, natural gas (NG)/syngas to methanol. The rich carbon source from cement industry could be used as carbon source for NG to MeOH.

- Demonstrated decision making strategy via exploring and understanding the problem and provide references from eco-techno economic analysis and political aspects.
- Provided reference cases for steel manufacture on three continents (North America, Asia, and Europe) for deciding whether to build CCPP or CBMeOH, or do nothing. These can also be used as reference cases in other energy and carbon-intensive industries, for example, the cement industry, glass industry, etc.
- Demonstrated that decision making is highly geographically related. Decision making with considering the location's own market, political decision, energy source distribution, etc. is highly recommended.

Acknowledgments

I would like to thank my family for their love, suggestions, and support. Thanks to my parents for providing me with warmth and open-mindedness, and to my two older brothers who are always there to give me valuable suggestions when I am feeling lost in my studies or life. Their spirit of self-reliance and self-improvement is a continual source of inspiration that drives me to become a stronger and more independent person.

I would also like to express my sincere gratitude to my supervisor, Dr. Thomas A. Adams II, who provided me with no shortage of encouragement and motivation. Dr. Adams was incredibly accessible, and he always had time to provide support and suggestions to help me overcome issues related to research, academic activities, or anything else I may have needed help with. Needless to say, I feel very fortunate to have had him as my Ph.D. supervisor.

In addition, I would like to thank my other two committee members, Dr. Vladimir Mahalec and Dr. Joseph McDermid. I was inspired by Dr. Mahalec's lectures on scheduling and planning, and how ProMV could be used to analyze multivariate big data. With respect to my research, Dr. Mahalc always asked tough questions that forced me to think about my project from a different angle and learn new things. As director of the Steel Research Center, Dr. McDermid is an expert in steel manufacturing and has a very deep understanding of the various aspects of the steel manufacturing process. Importantly, Dr. McDermid's easygoing nature made it easy to seek him out for help with technical issues, such as figuring out how to get the projector to work. Dr. Mahalec's and Dr. McDermid's assistance helped to make my committee meetings and my Ph.D. studies in general much less stressful and more productive.

Another group of people to whom I would like to express special thanks is my fellow students at MACC, as they always managed to make campus a happy place for me, whether it was during games of volleyball together or sharing birthday cakes in the office. In particular, I would like to thank

Haoxiang Lai, Leila Hoseinzade, Pranav Bhaswanth Madabhushi, Ikenna J. Okeke, Yingkai Song, Sayyed Faridoddin Afzali, Huiyi Cao, Yingwei Yuan, and Yurong Diao for their help and support in study and daily life. My life at McMaster would have been much less easy and colorful without this wonderful group of people.

Last, but certainly not least, I would like to thank the staff in the main office. Thanks to Michelle for always setting up the meeting room and for her endless support with administrative issues, and thanks to Kristina Trollip for her help with software purchases, conference reimbursement, and so many other things.

Truly, your help and support has made my four years at McMaster an experience that I will cherish forever.

Table of Contents

List of Abbreviations

AMD	ArcelorMittal Dofasco
BFG	Blast furnace gas
BOFG	Basic oxygen furnace gas
CCPP	Combined cycle power plant
CCS	Carbon capture and storage
CDR	CO_2 dry reforming
CEPCI	Chemical engineering plant cost index
CO_2e	CO_2 equivalents
COG	Coke oven gas
CSR	Combination of CO_2 and steam reforming
EAF	Electric arc furnace
FOB	Free-on-board
GAMS	General Algebraic Modeling System
GHG	Greenhouse gas
GT	Gas turbine
HHV	High heating value
HP	High pressure
IGCC	Integrated gasification combined cycle
IP	Intermediate pressure
LCU	Local currency unit
LP	Low pressure
LTWGS	Low temperature water-gas shift
MDEA	Methyl diethanolamine

MEA	Monoethanolamine
MeOH	Methanol
MTSR	Middle temperature sulfur removal
NCPO	Non-catalyst partial oxidization
NG	Natural gas
NPV	Net present value
POX	Partial oxidization
PPP	Purchasing power parity
PSA	Pressure swing adsorption
RWGS	Reverse water-gas shift
SMR	Steam methane reforming
SQ	Status quo
ST	Steam turbine
TCI	Total capital investment
TFC	Total fixed cost
TFCI	Total fixed capital investment
TOC	Total operation cost
TPC	Total production cost
TR	Total revenue
TSA	Temperature swing adsorption
U	Heating utility
ULCOS	Ultra-Low Carbon Dioxide Steelmaking
VHSV	Volumetric hourly space velocity
WGS	Water-gas shift

Declaration of Academic Achievement

This is a sandwiched thesis. As the author of this thesis, I confirm that I am the primary performer of all research and the primary author of all papers included in the proceeding chapters.

Chapter 1 Introduction

1. Background and Motivation

The steel manufacturing industry is one of the world's top industries in terms of CO_2 emissions. In 2017, the world's total CO_2 emissions output was 36.15 billion tonnes [1]. According to the World Steel Association [2], a total of 1730 million tonnes of crude steel was produced in 2017, with an average CO_2 emission rate of 1.83 tonnes CO_2 per tonne of steel produced. Thus, steel manufacturing accounted 3165.9 million tonnes of CO_2 in 2017, or 8.8% of all CO_2 emissions. As a result, governments have begun to implement stiffer carbon taxes [3] in an attempt to incentivize high-emissions industries to find new methods of cutting their CO_2 emissions.

According to the Worldsteel Association [4], there are two main steel production routes: the blast furnace-basic oxygen furnace (BF-BOF) route, which is used to produce about 75% of all steel; and the electric arc furnace (EAF) route, which is used to produce the other 25%. Recycled iron scrap or direct-reduced iron (DRI) are the main inputs in the EAF route, which is relatively less energy-intensive and emits less CO_2 than the BF-BOF route. However, the amount of recycled steel produced falls well short of satisfying growing international demand. As such, BF-BOF, which emits considerably more CO_2, remains the major route of steel production and, by extension, continues to receive the most attention with regards to CO_2 emission reduction.

The BF-BOF route includes pelleting, coke making, blast furnace, basic oxygen furnace, and downstream steel refining processes. Of these processes, the coke making process and the blast furnace process require the largest amount of energy and emit the most by-product off-gases, namely, coke oven gas (COG) and blast furnace gas (BFG). Much research has been devoted to developing ways of reducing the energy consumption and CO_2 emissions associated with these processes, with studies generally falling within one of four major areas. These areas of study are detailed below.

Technology innovation studies. In September 2004, a consortium of 48 companies and organizations from 15 European countries launched a cooperative research and development initiative to drastically reduce CO_2 emissions related to steel production. This consortium, known as ULCOS (Ultra-Low Carbon Dioxide Steelmaking), is supported by the European Commission and consists of Europe's major steel producers, energy and engineering partners, and research institutes and universities. The objective of this program was

to reduce the CO_2 emissions of today's best routes by at least 50%, which produced a number of potential GHG-reduction strategies. The systematic technological improvements brought about by the ULCOS program has enabled BF consumption to be reduced to 0.49 kilos of carbon-containing materials per kilo of hot metal produced. However, the best European steel plants are currently operating at the limits of what is technically possible, which means that further carbon reduction will simply not be possible without technological changes.

Out of a field of 80 potential breakthrough technologies, ULCOS identified the following four technologies as being the most promising [5]. (1) Top gas recycling blast furnace with CO_2 capture and storage (CCS). This technology uses recycled CO and CO_2 with pure O_2 instead of hot air as the oxidant in BF, which enables unwanted N_2 to be removed from the gas and makes it easier to separate and capture CO_2. (2) HIsarna with CCS, which combines coal preheating and partial pyrolysis in a single reactor consisting of a Cyclone Converter Furnace (CCF) for ore melting and a Smelting Reduction Vessel (SRV) for final ore reduction and iron production. This flexible technology uses significantly less coal, as it allows for the partial substitution of coal with biomass, NG, or even H_2. (3) ULCORED with CCS. Instead of coal or coke, this process uses gases produced by the partial oxidation of NG to produce direct reduced iron (DRI), which is then transferred to EAF for steel making. (4) Low-temperature (about 110 ˚C) iron electrowinning. Depending on the electricity mix used for electrolysis, this route is potentially carbon free. Significantly, the first three of these technologies are only able to achieve the goal of reducing CO_2 emissions by 50% with the use of CCS. Furthermore, these technologies are still in various stages of the testing process, mainly in the pilot plant and commercial test stage. Therefore, achieving the goal of a 50% reduction in CO_2 emissions with these methods will be quite challenging. Indeed, research groups have noted that the steelmaking industry has made great strides in reducing its energy consumption over the last fifty years, and that today's technologies are being operated at their best available capabilities. The Asia-Pacific Partnership framework for Clean Development and Climate has taken a plan to reduce 1.27 million tonnes of CO_2 emission per year from the steel industry by transferring to the best available technologies.

European countries are not the only ones exploring methods of producing steel via electrolysis. For example, Donald et al. [6] from the Massachusetts Institute of Technology studied a novel method of steelmaking using molten oxide electrolysis (MOE). Unlike low-temperature electrowinning, MOE requires

high temperatures to melt the iron ore. In addition, unlike other molten salt electrolytic technologies, MOE uses carbon-free anodes, which facilitates the production of oxygen gas at the anode. Among breakthrough technologies, MOE produces the lowest levels of CO_2 emissions per unit metal product. Allanore et al. [7] calculated that, assuming 0.9 faradaic efficiencies and 40% heat loss, MOE can achieve a minimum practical energy requirement of 10 MJ/tonne of Fe. This is considerably less than the best available cited BF/BOF route, which has an energy requirement of 17.9 MJ/tonne of Fe. However, this method is not without its challenges. In particular, there are only a small number of metals that can withstand MOE's operating temperature of approximately 1600 ˚C (iron ore melting usually in the range of 1250 ˚C to 1540 ˚C). In addition, electrolysis requires the availability of large quantities of CO_2-free anodes. Two additional key considerations in utilizing this process relate to determining the scale at which it can operate on at self-heated dimensions, and finding an inert anode that is economical relative to tonnage metal production and scarcity.

Researchers in other countries have also tested and proposed alternative technologies for reducing CO_2 emissions. For instance, Hasanbeigi et al. [8] discussed and compared twelve different technologies, with the COREX and FINEX being identified as two of the more promising options. COREX is an industrially and commercially proven steel-reforming process that allows hot metal to be produced directly from iron ore and non-coking coal. The advantages of COREX include a 20% reduction in CO_2 emissions, lower energy consumption, reduced investment and operation costs, and oxygen savings of 18%. The South Korean steel manufacturer, POSCO, uses the FINEX process. In this process, iron ore is not pelletized; rather, it is charged in fine particles through several stages of counter-current flow with gas. Furthermore, the FINEX process requires less energy due to reduced use of non-coking coal.

Alternative fuels and reduction agents' studies. Biomass and natural gas (NG) are alternative fuels and reduction agents that have been studied for use in the BF-BOF route. In their review paper, Mousa et al. [9] noted that using biomass instead of coal can reduce net CO_2 emissions by between 31-57% in life cycle analyses. However, Mousa et al. [9] also found that the use of biomass products, such as charcoal, reduced the strength of the coke and increased the coal's softening temperature, consequently reducing fluidity. In addition, the use of biomass has other major drawbacks, such as: a lack of information about available biomass

resources (location, season, quantity, quality, etc.) and upgrading technologies; lower production rates; technical problems in industrial implementation; and high market competition from fossil fuels.

In another study, Sohn [10] examined the use of H_2 as a reduction agent that reacts with fine iron oxide concentrates in a suspension reduction process. Their results demonstrated the considerable energy and environmental benefits of this new approach, which were largely due to the elimination of the coke-making and the pelletization/sintering steps required in the current steelmaking process. Specifically, Sohn's new technique provided 38% in energy savings compared to the current BF process, and it drastically reduced more than 1.1 tonnes of CO_2 per tonne of hot metal generated by the use of coke in the BF. In another study, Nogami et al. [11] examined the effects of intensive H_2 injection into the BF, finding that the coke injection rate decreased with H_2 injection. However, this approach also had one key drawback: it led to decreased temperature levels in the stack section, which in turn led to decreased top gas temperatures and delays in the reduction reaction in the stack section.

Scheduling and planning studies. The steel-production process is unstable, and both the production and consumption of by-product gases tend to fluctuate. In an attempt to reduce these fluctuations, steel enterprises have begun to install buffer units like gas holders and boilers. However, temporary excesses or shortages of by-product gases often occur due to limitations in the capacity of the by-product gasholders, which can lead to higher operating costs, environmental pollution, and even threaten proper production. Thus, research has found that it is imperative to optimize the scheduling of the by-product gas system. As noted in a review paper by Zhao et al. [12] [13], off-gas is mainly used in the iron and steel making system, with the remainder being used in the on-site power plant. They also point out that scheduling under a time-of-use power price is quite different from scheduling under a flat power price, and that scheduling under the former could reduce electricity purchase costs by 29.7%.

Off-gas utilization studies. Off-gas is used either to produce electricity in order to increase energy recovery efficiency, or to produce methanol in order to fix CO_2 into chemical products. The composition of the studied off-gas are shown in the following table.

Table 1. Off-gas composition. * in ppmv [14]

	HHV (MJ/kg)	T (°C)	P (bar)	Composition (vol. %)									
				C_2H_2	CH_4	CO	CO_2	H_2	N_2	O_2	H_2S*	CS_2*	C_4H_4S*
COG	22.6-32.6	35	1.45	1.5-3.-	22-28	5.0-9.0	1.0-3.5	45-60	3.0-6.0	0.1-1.0	3420-4140	72-102	20-40
BFG	2.6	28	1.44	-	-	23.5	21.6	3.7	46.6	0.6	-	-	-

As Table 1 shows, COG has much higher HHV compared to BFG, while BFG has a much larger production rate (its volume is almost 14 times that of COG). COG mainly contains H_2 and CH_4, which makes it a good hydrogen source, but its sulphur content is significant. Depending on the downstream process requirement, the desulphurization process might vary (further details on desulphurization will be shown in Chapter 2 and 3). BFG contains higher percentage of CO_2 and CO, which makes it a good carbon source. Depending on the market requirements, hydrogen can be extracted from off-gas, or it can be used to produce NG [15]. As the biggest steel producer, China has the most experience in dealing with off-gas utilization, with the most common off-gas utilization method being the production of methanol from COG [14]. In addition, some Chinese companies have been producing NG from off-gas due to the relative lack of NG in China [16]. In contrast, North America's extremely cheap NG prices makes the production of NG from off-gas economically disadvantageous.

Of the above discussed types of study, technology innovation requires a relatively longer time before commercialization. Furthermore, the adoption of alternative fuels or reduction agents can also take some time, as such decisions must be supported by experimental data. Since planning and scheduling are not mainly concerned with reducing CO_2 emissions, this work will focus on the fourth type of study: off-gas utilization. In particular, this work will study and compare how off-gas can be utilized for the highly efficient production of electricity and methanol.

Given that this work was conducted in Ontario, Canada, it would be worthwhile to explain the decision to focus on methanol production rather than ethanol production. Methanol and ethanol can both be used in standard automobile engines without causing significant changes to the engine's structure, which makes them

the most suitable known alcohols for spark-ignition engines [17]. Iliev found that increasing the amount of methanol or ethanol in the fuel can decrease CO and HC emissions, but can also cause a major increase in NO_x at concentrations above 30 vol.% (M30 or E30). Nonetheless, blended fuel is more economically beneficial than straight fossil fuels and produces lower levels of air pollutants.

In North America, especially the USA, ethanol is largely produced via the fermentation of corn and potatoes per government regulations [18]. For example, in 2018, President Trump directed the Environmental Protection Agency (EPA) to allow year-round sales of E15 nationwide. However, such directives could serve to exacerbate food shortages, as there will be greater incentive for farmers to grow corn rather than other crops. Ontario is also planning to achieve the goal of E15 by 2050 in order to achieve its emission-reduction goals [19]. Following Brazil, which is the world's second largest ethanol producer, Brazil's ethanol production mainly comes from the fermentation of starchy corn or sugarcane [18]. Although it is also possible to produce ethanol using a syngas synthesis process, methanol production via thermo-chemical processes is much more energy utilization efficient. Ethanol requires a longer process which is usually synthesized from methanol or DME [20].

Although ethanol is relatively less toxic than methanol (a concern if spilled during shipping), both are degradable and more environmentally friendly than gasoline [21]. Nonetheless, methanol is better in the long run, as it is a convenient medium for storing energy and can easily be transported and dispensed as a fuel. Furthermore, methanol can be produced by chemically recycling CO_2, which can be found naturally in the air or readily captured from atmosphere-polluting industrial emissions [22]. Methanol also has a higher octane rating (117) than ethanol (114), which means a higher compressor ratio, faster acceleration speeds, and more efficient energy utilization [2019 Ethanol industry outlook]. Notably, methanol has the distinction of being the safest motor fuel due to being much less flammable than gasoline, a fact that has led to its adoption by car racing leagues [21]. The prevalence of methanol-blended gasolines in the market grew from 7% to 9% between 2010 to 2015, while methanol-to-olefins increased from 0% to 18% [23]. IHS Markit predicts that nearly 1 in 5 tonnes of methanol will be used in MTO processes in China, with Northeast Asia (dominated by China) accounting for nearly 70% of global methanol demand by 2021, followed by North America at 9% and Western Europe at 8%. The great global demand for methanol is not only for use in gasoline blending or MTO;

rather, methanol can be used to synthesize a variety of other compounds, such as acetic acid, formaldehyde, silicone, methyl methacrylate, bio-diesel (replacement for ethanol), dimethyl-ether, marine fuel, and MTBE. For the above-discussed reasons, off-gas to methanol, rather than ethanol, was chosen as the focus of this study.

2. **Research outline**

The major goal of this research was to find a readily accessible solution that would enable steel manufactures to further minimize their CO_2 emissions, thereby reducing their environmental impact. This work is based on a local steel manufacturing company, ArcelorMittal Dofasco (AMD), which is located in Hamilton, Ontario, Canada. The three main by-products from AMD's steel manufacturing operations are coke oven gas (COG), blast furnace gas (BFG), and basic oxygen furnace gas (BOFG). COG and BFG are continuous by-products of the manufacturing process, while BOFG is an intermittent by-product. Therefore, a steady flow rate of COG and BFG is assumed. Additionally, given its intermittent status, the utilization of BOFG is not considered in this study.

This thesis contains five chapters. This chapter, the introduction, has provided an overview of the issues and technologies associated with CO_2 emissions reduction strategies in the steel industry, in addition to outlining the chapters that comprise the remainder of this work.

Chapter 2. This chapter analyzes the benefits of upgrading the status quo electricity generation system on-site to a more energy-efficient system, a combined cycle power plant (CCPP). In the status quo system, COG is combusted to boil lower pressure water in order to produce a limited amount of electricity and to distribute heat. The energy recovery efficiency of the status quo system is around 15%. Based on the same amount of available COG, I propose the use of a CCPP system, which uses a gas turbine. In order to satisfy the low sulfur content requirement, a gas pre-treatment step is necessary to remove bulk H_2S from COG. In this step, an MDEA solvent is used to remove more than 99% of H_2S at relatively high pressure (16 bar). The sweetened gas is then fed to the combustor, where it combusts with compressed air. The temperature of the exhaust gas in the combustor is controlled below 1260 ℃. Since the gas exiting the gas turbine is still very hot, thermal energy is further recovered by a series of heat exchangers. Additionally, more electricity is

produced via high-, intermediate-, and low-pressure steam turbines. The CCPP system was first modeled in ProMax for H_2S removal before being fed into Aspen Plus for CCPP simulation. A surrogate model was coded in General Algebraic Modeling System (GAMS) to find the optimized operation conditions in order to maximize the net present value (NPV). The systems were tested for five different locations—Ontario, the USA, Finland, Mexico, and China—taking into consideration factors such as purchasing parity, carbon tax, electricity carbon intensity, and electricity price. The results showed that, under 2016 conditions, the use of a CCPP system produced positive NPV for all five locations, with reduced indirect CO_2 emissions of 3% compared to AMD's annual emissions. Thus, the results demonstrate that the CCPP system outperforms the status quo system from both an economic and CO_2 emissions reduction perspective.

One point worth noting is that AMD has actually upgraded its on-site power plant from a single low-pressure steam turbine to a combined gas turbine and steam turbine, which has helped to increase its energy recovery capabilities. Though the size of the upgraded system is different from the proposed CCPP system, the idea is similar. In fact, AMD's actual on-site power plant upgrading costs proved to be similar to my independently determined projections. The fixed capital cost of my work was 0.29 $/kWh, while AMD's much smaller upgrade had a fixed capital cost of 0.30 $/kWh. This energy-saving upgrade was partially funded by a $10 million grant from the provincial government [24].

Chapter 3. This chapter focuses on another off-gas utilization approach: the conversion of COG and BFG into methanol (CBMeOH). Although methanol production from COG has been commercialized and operating well in Chinese plants since 2004, the utilization of BFG as a carbon source has not previously been considered as a commercially viable option. In addition, sulfur removal has always been a difficult process under the traditional method, generally requiring two-stages of hydrodesulfurization. Problematically, the fluctuations in temperature that occur during these hydrodesulfurization steps inhibit the efficiency of the methanol production process. Furthermore, since this work takes AMD as a case study, the profitability of building a methanol plant in Ontario remains unknown. Hence, this chapter focuses on finding a more efficient desulphurization system and determining whether the use of BFG as a carbon source in a CBMeOH system is a viable option for reducing CO_2 emissions in the steel industry. A special catalyst-packed reactor (CSR) with CO_2 and steam as an oxygen source is used to convert the methane in COG into CO and H_2, while at the same

time converting thiophene (one of the most stable sulfur contents) into H_2S, which is then removed via a middle-temperature removal process. The best H_2/CO mole ratio is also adjusted in this unit, which removes the need for a water-gas shift reactor downstream. Economic analyses of this new design were conducted for five locations: Ontario, the USA, Finland, Mexico, and China. Together with previous work (Chapter 2), the results show that the CBMeOH plant is the most profitable option in Ontario, the USA, Mexico and China, while the CCPP plant would be the most profitable option in Finland. These results are based on a probability distribution of market prices that mirrors the actual market conditions over the past 13 years in each market. Notably, the USA's profitability was highly related to the price of methanol.

Chapter 4. This chapter features environmental analyses of the status quo, CCPP, and CBMeOH systems from a life cycle perspective. This life cycle analysis (LCA) is based on previous two chapters' work. The system boundary for these analyses included both cradle-to-gate and gate-to-gate boundaries. Since the upper streams of COG and BFG were the same for all three systems, they were not considered in these analyses. The gate-to-gate boundary was used to capture the differences in how each system uses the off-gas, while the cradle-to-gate boundary was used to capture the differences between the systems in terms of utility, solvent, and catalyst usage. The data used in these analyses was mainly obtained from the previous study and the Ecoinvent V3.5 database. In all cases, the most correct available data were used. As with the analyses in Chapters 2 and 3, all five locations were considered (i.e., Ontario, the USA, Finland, Mexico and China). The analyses were conducted by running four LCA tools in SimaPro v9: TRACI, CML-IA, ReCiPe2016, and IMPACT2002+. The results showed that the CBMeOH system is the most environmentally friendly option for Ontario, Finland, and China, while the CCPP system is the best environmental option for the USA and Mexico.

Chapter 5. This chapter presents the overall conclusion of this thesis and potential directions for future study.

Chapter 2 Optimization of Coke Oven Gas Desulfurization and Combined Cycle Power Plant Electricity Generation

The content of this chapter has been published in a peer-reviewed journal:

Lingyan Deng, and Thomas A. Adams II. *Optimization of Coke Oven Gas Desulfurization and Combined Cycle Power Plant Electricity Generation*. Industrial & Engineering Chemistry Research 57.38 (2018): 12816-12828.

I&EC research
Industrial & Engineering Chemistry Research

Article

Cite This: Ind. Eng. Chem. Res. 2018, 57, 12816−12828

pubs.acs.org/IECR

Optimization of Coke Oven Gas Desulfurization and Combined Cycle Power Plant Electricity Generation

Lingyan Deng and Thomas A. Adams II*

Department of Chemical Engineering, McMaster University, 1280 Main Street West, Hamilton, Ontario L8S 4L7, Canada

Supporting Information

ABSTRACT: Many steel refineries generate significant quantities of coke oven gas (COG), which is in some cases used only to generate low pressure steam and small amounts of electric power. In order to improve energy efficiency and reduce net greenhouse gas emissions, a combined cycle power plant (CCPP) where COG is used as fuel is proposed. However, desulfurization is necessary before the COG can be used as a fuel input for a CCPP. Using a local steel refinery as a case study, a proposed desulfurization process is designed to limit the H_2S content in COG to less than 1 ppmv, and simulated using ProMax. In addition, the proposed CCPP plant is simulated in Aspen Plus and is optimized using GAMS to global optimality with net present value as the objective function. Furthermore, the carbon tax is considered in this study. The optimized CCPP plant was observed to generate more than twice the electrical efficiency when compared to the status quo for the existing steel refinery. Thus, by generating more electricity within the plant gate, the need to purchase electricity reduces, and hence reducing the lifecycle of CO_2 emissions considerably.

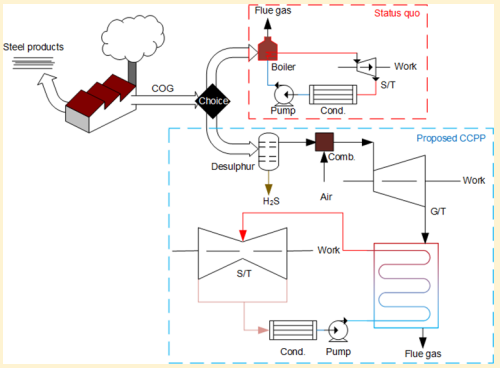

1. INTRODUCTION

The steel industry faces significant challenges with high greenhouse gas (GHG) emissions arising from the use of carbon as a required reagent in the primary iron oxide reduction step of the steelmaking process. For example, the ArcelorMittal Dofasco (AMD) refinery in Hamilton, Ontario, Canada, which produces 4.5 million tonnes of steel per year, also emits about 5.0 million tonnes of CO_2 equivalents (CO_2e) per year.[1] As the largest steel making company in Ontario, it is the largest single emitter of CO_2 in this province, emitting 75.0% more GHGs than the second and third largest emitters (which are also steel refineries).[2] Moreover, the Canadian government has proposed a minimum carbon tax scheme in which CO_2 emissions would be taxed at $10/tonne in 2018, rising to $50/tonne in 2022.[3] This translates to an extra $250 million per year in taxes for the refinery, which has serious implications on the profitability of the business and therefore incentivizes steel refineries to reduce their emissions wherever possible.

One of the primary sources of CO_2 emissions from steel refineries is associated with the large amounts of byproduct gases, such as coke oven gas (COG), blast furnace gas (BFG), and basic oxygen furnace gas (BOFG). Traditionally, these byproduct gases are recycled or reused where possible for heat or for metallurgical purposes, or flared for disposal when reuse is not possible. However, these gases potentially have a much higher value, which is often not exploited in practice. For example, Ghanbari and co-workers[4,5] and Bermudez et al.[6] examined several different ways of producing synthesis gas from various byproduct gases. When properly cleaned and upgraded, off-gases can be converted into more valuable products using the right kind of catalysts, thus creating a wide variety of chemicals and fuels. This concept is known as off-gas valorization. However, there is not always a business case for this, depending on the jurisdiction and situation of each refinery. An older but still relevant benchmark study of the Iron and Steel Industry in Canada found that the average efficiency improvement potential from off-gas valorization is between 20.0% to 30.0%.[7]

China produces about 50.0% of the world's crude steel,[8] and as such, China has the most industrial experience in utilizing steelmaking off-gas. Chinese steel manufacturers developed various options of utilizing their off-gases, especially coke oven gas (COG). COG is either used as fuel in combined cycle power plant,[9−11] for methanol synthesis,[12,13] for natural gas synthesis,[14] or as a source of H_2 through extraction.[6,15] However, these processes are widely different and are currently in various stages of development. Though the COG used for methanol synthesis has been commercialized successfully since 2004 in China, there is less of a business case for this in other countries using current technology.

The status quo of the AMD refinery in Hamilton and many of its Chinese counterparts is to use COG combustion to

Received: January 18, 2018
Revised: August 27, 2018
Accepted: August 28, 2018
Published: August 28, 2018

DOI: 10.1021/acs.iecr.8b00246
Ind. Eng. Chem. Res. 2018, 57, 12816−12828

generate low pressure steam to power steam turbines (generating electricity), or for other process needs.[11] However, the efficiency is usually low, at about 15.0% by higher heating value (HHV). Therefore, in order to increase the thermal efficiency, an optimized combined cycle power plant (CCPP) for COG is proposed in this work using the AMD Hamilton refinery as a case study. Although there are steel refineries in Brazil[16] and China[10] which use CCPPs powered by a mixture of BFG and COG, a COG-only CCPP had only been studied from a simulation standpoint.[9] Furthermore, there is no previous study found in the literature where an optimal design of a COG-based CCPP system as a whole was carried out to the best of our knowledge. In addition, this is the first work to quantify both the economic and environmental benefits of avoiding grid electricity use by switching to the COG-based CCPP system in the Canadian context. The geographical context is important because the benefits of the proposed system are strongly dependent on the price of grid electricity, and local carbon emissions taxes or regulations. Because of this, the analysis in this paper considers the various trade-offs of applying the CCPP system at different electricity prices and carbon emission taxes.

2. METHODOLOGY

2.1. Available Gas Qualities. Typical conditions of available COG are shown in Table 1.[15,17] Note that COG has about half of the high heating value of natural gas (950−1150 Btu/ft^3),[18] which is high enough to use for combustion-based electricity generation. This work uses COG flow rates and qualities provided by AMD Hamilton, but for confidentiality reasons, only ranges and/or normalized data are reported in this paper when referring to existing commercial processes. For a sense of scale, the flow rate of the COG is enough to produce on the order of 20.0−80.0 MW of electric power with the classic steam cycle and is available in approximately continuous amounts.

Table 1. Typical Characteristics of Available Coke Oven Gas

component	COG
temperature (°C)	35.0
pressure (bar)	1.44
HHV (Btu/ft^3)	400−570
HHV (MJ/kg)	22.6−32.4
Chemical Composition (volume fraction)	
%C_2H_2	1.50−3.00
%CH_4	22.0−28.0
%CO	5.00−9.00
%CO_2	1.00−3.50
%H_2	45.0−60.0
%N_2	3.00−6.00
%O_2	0.100−1.00
H_2S (ppmv)	3420−4140
CS_2 (ppmv)	82.0−92.0
thiophene (C_4H_4S) (ppmv)	26.0−34.0

2.2. COG Desulfurization. The COG at AMD Hamilton contains H_2S, CS_2, and thiophene (C_4H_4S) with approximate ranges shown in Table 1. Typically, these sulfur compounds need to be removed before COG can be used for combustion or other purposes. Currently, the status quo at AMD Hamilton is to use a sulfur removal process that removes some, but not all, of the sulfur compounds. However, in the proposed CCPP design, the COG is combusted at high-pressure, which requires the COG to be much sweeter. The maximum H_2S concentration that can be tolerated is 4 ppmv as a design requirement[19] which is a three-order-of-magnitude reduction in sulfur content. Therefore, we have designed and simulated a sulfur removal system that is different from the process used at AMD Hamilton to sweeten the COG to the acceptable levels.

Our proposed COG-sweetening system is designed for H_2S removal only. Thiophene is a heterocyclic compound that has very stable chemical bonds and is commonly removed from oil and coal by a hydro-desulfurization processes at high pressure.[20] A much more expensive two-stage hydrodesulfurization step is required[21] to remove thiophene from COG. For the case study of AMD Hamilton, removing mainly the H_2S and some CS_2 at the same time is sufficient to meet environmental emission standards of the postcombustion flue gas and avoid damage to the equipment.[22] Therefore, thiophene removal is not studied in this work.

Four potential solvents were considered for the sulfur absorption and stripping process, as shown in Table 2. The H_2S removal process is essentially the same for each solvent, as shown in Figure 1. First, fresh solvent is contacted countercurrently with COG in an absorber where it absorbs the acid gases. Then, the loaded solvent is sent to a stripper, which separates the acid gases from the solvent producing lean solvent in the bottoms which then is recycled to the absorber. Depending on the solvent used, it may be necessary to operate the absorber at a high pressure, thus requiring an additional COG compression step. A small amount of makeup solvent is required to account for any solvent losses through the sweetened COG product and the captured sulfur gases.

Table 2. Comparison of Different Solvents[23] Binary Effects with Sulfur Compounds

	Rectisol	MDEA	MEA	DGA
solvent type	physical	aqueous	amine	aqueous amine
typical application	coal to MeOH	IGCC	commercialized for postcombustion	commercialized for NG sweeting
		Relative Volatility (Chemical/Solvent) at 16 bar		
temp. range (°C)	−60.0 to 150	−70.0 to 410	−80.0 to 300	−70.0 to 370
H_2S	127−5000	458−3.60 × 10^8	369−6.90 × 10^7	42.5−7.27 × 10^4
CS_2	1.93	8.62−33.0	28.9−199	7.87−19.4
C_4H_4S		5.58−9.56	20.0−25.5	4.97−6.20
		Pressure (bar)		
absorber	17.0	16.2	1.00	1.00
stripper	3.40—17.0	2.00		1.00

DOI: 10.1021/acs.iecr.8b00246
Ind. Eng. Chem. Res. 2018, 57, 12816−12828

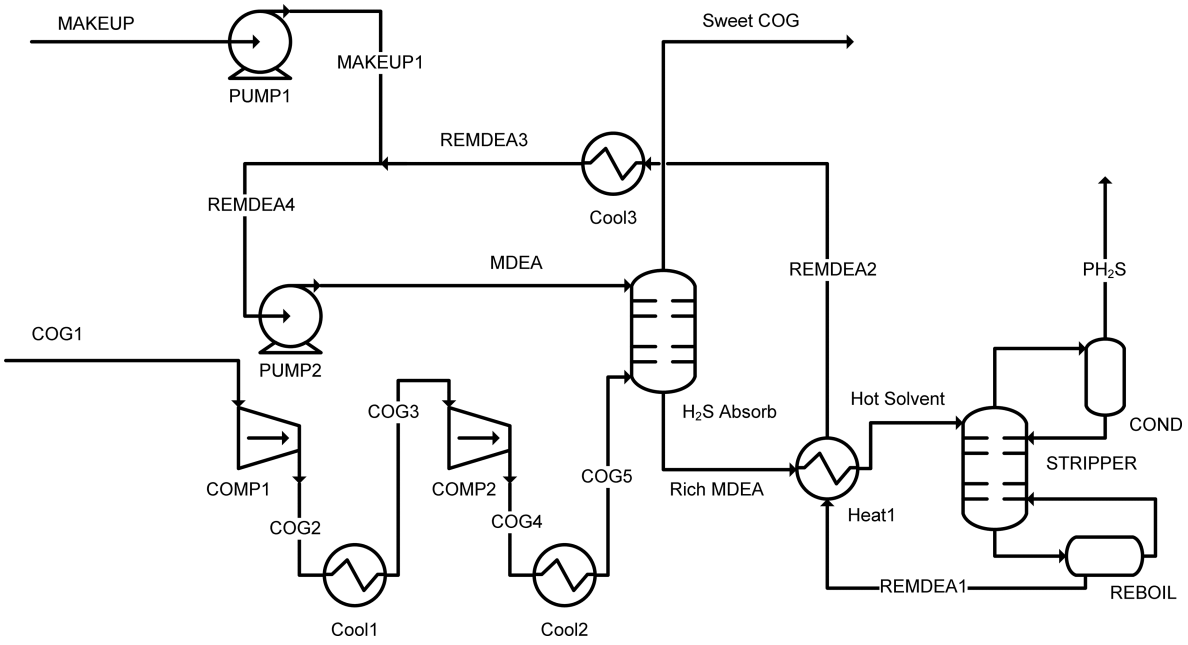

Figure 1. COG desulfurization process proposed.

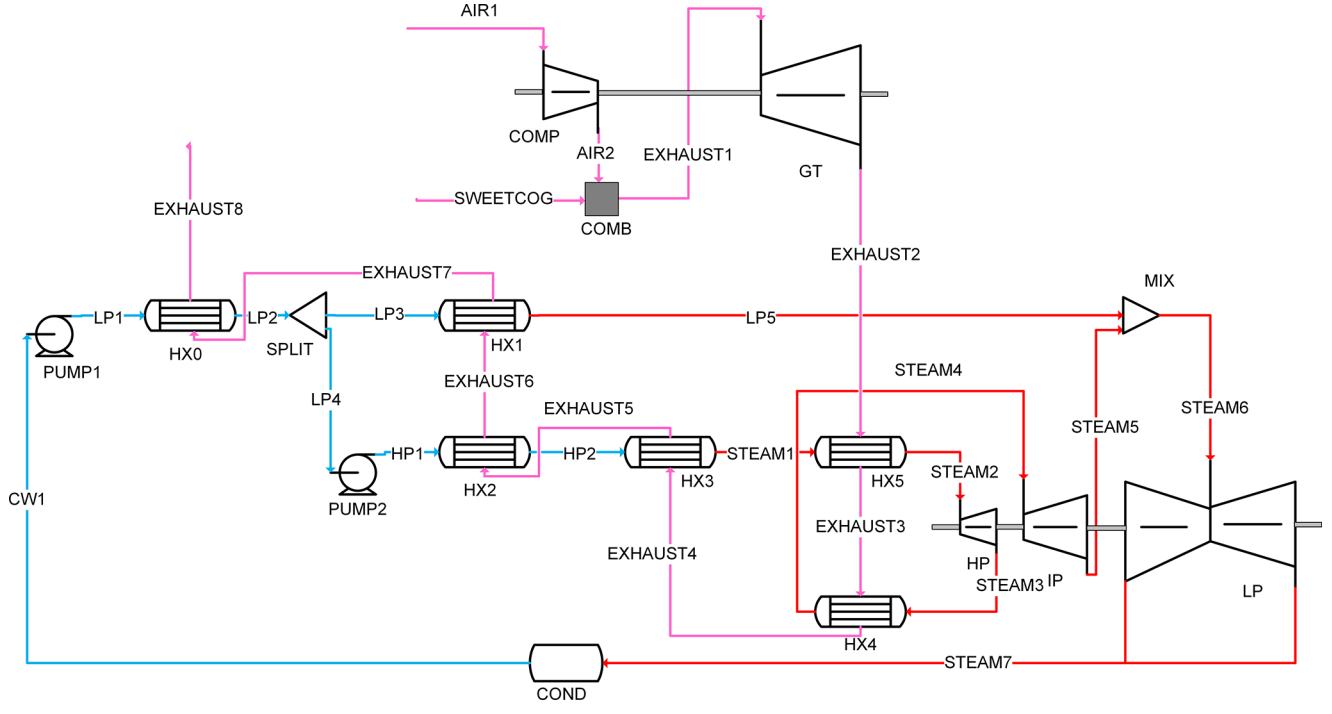

Figure 2. Proposed combined cycle power plant design.

The Rectisol process is preferred at low temperatures, usually in the range of −60 to −40 °C. This is not likely to be a good choice for our process due to higher temperature downstream. MEA and MDEA are have high relative volatility with respect to H_2S. However, unlike that for MDEA, the selectivity difference of H_2S and CO_2 is small when using MEA. MEA for H_2S removal is recommended only when CO_2 is not present. DGA is good for a small amount of H_2S removal, and it has a low sour gas loading capacity. In addition, DGA also selects CO_2 over H_2S. In this work, our major concern is to remove H_2S, thus MDEA was chosen. Although the high pressure MDEA-based process requires the use of expensive compressors, from a systems perspective this is not a bad choice because the sweetened COG has to be compressed to high pressure anyway for combustion in a gas turbine (GT). Thus, the cost of compression is relatively independent of the choice of solvent. A more comprehensive techno-economic analysis would be needed in order to select the best solvent at the systems level, but this is outside of the scope of the current work. The MDEA selection provides a reasonable and effective base case for use in analysis.

The process of Figure 1 was simulated in the commercial software package ProMax using the amines physical properties package. The TSWEET Kinetics column type is used to

DOI: 10.1021/acs.iecr.8b00246
Ind. Eng. Chem. Res. 2018, 57, 12816−12828

simulate the absorber and the TSWEET Stripper column process model is used to model the stripper. These models are specifically designed for gas sweeting applications with amines such as MDEA. The design was made using the heuristics suggested by Adams et al.[23] with manual adjustments. Some trial and error was used to estimate the required amount of solvent needed, the number of stages, and the heat required to raise the temperature of the rich solvent before entering the stripper.

2.3. Combined Cycle Power Plant Design. The stream conditions of the sweet COG stream as computed by ProMax MDEA desulfurization simulation was implemented as the feed stream in the CCPP design conducted in Aspen Plus. The design of the proposed CCPP is shown in Figure 2. The sweet COG (after MDEA desulfurization) is combusted with compressed air at 16.0 bar. Interstage coolers are used to ensure that the air temperature does not exceed 250 °C in the compressor. The flow rate of air is chosen such that the combustion temperature is 1240 °C, which is typical of gas turbine inlet temperatures (for example, Lin et al.[24] reports a value of 1260 °C before expansion in the GT). A temperature of 1240 °C was chosen because with the specified GT outlet pressure of 1.7 bar, the predicted GT outlet temperature is just under the HX5 material temperature limit of 650−700 °C.[25] The GT modeled is based on a 9FA class of GE Power turbine with an isentropic efficiency close to 0.9.[24]

The remaining thermal energy from the exhaust gas is captured through a series of heat exchangers in the bottoming cycle before the exhaust gas is vented to the atmosphere. In the heat exchangers, the gas enters through the shell side, while high pressure steam/water enters through the tube side. The pressure drop is an important factor to be considered. The pressure drop in the shell side for every heat exchanger in the CCPP section is assumed to be 0.1 bar.[26] For the tube sides, the pressure drop is assumed to be 0.3 bar for HX0, 0.4 bar for HX1, 0.8 bar for HX2, 0.8 bar for HX4 and HX5, and 1.2 bar for HX3, based on the recommendations of Gicquel.[26] To make sure that the pressure of the flue gas is high enough to be emitted to open air through a stack without an exhaust fan, the outlet pressure of the GT exhaust is set to 1.7 bar.

The heat transfer coefficient depends on the flow phase conditions in both the shell side and tube side.[27] The heat transfer coefficient is always higher for liquid−liquid than for gas−vapor phase in shell-tube side. For the gas phase in the shell side and liquid phase in the tube side, the heat transfer coefficient without phase change is in the range between 227 and 454 $W/m^2/K$.[27] For vaporization in the tube side, the heat transfer coefficient is much higher, which is more than 1000 $W/m^2/K$. Details of the assumptions chosen for this work are shown in the Supporting Information Table S1.

Most bottoming processes consist of high pressure (HP), intermediate pressure (IP), and low pressure (LP) steam turbines (ST) when the bottoming cycle has the ability to generate more than 20.0 MW of power, and the temperature of the available waste heat from the COG exhaust is high enough to a support steam pressures up to 100 bar.[28] In this study, since total work generated at the bottoming process will exceed 20.0 MW, a three-stage steam turbine system was designed.

To recover as much thermal energy as possible, process water is fed to a low pressure heat exchanger. Then it is split into low pressure and high pressure pathways. The low pressure stream goes through a low pressure economizer, and an evaporator. The high pressure stream is pumped to 123 bar and then sent to a high pressure economizer, an evaporator, and a superheater. The HP steam feeds the HP ST. The HP ST exhaust is reheated before being fed to the IP ST. The stream leaving the IP ST is mixed with the LP steam from the LP superheater and fed into the LP ST. The stream leaving of LP ST is condensed and recycled back to the low pressure pump. The isentropic efficiency of the HP, IP, and LP steam turbines are assumed to be 0.88, 0.89, and 0.86, respectively.[24]

To model the CCPP in Aspen Plus, the PR-BM thermodynamic property package was used to predict the physical properties of all the gas phase unit operations including the fluid properties on the shell side of the heat exchangers. The STEAMNBS thermodynamic property model was used for all water/steam related unit operations such as the tube side of the heat exchangers in the bottoming cycle. In the Aspen Plus model, all heat exchangers were modeled using HEATX block, the condenser was modeled with a HEATER block, the combustion step was modeled using RGIBBS assuming equilibrium was reached, and all turbomachinery was modeled using assumed isentropic efficiencies as noted previously.

2.4. Economic Analysis of the System. Electricity generated by turbines is the main product of this system. Although the status quo and the CCPP will both emit approximately the same flow rates of GHGs (as measured in CO_2e) in absolute terms, the CCPP results in lower indirect emissions associated with the reduced amount of grid electricity purchased for the balance of the plant (since the AMD refinery consumes more electricity than the CCPP produces). As such, we assume that the value of that reduction in GHG emissions will return to the company in the form of lower CO_2 carbon taxes.

The net present value (NPV) can be formulated as shown in eq 1.

$$\mathrm{NPV} = \mathrm{AF}(\mathrm{TR} - \mathrm{TOC} - \mathrm{TPC}) - \mathrm{TCI} \tag{1}$$

$$\mathrm{AF} = \frac{1 - (1 + r)^{-t}}{r} \tag{2}$$

where AF represents the annuity factor, TR represents the annual revenue ($), TOC represents the annual operating cost ($), TPC represents the total production cost ($), and TCI represents the total capital investment ($). For the annuity factor function (eq 2), r represents the interest rate and t represents the lifetime (yr).

The economic analysis in this work uses a business-case comparison against the status quo in order to quantify the value-added by replacing the existing power system with CCPP. This means that the revenues and production costs used in eq 1 are representations of a value instead of actual revenues and expenses. For example, the annual value of electricity of the COG CCPP case is the value of the additional net electricity production over and above the existing process which produces power at a lower rate from the same amount of COG. This additional net work ($W_{\mathrm{add.}}$) is defined in eq 3 as follows:

$$W_{\mathrm{add}} = -W_{\mathrm{COMP}} + W_{\mathrm{GT}} - \sum_{j=1}^{2} W_{\mathrm{PUMP},j} + \sum_{k=\mathrm{LP,IP,HP}} W_{\mathrm{ST},k} - W_{\mathrm{current}} \tag{3}$$

DOI: 10.1021/acs.iecr.8b00246
Ind. Eng. Chem. Res. 2018, 57, 12816−12828

where W_{COMP}, $W_{PUMP,j}$, W_{GT}, $W_{ST,k}$, and $W_{current}$ represent work (kW) consumed by compressor and pumps, work generated by gas turbine and steam turbine, and the net work currently produced using the status quo system, respectively. The value for $W_{current}$ was provided for this case study by AMD Hamilton but is not disclosed for privacy reasons. This value-added electricity is priced at grid electricity purchase prices including delivery (not wholesale prices) because the primary value of the CCPP is to offset AMD Hamilton's grid electricity purchases, which far exceed the power produced by the COG CCPP. Similarly, under a carbon tax, there is value in the reduction of GHG emissions priced at the carbon tax rate. Although the actual GHG emissions will be reduced indirectly (through reduced grid electricity generation), it is assumed that the value of the reduction in emissions in a fair system will be ultimately returned to AMD. Assuming 8000 annual working hours per year, the annual revenue becomes

$$\mathrm{TR} = 8000\ \mathrm{h/yr}\, W_{add}(x_{elec} + R_{CO_2}) \tag{4}$$

$$R_{CO_2} = \omega_{CO_2}\mathrm{Tax}_{CO_2} \tag{5}$$

where x_{elec} represents the price of electricity ($/kWh), R_{CO_2} represents the revenue from carbon tax ($/kWh). ω_{CO_2} represents the carbon intensity of the electrical grid (tCO_2e/kWh), and Tax_{CO_2} represent the tax of CO_2 ($/$tCO_2e$). In this study, these parameters are assumed to be constant during the lifetime of the process.

The annual operating costs include COG consumption, MDEA makeup solvent costs, and utility costs. The makeup water flow rate is computed, but the costs of makeup water is assumed to be zero. Although other studies assumed prices for COG based on heating content,[29] it is not appropriate to use a value of COG for our case study. This is because we consider the difference in value between the status quo and the proposed COG CCPP use case. Since it has the same value in both cases (i.e., a waste product with a very limited market), the value added (or extra cost) is zero and so it does not appear in the equation for the production costs. Thus, the annual operating costs include only the extra costs associated with the purchase of makeup MDEA and utility costs over and above the utility water requirements of the status quo:

$$\begin{aligned}\mathrm{TOC} = 8000\frac{\mathrm{h}}{\mathrm{yr}}(&x_{MDEA}m_{MDEA,makeup} + x_{cond}Q_{cond} \\ &+ x_{reb}Q_{reb} + x_{CW}(Q_{comp} + Q_{cool,MDEA} + Q_{CCPP} \\ &- Q_{SQ}))\end{aligned} \tag{6}$$

where x_{MDEA} represents the price of MDEA ($/kg), $m_{MDEA,makeup}$ represents the flow rate of makeup MDEA (kg/h), x_{cond} and x_{reb} represent the prices of the condenser and reboiler utilities ($/GJ) in the desulfurization section, respectively, Q_{cond} and Q_{reb} represent the duties of the condenser and reboiler utilities (GJ/h) in the desulfurization section, respectively, x_{CW} is the price of cooling water ($/GJ), Q_{comp} represents the total interstage cooling duty of the COG and air compressor, $Q_{cool,MDEA}$ represents the cooling duty of recycling MDEA solvent in desulfurization process, and Q_{CCPP} and Q_{SQ} are the total condenser duties (GJ/h) of the steam sections of the COG CCPP and status quo plants, respectively.

The total annual production cost is defined in Table S2. The TPC ($/yr) is calculated according to page 604 of the book of Seider et al.[27] It includes operations (labor-related), maintenance cost, operating overhead, property taxes and insurance, depreciation, and general expenses. Note that for this analysis, we assume that the TPC of the status quo is zero, due to the lack of publically available data for the TPC of the existing system at the AMD Hamilton refinery. Thus, this serves as a very conservative estimate of the value of the COG CCPP system. In other words, a strong business case would be made for the CCPP system if the NPV and other economic criteria are favorable even with this assumption. Q_{SQ} is estimated according to the size of the status quo. It is assumed that the pressure inlet and outlet of the LP ST in both the status quo and the COG CCPP are the same. Thus, the heat duty (Q_{SQ}) is linearly regressed with respect to the amount of work generated in the LP ST.

The equipment required in this new CCPP includes a compressor, a combustor, a gas turbine, two pumps, six heat exchangers, three steam turbines, and the equipment of the whole desulfurization process. Thus, the total free-on-board (F.O.B.) cost (C_{fob}) is calculated as eq 7:

$$\begin{aligned}C_{fob} = C_{COMP} + C_{COMB} + C_{GT} + \sum_{1}^{2} C_{PUMP,j} \\ + \sum_{1}^{2} C_{motor,j} + \sum_{0}^{5} C_{HX,i} + \sum_{k} C_{ST,k} + C_{MDEA}\end{aligned} \tag{7}$$

where C_{COMP}, C_{COMB}, C_{GT}, $C_{PUMP,j}$, $C_{motor,j}$, $C_{HX,i}$, $C_{ST,k}$, C_{MDEA} represent the F.O.B cost of the compressor, combustor, gas turbine, pumps, pump motors, heat exchangers, steam turbines, and desulfurization process, respectively.

The equipment free on board (F.O.B.) cost of topping cycle equipment is based on 1982 prices[30] while the bottom cycle equipment is based on 2006 prices.[27] To convert the cost to present cost, the Chemical Engineering Plant Cost Index (CEPCI)[31] for 2016 is used. For this research, these F.O.B. costs are converted to 2016 CAD with the following equation.

$$\text{present cost} = \text{base cost}\frac{\mathrm{CEPCI}_{new}}{\mathrm{CEPCI}_{old}}\mathrm{PPP} \tag{8}$$

where PPP is the purchasing power parity of Canada[32] relative to that of the United States in this case since the cited equipment cost curves are for US applications. Also, we note that the topping cycle equipment cost projections, although old, are the most recent we could find in the peer-reviewed literature and continue to be used in recent studies.[30] However, an online database of user-supplied actual purchase prices indicated that the cost for a similar topping cycle equipment at a similar scale was around $10 million for the equipment purchase costs.[33] Although we did not use this price because it is not verifiable or peer reviewed, when the cost of installation (including shipping, piping, etc.) using assumed capital investment factor by Seider et al.[27] is considered, the total installed cost would be in the range of $30−60 million. The installed cost predicted using the peer-reviewed correlations and the CEPCI is within this range and therefore is a reasonable estimate for this analysis.

The total capital investment (TCI) includes the F.O.B. costs and any related costs such as shipping, installation, construction, construction overhead, contractor engineering, contingencies, depreciation, land, royalties, start-up, and total

DOI: 10.1021/acs.iecr.8b00246
Ind. Eng. Chem. Res. 2018, 57, 12816−12828

working capital. A detailed calculation of the TCI is shown in Table S3.[27]

The compressor cost (C_{COMP}) is correlated to the mass flow rate of air (m_{air}: kg/h), its compression efficiency (η_{comp}), outlet to inlet pressure ratio, and number of compression stages (N):[30]

$$C_{COMP} = \left(\frac{1}{N}\right)\left(0.01975\frac{m_{air}}{0.9 - \eta_{comp}}\right)\left(\left(\frac{P_{air}^{out}}{P_{air}^{in}}\right)^{1/N}\right)\left(\ln\left(\frac{P_{air}^{out}}{P_{air}^{in}}\right)\right) \quad (9)$$

The cost of the combustor (C_{COMB}) is correlated to mass flow rate of air, outlet ($P_{g,COMB}^{out}$) to inlet (P_{air}^{in}) pressure ratio, and outlet temperature ($T_{g,COMB}^{out}$).[30]

$$C_{COMB} = \left(0.0128\frac{m_{air}}{0.995 - \frac{P_{g,comb}^{out}}{P_{air,comb}^{in}}}\right)(1 + \exp(0.018T_{g,COMB}^{out} - 26.4)) \quad (10)$$

The cost of the gas turbine (C_{GT}) is correlated to mass flow rate of gas (m_g: kg/h), and is affected by inlet to outlet pressure ratio, inlet temperature (T_g^{in}), and efficiency of the turbine (η_{GT}):[30]

$$C_{GT} = 0.13315\left(\frac{m_g}{0.92 - \eta_{GT}}\right)\left(\ln\left(\frac{P_g^{in}}{P_g^{out}}\right)\right)(1 + \exp(0.036T_g^{in} - 54.4)) \quad (11)$$

The F.O.B. cost of pumps $C_{PUMP,j}$ is correlated to pump type ($F_{t,pump}$), material type ($F_{m,pump}$), and the base cost of that pump ($C_{B,PUMP,j}$). Considering the large amount of water to be pumped, a centrifugal pump is chosen in this paper.[27]

$$C_{PUMP,j} = F_{t,pump}F_{m,pump}C_{B,PUMP,j} \quad (12)$$

The base cost of the pump as calculated by eq 13 is correlated to shape factor (S),[27] while the shape factor is a function of water flow rate (V) in gallons/min, and pump head (H) in feet.

$$C_{B,PUMP,j} = \exp\left(9.7171 - 0.6019\ln(S_j) + 0.0519(\ln(S_j))^2\right) \quad (13)$$

$$S_j = V(H)^{0.5}, \quad S_j \in [400, 1E5] \quad (14)$$

A centrifugal pump is usually driven by an electric motor. Depending on which type of motor used, the motor-type factor ($F_{t,motor,j}$) will apply. The cost of an electric motor is a function of the horsepower consumption ($HP_{pump,j}$):[27]

$$C_{motor,j} = F_{t,motor,j}\exp(5.8259 + 0.13141\ln(HP_{pump,j}) + 0.053255(\ln(HP_{pump,j}))^2 + 0.028628(\ln(HP_{pump,j}))^3 - 0.0035549(\ln(HP_{pump,j}))^4) \quad (15)$$

The electricity needed for the pump is factored into the net output of the CCPP.

A fixed head type heat exchanger is chosen in this work.[27] The base cost ($C_{B,HX,i}$) of a heat exchanger is a function of heat exchange area A_i.

$$C_{B,HX,i} = \exp(11.2927 - 0.9228\ln(A_i) + 0.09861(\ln(A_i))^2) \quad (16)$$

The F.O.B. cost of heat exchanger ($C_{HX,i}$) is correlated to the material type ($F_{m,HX}$), length of the tube ($F_{L,HX}$), the shell side pressure factor ($F_{p,HX}$), and the base cost ($C_{B,HX,i}$).

$$C_{HX,i} = F_mF_LF_pC_{B,HX,i} \quad (17)$$

The pressure factor is a function of pressure (in psig) in the shell side as shown in following equation, which is applicable from 100 to 2000 psig:

$$F_p = 0.9803 + 0.018\frac{P}{100} + 0.0017\left(\frac{P}{100}\right)^2 \quad (18)$$

HP and IP steam turbines are noncondensing while the LP stream turbine is a condensing type. In addition, the size of the LP steam turbine is larger than the normal steam turbine; two parallel LP ST are used. The F.O.B. purchase cost of the steam turbine is shown in the following equation from Seider et al, page 591.[27]

$$\left.\begin{aligned} C_{ST,k} &= 9400(W_{ST,k}/0.7355)^{0.41}, \quad k = \text{HP, IP} \\ C_{ST,k} &= 50000(W_{ST,k}/1.471)^{0.41}, \quad k = \text{LP} \end{aligned}\right\} \quad (19)$$

To build a new plant, the payback period is a crucial criterion. As eq 20 shows, the payback period (y) is calculated using a shortcut approach:

$$y = \frac{TCI}{TR - TOC - TPC} \quad (20)$$

2.5. Optimization of the System. An optimization approach was used to determine the design parameters for the CCPP. Although the ProMax and AspenPlus simulations are useful for rigorous performance and stream output predictions, they are not directly amenable to rigorous global optimization due to their complexity. Instead, a simplified model of the chemical plant was used in a mathematical programming framework to determine the optimal plant design. The rigorous ProMax and Aspen Plus models were used for the creation of certain reduced models as well as for the validation of the optimization results. The CCPP system design has certain fixed conditions such as some of the steam turbine pressures and temperature which are shown in Table S4. The key decision variables are the surface area of each heat exchanger A_i, the process water flow rate (m_{H_2O}), and the split fraction ($1 - \gamma$) of the process water going to the LP steam turbine. The optimization formulation is shown in the following equations.

$$\text{maximize}_{A_i, m_{H_2O}, \gamma, S_j} \text{NPV}(A_i, m_{H_2O}, \gamma, S_j) \quad (21)$$

Subject to

$$\left.\begin{aligned} m_g(h_{g,i}^{in} - h_{g,i}^{out}) - m_{H_2O}(h_{H_2O,i}^{out} - h_{H_2O,i}^{in}) &= 0, \ i = 0 \\ m_g(h_{g,i}^{in} - h_{g,i}^{out}) - \gamma m_{H_2O}(h_{H_2O,i}^{out} - h_{H_2O,i}^{in}) &= 0, \ i = 2 - 5 \\ m_g(h_{g,i}^{in} - h_{g,i}^{out}) - (1 - \gamma)m_{H_2O}(h_{H_2O,i}^{out} - h_{H_2O,i}^{in}) &= 0, \ i = 1 \end{aligned}\right\} \quad (22)$$

DOI: 10.1021/acs.iecr.8b00246
Ind. Eng. Chem. Res. 2018, 57, 12816−12828

$$m_g(h_{g,i}^{in} - h_{g,i}^{out}) - U_i A_i \Delta T_{LM,i} = 0,$$
$$A_i \in [14.0, 1120], \quad i = 0 \text{ to } 5 \tag{23}$$

$$m_{H_2O}(h_{cond,ccpp}^{out} - h_{cond,ccpp}^{in}) - Q_{cond,ccpp} = 0 \tag{24}$$

$$\Delta T_{LM,i} - \frac{(T_{g,i}^{in} - T_{H_2O,i}^{out}) - (T_{g,i}^{out} - T_{H_2O,i}^{in})}{\ln\left(\frac{T_{g,i}^{in} - T_{H_2O,i}^{out}}{T_{g,i}^{out} - T_{H_2O,i}^{in}}\right)} = 0,$$
$$i = 0 \text{ to } 5 \tag{25}$$

$$\left.\begin{aligned} h_l - (a_l T_l - b_l) = 0 \\ h_g - (a_g T_g - b_g) = 0 \end{aligned}\right\} \tag{26}$$

$$h_{mix} - ((1 - \gamma)h_{LP} + \gamma h_{IP}) = 0 \tag{27}$$

$$\left.\begin{aligned} W_{pump,j} - m_{H_2O,j}(h_{H_2O,j}^{out} - h_{H_2O,j}^{in}) = 0, \quad j = 1 \\ W_{pump,j} - \gamma m_{H_2O,j}(h_{H_2O,j}^{out} - h_{H_2O,j}^{in}) = 0, \quad j = 2 \end{aligned}\right\} \tag{28}$$

$$\left.\begin{aligned} W_{ST,k} - \gamma m_{H_2O,k}(h_{H_2O,k}^{out} - h_{H_2O,k}^{in}) = 0, \quad k = \text{HP, IP} \\ W_{ST,k} - m_{H_2O,k}(h_{H_2O,k}^{out} - h_{H_2O,k}^{in}) = 0, \quad k = \text{LP} \end{aligned}\right\} \tag{29}$$

$$\left.\begin{aligned} T_{g,i}^{out} - T_{g,i}^{in} < 0 \\ T_{H_2O,i}^{in} - T_{H_2O,i}^{out} < 0 \\ T_{H_2O,i}^{out} - T_{g,i}^{in} < 0 \\ T_{H_2O,i}^{in} - T_{g,i}^{out} < 0 \end{aligned}\right\}, \quad i = 0 \text{ to } 5 \tag{30}$$

where NPV(A_i $m_{H_2O,\gamma Sj}$) is the nonlinear net present value function as computed by eqs 1 through 19, h represents the enthalpy of a process liquid and gas in J/kg, subscripts H_2O, g, and l represent water or steam streams, gas streams, set of streams whose enthalpy are linear modeled, stream after the MIX block, and intermediate pressure and low pressure streams before the MIX block, respectively. Superscripts out and in denote the output and input of the heat exchanger. The heat transfer coefficient (U_i) is constant as shown in Table S1. $\Delta T_{LM,i}$ represents the log mean temperature difference of each heat exchanger, which is the driving force of each heat exchanger. T represents temperature in °C, and a and b represent constants of the linear regression model for enthalpy. Notice that for each stream in the bottoming cycle as shown in Figure 2, the pressure of each stream is fixed. The temperature of the streams that goe into the HP and IP stream turbines is also fixed as shown in Table S4. Since HX1 and HX3 are evaporators, their steam temperatures are also fixed. This helps constrain the temperature range for the unknown streams. In addition, each stream is guaranteed to have a single phase. If the temperature is not specified, a linear model is used to estimate the enthalpy of that stream. Thus, the enthalpy of each stream can be represented by eq 26. For those streams with specified temperature, the enthalpy is constant.

Equation 22 to eq 29 are the equality constraints of the optimization problem. Equation 22 is the energy balance between shell side and tube side. Equation 23 is the energy balance of the heat exchanger with heat exchange area bounded in a given range [14.0, 1120] m^2. Equation 24 is the energy balance of the condenser in CCPP. The thermal energy decreasing in the recycled process water is the amount that the condenser removed. Equation 25 is the heat exchanger driving force. The coefficients in eq 26 and eq 27 are determined by linear regression of the STEAMNBS/PR-BM model in Aspen Plus over the relevant temperature range with a good fit (R^2 greater than 0.99). The temperature range for stream STEAM6 is [205.3, 269.9] °C, while the temperature for gas is in the range of [50.2, 692.0] °C.

The flow rate of COG, the GT inlet temperature, and GT inlet pressure are set as a fixed value according to design requirement as mentioned in Table S4. The net work generated in the topping process is fixed. Thus, the work of compressor and GT is a known constant value. For pumps and steam turbines, the working fluid is water/steam. Thermal energy is converted to mechanical energy. The work consumed by pump ($W_{pump,j}$) and work generated by steam turbines ($W_{ST,k}$) could be calculated in the form of enthalpy change. Thus, the work is calculated in the eqs 28 and 29.

Equation 30 ensures that there is no temperature crossover in each heat exchanger. Setting a minimum approach temperature (or pinch point) is not necessary because small approach temperatures (which would result in extremely high heat exchanger areas) are automatically avoided because of the economic objective. Most variables were left unbounded except for the temperature of the flue gas exhaust (EXHAUST8) which had a lower safety bound of 75 °C.

The above simplified model of the CCPP was constructed in the General Algebraic Modeling System (GAMS) version 24.7.4. There were 85 variables in total, including the 10 decision variables. When using the solver BARON (version 16.8.24) to find the global optimum, we found that it would typically take about 0.33 s or less to converge given a good initial guess. Without any initial guess, the solver would abort due to domain of definition errors (for example, pump cost eq 13 would fail if no initial value for the pump shape factor is provided, since GAMS treats all the variables as zero when no initial value is provided). Although Aspen Plus simulation results were used to generate initial guesses, some of these guesses would still be quite poor, often requiring large computation times. To shorten the overall calculation time with a poor initial guess, we used a different strategy to approach the optimization of the system by using a series of solvers, in the order of IPOPT → CONOPT → BARON. This not only resulted in finding global optimums consistently, but shorter calculation times on the order of 0.12 s. Specifically, IPOPT (version 3.12) was used to find an initial feasible point for the problem, which it can do very quickly because we already have a good feasible initial guess from our Aspen Plus base case simulation. This initial feasible point was used as an initial guess for CONOPT (version 3.17A), which was used to find a guaranteed local optimum. The local optimum was used as initial guess for BARON (version 16.8.24), which found the global optimum quickly with such a good initial guess (and in fact that local optima is very often the global optimal). For this case study, the total CPU time for IPOPT function evaluations was around 0.05 s, the CONOPT solver was trivially fast, and with the total CPU time for BARON once initialized was around 0.07 s.

DOI: 10.1021/acs.iecr.8b00246
Ind. Eng. Chem. Res. 2018, 57, 12816−12828

Table 3. Design Parameters and Simulation Results for the MDEA Process

Compression			
compressor 1 outlet pressure (bar)	5.00	comp 1 work (MJ/kg COG)	0.370
compressor 2 outlet pressure (bar)	16.2	comp 2 work (MJ/kg COG)	0.400
Absorber			
gas inlet temperature (°C)	46.6	sweet COG H_2S Content (ppmv)	0.100
solvent inlet temperature (°C)	46.6	sweet COG CS_2 Content (ppmv)	80.2
solvent rate (kg solvent/kg COG)	1.77	sweet COG C_4H_4S Content (ppmv)	25.5
number of stages	18.0		
Stripper			
number of stages	8.00	H_2S recovery (1-kg H_2S in product/kg H_2S in feed)	99.8%
CS_2 recovery (1-kg CS_2 in product/kg CS_2 in feed)	0.460%	C_4H_4S recovery (1-kg C_4H_4S in product/kg C_4H_4S in feed)	5.36%
reflux ratio	10.0	boilup ratio	3.44
cooling duty (MJ/kg feed)	2.17	heat duty (MJ/kg feed)	0.570
distillate temperature (°C)	40.0	bottoms outlet temperature (°C)	210
Makeup			
water makeup/losses (kg H_2O added per kg H_2O in solvent absorber feed)	0.011	MDEA makeup/losses (kg MDEA added per kg MDEA in solvent absorber feed)	7.80×10^{-6}

3. RESULTS AND DISCUSSION

3.1. Desulfurization Results. The key design parameters and ProMax simulation results are shown in Table 3. Two-stage of compressors were used. The second compressor consumed 8% more power than the first compressor. The makeup water flow rate is about 1.10% of the flow rate of the bulk solvent requirement. The makeup MDEA flow rate is very low, which means that there is very little solvent loss in the desulfurization process. The desulfurization process achieved 99.8% of H_2S removal, while little of the organic sulfur compound CS_2 and thiophene (C_4H_4S) were removed as expected. However, the H_2S content in the sweet COG is less than 1.00 PPMV, meaning that the total sulfur content is low enough to use in the gas turbine, despite the presence of CS_2 and thiophene.

3.2. GAMS Model Match with Aspen Plus. The parameters that were used to calculate the capital cost of the system are shown in Table S3. The pressure in the shell side of the heat exchanger drops from 1.70 to 1.10 bar (30.7 to 39.4 psig). According to eq 18, the pressure factor (F_p) for the heat exchanger is in the range from 0.986 to 0.988, thus it was approximated to 0.988 for all cases instead of having an equation for calculating F_p in GAMS. The longest standard tube length is 20.0 ft (6.10 m), which in this paper was chosen for heat exchanger calculations considering the area of each heat exchanger was in the order of 1000 m^2. For the pump impeller, cast iron is inferior to bronze in corrosion, erosion, and cavitation resistance. Stainless steel impellers have the highest resistance of corrosion, erosion, and cavitation, but it is more costly. Thus, bronze material is chosen for both the impeller and the casing.[34] There are three types of electric motor that could be used for the pump: open, drip-proof enclosure, size range from 1 to 700 Hp; totally enclosed, fan-cooled, size range from 1 to 250 Hp; and explosion-proof enclosure, size range from 1 to 250 Hp. The pump is used to pump water, which is relatively safe and has no large temperature increase, thus an open, drip-proof enclosure type is chosen.

For the utility costs, 450 psig steam (235.8 °C) was chosen for the desulfurization reboiler utility. The HRSG condenser, distillation condenser, and interstage coolers for compressors all use cooling water (assuming an operating temperature range of 32 to 49 °C). The corresponding price of utilities is shown in Table S5, based on ref 27.

The base case uses Ontario's global adjusted electricity price (11.2 ¢/kwh),[35] an interest rate of 15.0%, a lifetime of 30 years, Ontario's electricity grid carbon intensity of 40 gCO_2eq/kWh,[36] and Ontario's average carbon tax in 2017, which is $18.1/tonne.[37] Although the current carbon tax system in Ontario includes a complex arrangement of emissions credits, we assume that all of the associated CO_2 emissions are taxable. To validate the reduced model used in GAMS, the optimal decision variables determined by GAMS were used as inputs to the Aspen Plus simulation, and the Aspen Plus results of key variables were compared, as shown in Table 4.

The temperature of the EXHAUST streams and two adjustable steam/water streams have a small error. The biggest

Table 4. Results of the Optimization Model (Using Simplified Models), and the Corresponding Results of Key Variables When the Design Was Simulated More Rigorously in Aspen Plus. Results Are for the Base Case

component	description	GAMS	Aspen Plus	error (%)
m_{air}	kg air/kg COG	28.5	28.5	0.00
m_{H_2O}	kg water circulated in bottoming process/kg COG	6.56	6.56	0.00
T_g^1	EXHAUST1 (T/°C)	1240	1240	0.00
T_g^2	EXHAUST2 (T/°C)	692	692	0.00
T_g^3	EXHAUST3 (T/°C)	634	634	−0.01
T_g^4	EXHAUST4 (T/°C)	599	599	−0.02
T_g^5	EXHAUST5 (T/°C)	510	511	−0.04
T_g^6	EXHAUST6 (T/°C)	445	446	−0.15
T_g^7	EXHAUST7 (T/°C)	191	190	0.41
T_g^8	EXHAUST8 (T/°C)	98.0	96.0	1.51
$T^6_{H_2O,vap.}$	STEAM6 (T/°C)	206	205	0.32
$T^7_{H_2O,vap.}$	STEAM7 (T/°C)	51.1	51.1	0.01
total power generated	MJ/kg COG	25.9	25.9	0
total net work	MJ/kg COG	13.3	13.3	0
total HX area	total HX area (m^2)	2150	2180	−1.15
topping net work	MJ/kg COG	7.93	7.93	0
bottoming net work	MJ/kg COG	5.40	5.38	0.37

DOI: 10.1021/acs.iecr.8b00246
Ind. Eng. Chem. Res. 2018, 57, 12816−12828

Table 5. Economic Analysis of Proposed COG CCPP Compared with Status Quo

	proposed COG CCPP				
	desulfurization	topping	bottoming	total	business as usual/status quo
MJ/kg COG		7.93	5.4	13.3	5.77
TCI (million $)	1.29	50.0	17.2	68.5	0
TOC ($/kW)				31.4	0
TPC ($/kW)				288	0
TR ($/kW)				512	0
payback period (yr)				5.77	0
NPV (million $)				9.51	0
installation cost ($/kW)		1359	685	1107	0

error is the temperature of stream EXHAUST8, which is the stack temperature. But all the errors are less than 1.51%, which is small. Thus, the result from GAMS optimization is reasonable, and the simplified GAMS model is good for further use with other parameters.

As Table 4 shows, every 1 kg of COG will need 6.56 kg of water in order to achieve the highest NPV for the CCPP. The total gross power generated is about 25.9 MJ/kg COG, while the total net work is 13.3 MJ/kg COG.

3.3. Economic Analysis. For the base case, the topping cycle generates about 59.5% of the total work, while the bottoming cycle generates 40.5% of electricity as shown in Table 5. According to M. Boyce,[28] the topping cycles of combustion systems usually generate around 60.0% of the power, which is very much in line with our results. The thermal efficiency of CCPP from natural gas can be as high as 60.0% when the outlet pressure of gas from GT is at atmospheric pressure as M. Boyce stated.[28] In this case, however, the thermal efficiency is about 34.7% because the HHV of COG is only about half that of natural gas. However, the proposed CCPP has more than twice the efficiency (15.0% high heating value) of AMD Hamilton's existing COG combustion power system.

The installation cost of the topping process is about 3 times that of the bottoming process. The high cost of the topping cycle might be the reason why a considerable number of steel refineries only use low pressure steam turbines even though they have lower energy recovery. The total installation cost of this proposed system is 1107 $/kW, which is higher than the common CCPP plant whose cost range falls between 600 and 900 $/kW.[28] However, this includes the desulfurization cost, which comprises 1.9% of the total cost. Without the desulfurization process taken into account, the CCPP installation cost would only be 1086 $/kW. The NPV of the business as usual scenario evaluates to $0 million according to eq 1. Thus, the CCPP plant is a good risk for an investment because it has a potential net present value of $9.51 million (including the benefits of reduced grid electricity purchases and reduced carbon taxes), within 6 years (payback period of 5.77 yr) and only $68.5 million in capital investment. In addition, the net lifecycle CO_2 emissions reduced is 84.1 gCO_2e/kg COG with the local carbon intensity of 40 gCO_2e/kWh. This represents a net lifecycle reduction in GHG emissions arising from COG combustion by about 5.28%. However, the direct CO_2 emission of AMD status quo is 995 gCO_2e/kWh, while the proposed CCPP reduces it to 430 gCO_2e/kWh.

3.4. Sensitivity Analysis of the System. Considering that the electricity price, carbon intensity, carbon tax, PPP, and annuity factor might change according to government policies and market effects, the business case for using the proposed system may change accordingly. Thus, the uncertainty of the above-mentioned five factors is considered in a sensitivity analysis. The worldwide electricity price ranges from 3.00 to 60.0 CAD ¢/kWh;[38−40] grid carbon intensity ranges from 2.05 to 4553 gCO_2 eq/kWh; the carbon tax rate ranges from 0.00 to 70.0 CAD $/tonne;[37,41] and the carbon tax revenue R_{CO_2} thus ranges from 0.00 to 0.319 CAD $/kWh. For the annuity factor, assuming that the interest rate range is 10.0−50.0% and the lifetime range is 10.0−50.0 years, the AF is in the range of 1.70−10.0. It is usually the case that countries with very high carbon intensity have little or no carbon tax. Also, when the carbon intensity is high, the PPP is high as well, which means the cost of applying this proposed COG CCPP is high. The optimization problem was resolved using 1000 different combinations of the economic parameters (electricity price, grid carbon intensity, carbon tax rate, and annuity factor), which were selected randomly using a uniform distribution within reasonable ranges of the uncertainty mentioned above. The global optimal design, however, was the same for all cases. The NPV is a function of electricity price, carbon tax rate, PPP, and annuity factor as eq 31 shows.

$$\mathrm{NPV} = \mathrm{AF}\left(\left(248.558\left(x_{\mathrm{elec}}\frac{1\$}{100¢} + R_{CO_2}\right) - \mathrm{PPP}(\$1.532) - \$14.2\right) - \mathrm{PPP}(\$54.003)\right) \times 10^6 \tag{31}$$

As the electricity price and carbon tax rate increases, the NPV increases. When the interest rate is 15.0%, lifetime is 30 years (meaning when AF is 6.57), and there is no carbon tax credit (which means that the carbon tax rate is zero), the electricity price could be as low as 10.8 CAD ¢/kwh to still have a positive NPV. If the price is lower than that, the CCPP is not recommended.

The payback period within the above range is given as eq 32.

$$y = \frac{\$54.003\mathrm{PPP}}{248.55788\left(x_{\mathrm{elec}}\frac{1\$}{100¢} + R_{CO_2}\right) - \$1.532\mathrm{PPP} - \$14.2} \tag{32}$$

For the base case, payback period is about 5 years. When the electricity price goes up to above 15.1 ¢/kwh, or R_{CO_2} goes above 0.157 $/kWh, the payback period will be reduced to 3 years.

Four other representative locations are chosen as a case study. These are China, USA, Finland, and Mexico, and each of them have different electricity price, carbon tax, carbon intensity of their electric grid, and PPP. Notice that the

DOI: 10.1021/acs.iecr.8b00246
Ind. Eng. Chem. Res. 2018, 57, 12816−12828

Table 6. Economic Analysis of COG CCPP Applied in Various Locations Assuming AF = 6.57

	Ontario, Canada	USA	Finland	Mexico	China	units	ref
PPP	1.27	1	0.905	8.57	3.47	LCU/USD	32
ω_{CO_2}	40	588	285	856	1064	g/kWh	42−45
Tax_{CO_2}	18.1	0	29.3	3.70	0	$/tonne	37, 41, 46
x_{elec} [a]	0.112	0.108	0.175	3.65	0.660	LCU/kwh	47−49
NPV	9.51	19.5	164	286	115	million USD	
Y	5.77	4.82	1.63	0.53	1.30	yr	

[a]LCU = local currency unit (Canada in CAD, USA in USD, Finland in Euro, Mexico in MXN, and China in RMB).

carbon intensity for USA, Finland, Mexico, and China are calculated as follows:

$$\omega_{CO_2} = (\text{CO}_2 \text{ emissions from electricity and heat production (\% of total fuel comb)} \times \text{total CO}_2 \text{ emission (kt)}) \Big/ \left(\text{electrical power consumption}\left(\frac{\text{kWh}}{\text{capital}}\right) \times \text{total population}\right) \quad (33)$$

The data used to calculate carbon intensity in eq 33 are from the World Bank, 2016.[42−45] Table 6 is the comparison between those cases as well as the AMD case.

For the five cases shown in Table 6, the values are based on AF = 6.57. Even though Finland has a very low carbon intensity (285 gCO_2e/kWh), it has very high carbon tax (29.32 $/tonne).[41] While for Mexico, its carbon intensity (856 gCO_2e/kWh) is about three times that of Finland, but its carbon tax is low (3.7 $/tonne).[42] For the USA case, even though its R_{CO_2} is zero, its capital cost is lower compared to the AMD, Canada case, and thus there is an even stronger business case for using COG CCP in the USA. For Mexico and China, not only are the economic gains large, but indirect CO_2 emissions can be reduced by 241 $ktCO_2e/yr$ and 299 $ktCO_2e/yr$, respectively, with the same COG flow rate per instance. As of 2016, China produced 808.4 Mt of crude steel.[50] If China applied this proposed COG CCPP, a COG production rate of the total CO_2 emission reduced would be 53.7 $MtCO_2e/yr$. For the whole world, the CO_2 emission reduction would be 108 $MtCO_2e/yr$.

The cost of CO_2 avoided (CCA) in this proposed COG CCPP is the extra costs of doing a "green" technology compared to a status quo, divided by the reduction in emissions as a result of that technology. This means that

$$\text{CCA} = \frac{\text{NPV}_{SQ} - \text{NPV}_{CCPP}}{30\text{yr}(8000\text{h}\omega_{CO_2}W_{add})} \quad (34)$$

where NPV_{SQ} and NPV_{CCPP} represent the net present value of the status quo and proposed COG CCPP. The NPV calculated in eq 34 are without revenue from the carbon tax. The CCA for Canada and China is −2.21 and −12.8 $/t$CO_2$e, respectively.

4. CONCLUSION

This paper proposed a design and examined the economics of a COG based fuel CCPP process. It was found that if the current steam power plant were replaced with the proposed CCPP, it could achieve $9.51 million in net present value under base case market conditions. The payback period is also relatively short. The potential environmental benefit for this particular case study, however, is relatively small, because the reduction in GHG emissions is associated with avoided electricity purchases from an electric grid which already has a low carbon intensity. But the impact of using this same technology in other markets is substantially different.

A sensitivity analysis was conducted that yielded a simple bilinear prediction of the NPV of this investment as a function of the annuity factor (easily computed from project lifetime and interest return rates), price of electricity, and the value of avoided carbon taxes (easily computed from grid carbon intensity and carbon taxes). However, this analysis does not include important case-specific factors such as the lost productivity due to lost electric power produced by the status quo system during the retrofit construction period, which would add to the cost. This also does not reflect the additional cost of other practical issues during this retrofit construction period such as having to add in more substations/transition lines to provide for lost power from the grid during retrofit so the rest of the refinery can still operate.

In a future work, we consider alternative COG disposal strategies, such as conversion to methanol or H_2. The potential advantages would be significantly lower direct grid CO_2 emissions from the plant and the displacement of fossil-based primary energy products (such as petroleum-derived methanol). However, this would be offset by increased grid electricity consumption, CO_2 emissions associated with indirect emissions of downstream product use, and the adoption of business activity which is typical for a steel refinery, such as liquid/gaseous chemical production and CO_2 sequestration. The CCPP approach presented in this study will serve as an important benchmark for comparative purposes.

■ ASSOCIATED CONTENT

Supporting Information

The Supporting Information is available free of charge on the ACS Publications website at DOI: 10.1021/acs.iecr.8b00246.

Pressure drop and heat transfer coefficients in heat exchangers; annual cost to operate the CCPP; factors for total capital investment; specified stream conditions based on the handbook in ref 28; parameters used in the base case calculation (PDF)

■ AUTHOR INFORMATION

Corresponding Author

*Tel.:+1 905 525 9140 ext.24782. E-mail: tadams@mcmaster.ca.

ORCID

Lingyan Deng: 0000-0002-4135-3537

Thomas A. Adams II: 0000-0002-9871-9851

Notes

The authors declare no competing financial interest.

DOI: 10.1021/acs.iecr.8b00246
Ind. Eng. Chem. Res. 2018, 57, 12816−12828

■ ACKNOWLEDGMENTS

This invited contribution is part of the I&EC Research special issue for the 2018 Class of Influential Researchers. Helpful collaborations and data from Ian Shaw and David Meredith (AMD) are gratefully acknowledged. This research was funded by the McMaster Advanced Control Consortium, of which AMD is a member.

■ NOMENCLATURE

Abbreviations

AMD = ArcelorMittal Dofasco
BFG = blast furnace gas
BOFG = basic oxygen furnace gas
CEPCI = chemical engineering plant cost index
CO_2e = CO_2 equivalents
COG = coke oven gas
FOB = free-on-board
GHG = greenhouse gas
GT = gas turbine
HHV = high heating value
HP = high pressure
IGCC = integrated gasification combined cycle
IP = intermediate pressure
LP = low pressure
MDEA = methyl diethanolamine
MEA = ethanolamine
NG = natural gas
NPV = net present value
ST = steam turbine

Roman and Greek symbols

A = heat exchange area (m^2)
AF = annuity factor
a, b = factors of calculating enthalpy
C = cost ($)
CCA = cost of CO_2 avoided ($/t$CO_2$e.)
γ = split fraction
F_L = tube length correction of heat exchangers
$F_{m,HX}$ = heat exchanger material factor
$F_{m,pump}$ = pump material factor
$F_{p,HX}$ = heat exchanger pressure factor
$F_{t,motor}$ = electric motor type factor
$F_{t,pump}$ = pump type factor
m = mass flow rate (kg/h)
N = number of compressor stages
η = efficiency of the equipment
ΔT_{LM} = log mean temperature difference
H = pump head (ft)
$Hp_{pump,j}$ = horse power consumption of pump (hp)
h = enthalpy of stream (J/kg)
p = pressure (bar)
P = shell side pressure (psig)
PPP = purchasing power parity
Q = duties of utility (GJ/h)
r = reducetion rate
R_{CO_2} = revenue from carbon tax ($)
S = shape factor
t = lifetime (year)
T = stream temperature (°C)
Tax_{CO_2} = carbon tax ($/ t CO_2e)
TCI = total capital investment ($)
TFC = total fixed cost ($)
TOC = annua operation cost ($)
TPC = total production cost ($)
TR = total revenue ($)
U = heat transfter coefficient (cal/sec-cm^2-k)
V = water flow rate (gallon/min)
W = work (kw)
ω_{CO_2} = carbon intensity in ecletric grid (tonne/kwh)
x_{cw} = price of cooling water ($/GJ)
$x_{elec.}$ = price of condenser utilities ($/GJ)
x_{cond} = electricity price ($/kwh)
x_{MDEA} = MDEA solvent price ($/kg)
x_{reb} = price of reboiler utilities ($/GJ)
y = payback period (yr)

Subscripts and Superscripts

add	additional
air	air
B	base cost
ccpp	combined cycle power plant
comb	combustor
comp	compressor
cond	condenser
cool	cooling process
current	current sinario
elec	electricity
g	exhaust gas
GT	gas turbine
H_2O	water or steam
HX	heat exchanger
i	number of heat exchanger
in	inlet
j	number of pump
k	LP, IP, and HP steam turbine
l	set of streams whose enthalpy are linear modeled
MDEA	MDEA solvent
motor	electric motor
new	updated cost index
old	original cost index
out	outlet
pump	pump
reb	reboiler
SQ	status quo
ST	steam turbine

■ REFERENCES

(1) Valeri, T. Greenhouse Gas Reporting Program data search: facility information. *ArcelorMittal Dofasco G.P.* [Online], 2016, https://climate-change.canada.ca/facility-emissions/GHGRP-G10091-2016.html (accessed May 22, 2018).

(2) Results of GHG Facility Data Search, Ontario. http://ec.gc.ca/ges-ghg/donnees-data/index.cfm?do=results&lang=en&year=2015&gas=all&fac_name=&prov=ON&city=&naics=all&submit=Submit&order_field=data_co2eq&order=DESC (accessed Aug 2, 2017).

(3) *Technical Paper on the Federal Carbon Pricing Backstop*; Environment and Climate Change, Canada, 2017; https://www.canada.ca/en/services/environment/weather/climatechange/technical-paper-federal-carbon-pricing-backstop.html.

(4) Ghanbari, H.; Pettersson, F.; Saxén, H. Sustainable Development of Primary Steelmaking under Novel Blast Furnace Operation and Injection of Different Reducing Agents. *Chem. Eng. Sci.* **2015**, *129*, 208−222.

(5) Ghanbari, H.; Saxén, H.; Grossmann, I. E. Optimal Design and Operation of a Steel Plant Integrated with a Polygeneration System. *AIChE J.* **2013**, *59*, 3659−3670.

DOI: 10.1021/acs.iecr.8b00246
Ind. Eng. Chem. Res. 2018, 57, 12816−12828

(6) Bermúdez, J. M.; Arenillas, A.; Luque, R.; Menéndez, J. A. An overview of novel technologies to valorise coke oven gas surplus. *Fuel Process. Technol.* **2013**, *110*, 150−159.
(7) *Tracking Industrial Energy Efficiency and CO_2 Emissions*; International Energy Agency, 2007.
(8) Worldsteel association. World steel in figures 2017, https://www.worldsteel.org/ (accessed July 17, 2017).
(9) Shi, W. Z.; An, L. S.; Chen, H. P.; Zhang, X. L. *Performance Simulation of Gas Turbine Combined Cycle with Coke Oven Gas as Fuel.* Power and Energy Engineering Conference, Wuhan, China, March 13−20, 2009.
(10) Yang, W. H.; Xu, T.; Li, W.; Chen, G.; Jia, L. Y.; Guo, Y. J. *Waste gases utilization and power generation in iron and steel works.*IEEE Intelligent Information Technology Application Workshops, Nanchang, China, Nov 21−22, 2009.
(11) Zhou, N. J.; Chen, A. M.; Luo, L.; Li, Y. L. Research and Application of Power Generation Schemes Using Coke Oven Gas. *Energy Conservation Technology.* **2008**, *26*, 202−205.
(12) Zhang, G. J.; Dong, Y.; Feng, M. R.; Zhang, Y. F.; Zhao, W.; Cao, H. C. CO_2 reforming of CH_4 in coke oven gas to syngas over coal char catalyst. *Chem. Eng. J.* **2010**, *156*, 519−523.
(13) Bermúdez, J. M.; Fidalgo, B.; Arenillas, A.; Menéndez, J. A. Dry reforming of coke oven gases over activated carbon to produce syngas for methanol synthesis. *Fuel* **2010**, *89*, 2897−2902.
(14) Man, Y.; Yang, S. Y.; Qian, Y. Integrated process for synthetic natural gas production from coal and coke-oven gas with high energy efficiency and low emission. *Energy Convers. Manage.* **2016**, *117*, 162−170.
(15) Razzaq, R.; Li, C. S.; Zhang, S. J. Coke oven gas: availability, properties, purification, and utilization in China. *Fuel* **2013**, *113*, 287−299.
(16) Modesto, M.; Nebra, S. A. Exergoeconomic analysis of the power generation system using blast furnace and coke oven gas in a Brazilian steel mill. *Appl. Therm. Eng.* **2009**, *29*, 2127−2136.
(17) Yang, Z. B.; Ding, W. Z.; Zhang, Y. Y.; Lu, X. G.; Zhang, Y. W.; Shen, P. J. Catalytic partial oxidation of coke oven gas to syngas in an oxygen permeation membrane reactor combined with NiO/MgO catalyst. *Int. J. Hydrogen Energy* **2010**, *35*, 6239−6247.
(18) George, T.; Armstrong, T.; Jobe, L., Jr. *Heating values of natural gas and its components*; NIST: Washington DC, 1982.
(19) Yuan, B. X.; Liu, J. L. Desulfurization and Purification in CCPP Power Generation by Coke Gas. *Shandong Chem. Ind.* **2015**, *44*, 190−192.
(20) Reynolds, M. A. *Organometallic modeling of the hydrodesulfurization (HDS) process: rhenium carbonyl-promoted CS bond cleavage and hydrogenation of thiophenes and benzothiophenes.* Ph.D. Thesis, Iowa State University, September 2002, 82−123.
(21) Yang, Z. R.; Jian, S. H.; Wu, Z. L.; Yang, Y. W. Discussion of feed gas purification technology for production of methanol from coke oven gas. *Natural Gas Chem. Ind.* **2011**, *36*, 42−45.
(22) O. Reg. 305/17. Environmental Protection Act: Ontario regulation 194/05, Industry emissions-nitrogen oxides and sulfur dioxide. R.S.O, https://www.ontario.ca/laws/statute/90e19 (accessed Sep 8, 2017).
(23) Adams, T. A., II.; Salkuyeh, Y. K.; Nease, J. Processes and Simulations for Solvent Based CO_2 Capture and Syngas Cleanup. *Reactor and Process Design in Sustainable Energy Technology*; Shi, F., Ed.; Elsevier; 2014; Chapter 6, pp 163−231.
(24) Lin, H.; Jin, H. G.; Gao, L.; Zhang, N. A polygeneration system for methanol and power production based on coke oven gas and coal gas with CO_2 recovery. *Energy* **2014**, *74*, 174−180.
(25) Kehlhofer, R.; Hannemann, F.; Rukes, B.; Stirnimann, F. *Combined-cycle gas & steam turbine power plants*; Pennwell Books: Oklahoma, 2009.
(26) Gicquel, R. Combined Cycle Power Plants. *Energy systems: a new approach to engineering thermodynamics*; CRC Press, 2011; Chapter 17.
(27) Seider, W. D.; Seader, J. D.; Lewin, D. R.; Widagdo, S. *Product and Process Design Principles: Synthesis, Analysis and Evaluation*; John Wiley & Sons, Inc., 2009.
(28) Boyce, M.. *Handbook for Cogeneration and Combined Cycle Power Plants*; American Society of Mechanical Engineers, New York, 2004.
(29) Modesto, M.; Nebra, S. A. Analysis of a Repowering Proposal to the Power Generation System of a Steel Mill Plant through the Exergetic Cost Method. *Energy* **2006**, *31*, 3261−77.
(30) Gorji-Bandpy, M.; Goodarzian, H. Exergoeconomic Optimization of Gas Turbine Power Plants Operating Parameters Using Genetic Algorithms: A Case Study. *Thermal Science* **2011**, *15*, 43−54.
(31) The Chemical Engineering Plant Cost Index. Chemical Engineering. http://www.chemengonline.com/pci-home (accessed June 5, 2017).
(32) The wold bank data. PPP conversion factor, GDP (LCU per international $). https://data.worldbank.org/indicator/PA.NUS.PPP?end=2016&name_desc=false&start=2016&view=bar (accessed Nov 10, 2017).
(33) Nye Thermodyamics Corp. Gas Turbine Prices by Output. http://nyethermodynamics.com/trader/outprice.htm (accessed Nov 10, 2017).
(34) Budris, A. R. *The Impact of Component Material Selection on Pump Reliability*. http://www.waterworld.com/articles/print/volume-30/issue-12/inside-every-issue/pump-tips-techniques/the-impact-of-component-material-selection-on-pump-reliability.html (accessed Oct 4, 2017).
(35) IESO. Price Overview. http://www.ieso.ca/en/power-data/price-overview/global-adjustment (accessed Nov 10, 2017).
(36) IESO. Ontario Energy Report. https://www.ontarioenergyreport.ca/pdfs/6001_IESO_Q4OER2016_Electricity_EN.pdf (accessed Nov 24, 2017).
(37) Taylar, P. S. The Coming National Carbon Tax Gap. *C2C Journal.* [Online] 2016. http://www.c2cjournal.ca/2016/11/the-coming-national-carbon-tax-gap/ (accessed May 23, **2017**).
(38) Eurostat statistics explained. Energy price statistics. http://ec.europa.eu/eurostat/statistics-explained/index.php/Energy_price_statistics (accessed Oct 19, 2017).
(39) Hydro Quebec. Comparison of electricity prices in major North American cities. http://www.hydroquebec.com/publications/en/docs/comparaison-electricity-prices/comp_2016_en.pdf (accessed Oct 20, 2017).
(40) The statistics portal. Global electricity prices by select countries in 2015 (in U.S. dollar cents per kWh. https://www.statista.com/statistics/263492/electricity-prices-in-selected-countries/ (accessed Nov 14, 2017).
(41) Carbon Tax Center. *Where carbon is taxed.* https://www.carbontax.org/where-carbon-is-taxed/ (accessed Sep 7, 2018).
(42) Worldbank. Population, Total. http://data.worldbank.org/indicator/SP.POP.TOTL (accessed May 19, 2017).
(43) Worldbank. CO_2 Emissions (Kt). http://data.worldbank.org/indicator/EN.ATM.CO2E.KT (accessed May 19, 2017).
(44) Worldbank. CO_2 Emissions from Electricity and Heat Production, Total (% of Total Fuel Combustion). http://data.worldbank.org/indicator/EN.CO2.ETOT.ZS (accessed May 19, 2017).
(45) Worldbank. Electric Power Consumption (kWh per Capita). http://data.worldbank.org/indicator/EG.USE.ELEC.KH.PC (accessed May 19, 2017).
(46) Altamirano, J. C.; Martinez, J. Mexico's 3 Big Steps towards Comprehensive Carbon Pricing. *World Resources Institute* [Online], April 14, 2017. http://www.wri.org/blog/2017/04/mexicos-3-big-steps-towards-comprehensive-carbon-pricing (accessed May 23, **2017**).
(47) U.S. Energy Information Administration. Electric power monthly. https://www.eia.gov/electricity/monthly/epm_table_grapher.php?t=epmt_5_6_a (accessed Nov 20, 2017).

DOI: 10.1021/acs.iecr.8b00246
Ind. Eng. Chem. Res. 2018, 57, 12816−12828

(48) Europe's Energy Portal. EU latest Energy Prices Report. https://www.energy.eu/historical-prices/EU-Latest/. (accessed Nov 20, 2017).
(49) Electricity Local. China Electricity Rates. https://www.electricitylocal.com/states/texas/china/ (accessed Nov 20, 2017).
(50) Worldsteel aAssociation. World steel in figures, 2017. https://www.worldsteel.org/en/dam/jcr:0474d208-9108-4927-ace8-4ac5445c5df8/World+Steel+in+Figures+2017.pdf (accessed Nov 23, 2017).

DOI: 10.1021/acs.iecr.8b00246
Ind. Eng. Chem. Res. 2018, 57, 12816−12828

Supporting information

Table S1. Pressure drop and heat transfer coefficients in heat exchangers

Heat exchangers	Description	Pressure drop (bar)		Heat transfer coefficient ($W/m^2/K$)
		Shell side	Tube side	
HX0	Gas-liquid HX	0.100	0.300	260
HX1	Vaporization	0.100	0.400	1100
HX2	Gas-liquid HX	0.100	0.800	260
HX3	Vaporization	0.100	1.20	1140
HX4	Gas-Vapor HX	0.100	1.00	140
HX5	Gas-Vapor HX	0.100	1.00	140

Table S2. Annual cost to operate the CCPP

Annual operation (hr) 8000			
Operations (labor-related)			*463800*
Direct wages and benefits (DW&B)	35	$/hr	*280000*
Direct salaries and benefits	15	% of DW&B	*42000*
Operating supplies and services	6	% of DW&B	*16800*
Technical assistance to manufacturing			*60000*
Control laboratory			*65000*
Maintenance (M)			
Wages and benefits (MW&B)	13	% of C_{TDC}	
Fluid handling process	3.5	% of C_{TDC}	
Salaries and benefits	25	% of MW&B	

Materials and services	100	% of MW&B
Maintenance overhead	5	% of MW&B
Operating overhead		
General plant overhead	7.1	% of M&O-SW&B
Mechanical department services	2.4	% of M&O-SW&B
Employee relations department	5.9	% of M&O-SW&B
Business services	7.4	% of M&O-SW&B
Property taxes and insurance	2	% of C_{TDC}
Depreciation		
Direct plant	8	% of (C_{TDC}-1.18 C_{alloc}
Allocated plant	6	% of 1.18 C_{alloc}
Cost of Manufacture (COM)	the sum of the above from DW&B	
General Expenses		
Selling (or transfer) expense	3	% of sales
Direct research	4.8	% of sales
Allocated research	0.5	% of sales
Administrative expense	2	% of sales
Management incentive compensation	1.25	% of sales
Total general expenses (GE)		
Total Production cost (C)	TPC = COM+GE	

Table S3. Factors for total capital investment

F.O.B. (Purchase) Costs	C_{fob}	Historical charts

Installation Costs	C_{inst}	$0.714*C_{fob}$
Construction Costs (Incl. Labor)	C_{cons}	$0.63*C_{fob}$
Total Direct Costs	C_{TDC}	$C_{TDC}=C_{fob} + C_{inst} + C_{cons}$
Shipping (Incl. Insurance & Tax)	C_{ship}	$0.08*C_{fob}$
Construction Overhead	C_{over}	$0.571*C_{fob}$
Contractor Engineering	C_{engn}	$0.296*C_{fob}$
Contingencies	C_{slop}	$0.15 - 0.35*C_{fob}$
Total Indirect Costs	C_{TIC}	$C_{TIC}=C_{ship} +C_{over}+C_{engn}+C_{slop}$
Total Depreciable Capital	C_{dep}	$C_{dep}=C_{TDC}+C_{TIC}$
Land (Pure Real Estate)	C_{land}	$0.02*C_{dep}$
Royalties	C_{royle}	$0.02*C_{dep}$
Startup Costs	C_{strt}	$0.02\text{-}0.3*C_{dep}$ (often 0.1)
Fixed Capital Investment	C_{FCI}	$C_{FCI}=C_{dep}+C_{land}+C_{royle}+C_{strt}$
Cash Reserves	C_{cash}	8.33% of total annual expense
Inventory	C_{inv}	1.92% of annual tangible sales
Accounts Receivable	C_{recy}	8.33% of total annual revenue
Accounts Payable	C_{payb}	8.33% of annual tangible expenses
Total Working Capital	C_{wc}	sum of this section $0.7\text{-}0.89*(C_{fob}+C_{ship})$
Total Capital Investment	C_{TCI}	(total FCI and working capital) $C_{TCI} = C_{FCI}+C_{WC}$

Table S4. Specified stream conditions based on the handbook[28]

Component	Temperature Inlet (°C)	Pressure Inlet (bar)	Temperature Outlet (°C)	Pressure Outlet (bar)

GT	1240	16.0	692	1.70
HP ST	540	120	318	25.0
IP ST	540	24.0	302	4.00
LP ST	339	4.00	51.0	0.130

Table S5. Parameters used in the base case calculation

Parameters	Description	Value	Parameters	Description	Value
$F_{m,\ HX}$	Carbon steel	1.00	$F_{t,\ PUMP}$	centrifugal	8.90
F_p	1.7 (bar)	0.981	$F_{t,\ motor}$	Open, drip-proof enclosure, 1 to 700 Hp	1
Fl	20 (ft)	1.00	x_{cond} & x_{cw}	Price of cooling water (US $/GJ)	0.048
$F_{m,\ PUMP}$	bronze	1.90	x_{reb}	Price of steam at 450 psig (US $/GJ)	8.13

Chapter 3 Techno-economic Analysis of Coke Oven Gas and Blast Furnace Gas to Methanol Process with Caron Dioxide Capture and Utilization

This chapter contributed to two works. One is the half PSE2018 Conference paper published in Computer Aided Chemical Engineering. The other one is a full paper published in the peer-reviewed Journal: Energy Conversion and Management. The full paper included work from the half paper and extended the analysis to more complete analysis. In this thesis, only the full paper is included.

Lingyan Deng, and Thomas A. Adams II. *Methanol production from coke oven gas and blast furnace gas*. Computer Aided Chemical Engineering. Vol. 44. Elsevier, 2018. 163-168.

Lingyan Deng, and Thomas A. Adams II. *Techno-economic analysis of coke oven gas and blast furnace gas to methanol process with carbon dioxide capture and utilization*. Energy Conversion and Management 204 (2019): 112315.

Energy Conversion and Management 204 (2020) 112315

Contents lists available at ScienceDirect

Energy Conversion and Management

journal homepage: www.elsevier.com/locate/enconman

Techno-economic analysis of coke oven gas and blast furnace gas to methanol process with carbon dioxide capture and utilization

Lingyan Deng, Thomas A. Adams II*

Department of Chemical Engineering, McMaster University, 1280 Main St. West, Hamilton, Ontario L8S 4L7, Canada

ARTICLE INFO

Keywords:
Coke oven gas
Blast furnace gas
COG desulphurization
CO_2 utilization
Economic analysis
Methanol production

ABSTRACT

This paper documents a process for converting coke oven gas (COG) and blast furnace gas (BFG) from steel refineries into methanol. Specifically, we propose the use of blast furnace gas (BFG) as an additional carbon source. The high CO_2 and CO content of BFG make it a good carbon resource. In the proposed process, CO_2 is recovered from the BFG and blended with H_2O, H_2, and CH_4-rich COG to reform methane. Optimized amounts of H_2O and CO_2 are used to adjust the $(H_2 - CO_2)/(CO + CO_2)$ molar ratio in order to maximize the amount of methanol that is produced. In addition, the desulphurization process was modified to enable the removal of sulfur compounds, especially thiophene, from the COG. The process design and simulation results reported herein were then used to determine any potential environmental and economic benefits. This research is based on off-gas conditions provided by ArcelorMittal Dofasco (AMD), Hamilton, Ontario. In order to determine which conditions are most desirable for this retrofit strategy, potential greenhouse gas reduction and economic benefits were analyzed. In particular, this analysis focused on the heating utility chosen for methane reformation prior to methanol synthesis. To this end, COG, BFG, and natural gas (NG) were compared. The results showed that using BFG/NG as a heating utility can produce greater economic gains, and that synthesizing COG + BFG to methanol results in greater economic and environmental gains than solely producing electricity (the status quo). Compared to current operating procedures, the proposed process could potentially increase net present values by up to $54 million. The carbon efficiency achieved was up to 72%. An additional 0.73 kg of CO_2 from BFG is needed for every 1 kg of MeOH produced. About 52% of feedstock energy is converted to MeOH, with another 33% recovered in the form of utilities. The exergy efficiency of the recommended version of the system is about 61%. The business case for converting CO_2 into methanol highly depends on the local electricity grid carbon intensity. For Ontario, it can reduce direct CO_2 emissions by 228 ktonne per year, and fix up to 246 ktonne CO_2 into methanol per year. In addition, analyses of location effects, CO_2 taxes, electricity prices, electricity carbon intensity, methanol prices, and income taxes indicated that MeOH production is highly recommended for Ontario, Mexico, the USA, and China applications. For USA, build MeOH plant is recommended for Finland, whether to do this retrofit or not is inconclusive. For Finland, the results are inconclusive, other strategies may be equally suitable. Aspen Plus Simulation files and other source code have been open-sourced and are available to the reader.

1. Introduction

In steel manufacturing, there are three major by-product off-gases: coke oven gas (COG), blast furnace gas (BFG), and basic oxygen furnace gas (BOFG). These gases mainly contain CH_4, CO, CO_2, H_2, and N_2. When these off-gases are combusted, large amounts of CO_2 are directly emitted to the atmosphere. Indeed, according to the World Steel Association [1], the average CO_2 emission rate is 1.9 tonnes for every tonne of crude steel cast. This figure is significant, as direct emissions from the steel industry contribute to about 7% of all anthropogenic CO_2 emissions [2]. However, CO_2 emissions can be reduced by improving the efficiency of the steelmaking process via different technologies or by upgrading how these off-gases are utilized.

For example, the Ultra-Low Carbon Dioxide Steelmaking (ULCOS) initiative aims to reduce CO_2 emissions by 50%, and its four selected breakthrough technologies have been achieving some progress towards this goal. The first of these technologies is a top-gas-recycling blast furnace that is equipped with a process designed to capture and store CO_2 (CCS). The CO_2 removed from the BFG is recycled as reduction agent, while pure O_2 is used as an oxidant, thus removing unwanted N_2

* Corresponding author.
E-mail address: tadams@mcmaster.ca (T.A. Adams II).

https://doi.org/10.1016/j.enconman.2019.112315
Received 20 August 2019; Received in revised form 13 November 2019; Accepted 14 November 2019
Available online 07 December 2019
0196-8904/

Nomenclature

CCA	Cost of CO_2 avoided ($/tonne$CO_2$e)
E	energy content (MJ/h)
Ex	exergy of stream (MJ/h)
NPV	Net present value ($M)
PPP	power purchasing parity (LCU/$)
R	exergy/energy ratio
TFCI	Total fixed capital investment ($M)
TPC	Total production cost ($M)
X	commodity price
η	energy efficiency
ψ	exergy efficiency
ω	carbon intensity (g/kwh)

Abbreviation

AMD	ArcelorMittal Dofasco
BFG	Blast furnace gas
BOFG	Basic oxygen furnace gas
CCPP	Combined cycle power plant
CCS	Carbon capture and storage
CDR	CO_2 dry reforming
COG	Coke oven gas
CSR	Combination of CO_2 and steam reforming
EAF	Electric arc furnace
HHV	Higher heating value
LCU	Local currency unit
LTWGS	Low temperature water-gas shift
MEA	Monoethanolamine
MeOH	Methanol
MTSR	Middle temperature sulfur removal
NCPO	Non-catalyst partial oxidization
NG	Natural gas
POX	Partial oxidization
PSA	Pressure swing adsorption
RWGS	Reverse water-gas shift
SMR	Steam methane reforming
TSA	Temperature swing adsorption
U	Heating utility
ULCOS	Ultra-Low Carbon Dioxide Steelmaking
VHSV	Volumetric hourly space velocity
WGS	Water-gas shift

from the air and making it easier to separate and capture CO_2 downstream. The second new technology is HIsarna, which also features a CCS process. This method consists of a reactor for coal preheating and partial pyrolysis, a melting cyclone for ore melting, and a smelter vessel for final ore reduction and iron production. This method requires the use of significantly less coal, and it is flexible insofar as it allows coal to be partially substituted with biomass, natural gas (NG), or even H_2. The third technology is ULCORED with CCS, which uses gases from the partial oxidation of NG instead of coal or coke. The direct reduction of iron ore is then transferred to the electric arc furnace (EAF) for steelmaking. Finally, the fourth technology is the low temperature (about 110 °C) iron electrowinning process. Instead of using coal or carbon compounds as reduction agents, this technology uses electrons and electrolytes to reduce the iron ore. Although electrowinning processes have the potential for zero CO_2 emissions, even without CCS, they are difficult to scale up.

These four options aim to reduce CO_2 emissions through new steelmaking technologies, but there is still a long way to go. The first three all require CCS, which can be practically impossible as steel refineries would need to be co-located near CO_2 sequestration sites and CO_2 pipelines would need to be constructed. The fourth technology though could achieve low CO_2 emissions without requiring CCS, but scaling-up to industrial size remains a major challenge. Hence this work focuses on other options for by-product off-gas valorization that are scalable, retrofittable, and do not require CCS. Throughout most of the steel manufacturing industry, COG is combusted for steam generation, which is subsequently used either for electricity generation using a low pressure steam turbine or as heat source. Deng and Adams [3] demonstrated that it is possible to retrofit the process by upgrading a COG-based low-pressure steam turbine system—which is a system present in many existing plants that combusts waste COG for steam generation—to allow it to function as a combined-cycle power plant (CCPP) to produce more electricity. Although this approach produces the same amount of direct CO_2 emissions, it can significantly reduce the amount of indirect CO_2 emissions because it requires less electricity to be purchased from the grid. Depending on the carbon intensity of the local power grid, this approach can reduce indirect CO_2 emissions by anywhere between 83.5 and 2221.1 gCO_2e/kgCOG. However, as the same authors have previously estimated [4], using COG to synthesize methanol (MeOH) instead of producing electricity may be an even more effective approach for reducing CO_2 emissions. In fact, researchers [5,6] are studying the potential of fixing CO_2 into MeOH as a method of CO_2 mitigation. Pérez-Fortes et al. [5] studied the techno-economic and environmental feasibility of using H_2 and CO_2 recovered from pulverized coal power plants as raw material for MeOH synthesis. Though it demonstrated a net CO_2 emission reduction, and has the potential of consuming 1.46 tonne CO_2/tonne MeOH, the high cost of the raw material prevents profitability. In this work, cheap raw materials are used instead, namely the by-products COG and BFG from steel manufacturing. It is a promising method with both CO_2 mitigation potential and profitability benefits for steel manufacturing. Therefore, this work will build upon these authors' previous work by conducting a techno-economic analysis of the COG + BFG to MeOH system.

A recent study by Kim et al. [7] examined the energy efficiency and economics of producing MeOH out of COG in a polygeneration system. In their study, MeOH was not the only expected product of the conventional COG to MeOH process; rather, heat, power, and MeOH were all proposed as being products of a single system. Significantly, the results showed that their approach increased energy efficiency from 38% to 53%. Furthermore, Kim et al. also analyzed MeOH's price trigger point. However, this analysis failed to demonstrate the effect of the carbon tax. Furthermore, their analysis underestimated desulphurization capital costs; they only considered H_2S removal due to the assumption that COG is purified and free of organic sulphur content. Moreover, it must be noted that, contrary to Kim et al.'s descriptions, the traditional COG to MeOH process does not separate H_2 out of COG via pressure swing adsorption (PSA) before steam methane reforming (SMR). The paper they cited [8] to support this claim actually says that the traditional H_2 recovery method (not for the purpose of producing MeOH out of COG) uses PSA to separate H_2 out of COG (A typical commercial method for converting COG to MeOH is shown in Fig. 1). As can be seen, instead of consuming CO_2, this polygeneration process actually produces significant amounts of direct and indirect CO_2 emissions [7]. In contrast, the method detailed in this paper aims to achieve negative net CO_2 emissions by fixing the CO_2 to the maximized production of MeOH. This approach has considerable potential, as one of the key findings of Kim et al.'s study was that it is more economically beneficial to produce a maximum amount of MeOH rather than produce more electricity and heat, but less MeOH.

Although some studies in the literature suggest a $(H_2\text{-}CO_2)/(CO + CO_2)$ molar ratio (S parameter) of 2.04 for MeOH production from syngas as the preferred ratio [9], this does not apply in our case.

For processes like the proposed one which uses COG and/or partial unreacted syngas recycling, the methanol synthesis reactor content can contain large amounts of N_2 and H_2O which have increased impacts on the balance-of-plant. For example, Hernández et al [10] suggested that S parameter should be within 1.75–2.5 with biogas as raw material when considering the balance-of-plant. Since COG is rich in H_2 and CH_4, its H_2/CO molar ratio is around 8, which is much higher than preferred ratio. Although coal gasification is traditionally the source of additional carbon, some researchers propose combusting half of COG for carbon source hence sacrifice the production of MeOH [11], this work proposed a process uses BFG as a carbon resource and maximize the production of MeOH. This idea is not new. Ghanbari et al. [12,13] proposed a polygeneration system in which BFG, COG, and BOFG are used as raw materials to generate electricity, dimethoxyethane, and/or MeOH. However, their work assumes that COG is sulphur free, which means that the desulphurization process was not considered in their economic analysis. Given that thiophene's stability makes it rather difficult to remove from COG, it is likely that Ghanbari et al.'s economic analysis underestimated the cost. Traditionally, methane in COG is converted to H_2 and CO via steam methane reforming. However, under this process, a reverse water-gas shift (RWGS) is required to adjust the S parameter due to high H_2 content. In addition, the MeOH synthesis process is very sulfur sensitive. The catalyst used in the MeOH synthesis process can very easily be deactivated by sulfur compounds, with sulfur tolerances as low as 0.1 ppmv [14,15]. The commercialized desulphurization method is a two-stage hydrodesulphurization process [16,17]. Wu [16] has also suggested using high-temperature non-catalyst partial oxidization (NCPO), as this approach is capable of cracking methane and thiophene at the same time. Evidence from this experiment has shown that with temperatures up to 900 °C, organic sulphur such as thiophene or CS_2 could be completely converted to H_2S with activated alumina in the presence of excess hydrogen [18]. In contrast, other researchers [19,20] have recently suggested using CO_2 dry reforming (CDR) directly for methane reforming, as this method could potentially shorten the COG to MeOH process by removing the RWGS process. Furthermore, due to the high temperature of CDR, thiophene could be converted to H_2S and then removed using a middle-temperature sulfur-removal process (MTSR). CDR is a promising technology due to its ability to convert methane, desulphurize thiophene, and adjust the S parameter; however, it requires high temperatures to mitigate the carbon deposition effect [20]. The combination of steam and CO_2 reforming (CSR) offers one viable method for increasing MeOH production and reducing the carbon deposition effect [21].

Therefore, we can conclude from the literature review that CSR is likely the best approach to create a process that reduces CO_2 emissions in steel refining and also does not require CCS. Moreover, the important individual components of the system are commercially available or technologically viable at scale, and so they can be used immediately without the need for further research to develop new materials or technologies (like electrowinning) at scale. These properties make it potentially the most commercially attractive option compared to the other four approaches because it has the fewest barriers to development. However, there are some key knowledge gaps in the literature that need to be overcome before the CSR approach can be commercialized, which we address in this work:

1. *Organic sulfur*. Some organic sulphur compounds present in COG present a major challenge for this process because they will poison downstream methanol synthesis catalysts. Thiophene is especially difficult to remove. All previous studies in the literature on COG to methanol have not considered this aspect of process synthesis. In this work, we specifically address this gap in thiophene considerations by presenting a novel desulfurization process that takes all of the forms of sulphur into account. Without this step, methanol synthesis could not be achieved practically.
2. *CO_2 utilization from BFG*. Previous studies looking at methanol synthesis through the CSR route have used CO_2 sources from outside the steel manufacturing process, such as coal combustion. However, our paper is the first to study the capture and utilization of CO_2 from elsewhere in the refinery, particularly from BFG. We also analyse how using BFG can impact the balance of plant because we are changing its makeup. This is important to address because sourcing large amounts of high-purity CO_2 from outside the refinery is not usually practical in most retrofit scenarios, and so this gap must be addressed to improve the chances of commercialization.
3. *Eco-Techno-economic analyses*. There is a major gap in the literature in terms of understanding and assessing the value of the CSR concept in terms of both economic and environmental objectives. In this work, we address this gap by a detailed analyses of a CSR retrofit, and we consider the application of this concept in five different geopolitical regions because the economics and environmental impacts are strongly influenced by the local electricity grid, local market prices, and local carbon taxes. This knowledge gap is important to address because the decision whether to retrofit a steel refinery with the COG + BFG to MeOH process depends highly on these issues.

2. Methodology and process description

There are six main steps involved in producing MeOH with COG and BFG as raw materials: first, recover the CO_2 from the BFG; second, remove the sulphur compounds from the COG; third, mix the purified COG and CO_2 and convert them to H_2 and CO in the CSR unit; fourth, adjust the S parameter and synthesize the MeOH; fifth, recycle most of the unconverted gas in order to increase production rate and purge the remaining unconverted gas to avoided inert gas accumulation; and finally, purify the MeOH. It is important to note that there may be overlap between these steps; for example, although it is responsible for removing thiophene from the COG, the CSR unit is also involved in converting methane. In addition, since the COG-sulphur-removal (mainly H_2S via Rectisol) process has already been commercialized, the related simulations have also been previously verified. As these simulations have shown, capital costs and operation costs are linearly related to the amount of H_2S that is removed [22]. Therefore, there is no further need to verify these simulations in this work. Furthermore, the kinetic equation used in the MeOH synthesis model has also been widely used and verified [23,24]. The only aspect of the CSR process that requires verification is the methane conversion process, which is detailed in Section 2.2.1. To enhance readability, the following discussion will be organized based on the six steps outlined above. The final proposed MeOH synthesis process is shown in Fig. 2.

2.1. Additional carbon resource from BFG

Among the three main off-gases produced in steel manufacturing, COG has the highest calorific value and a high H_2 content, while BFG has a low calorific value, but is generally produced in the largest volumes (about 14 times that of COG). The third off-gas, BOFG, is produced in batch mode and will not be considered in this particular paper. Traditional BFG consists of about 23 vol% CO_2 and 22 vol% CO, with the remainder mostly being made up of N_2. Detailed compositions of COG and BFG are shown in Table 1.

BFG is usually combusted to produce low-grade heat for use in the steel manufacturing process, which results in very high CO_2 emissions. The proposed method is based on the idea that, rather than using CO_2 from coal gasification, it may be more effective to recover and use the CO_2 from the BFG for COG methane reforming and S parameter adjustment. There are three main techniques for separating CO_2 from BFG: PSA, membrane separation, and monoethanolamine (MEA) absorption. A comparison of these techniques was conducted in order to identify the most suitable method for use in our proposed COG + BFG to MeOH process. This comparison process is detailed in the following sub-sections.

Table 1
COG and BFG compositions. * in PPMV. Source: [25,26].

	HHV (MJ/kg)	T (°C)	P (bar)	Composition (vol.%)									
				C_2H_2	CH_4	CO	CO_2	H_2	N_2	O_2	H_2S*	CS_2*	C_4H_4S*
COG	22.6–32.6	35	1.45	1.5–3.0	22–28	5.0–9.0	1.0–3.5	45–60	3.0–6.0	0.1–1.0	3420–4140	72–102	20–40
BFG	2.6	28	1.44	–	–	23.5	21.6	3.7	46.6	0.6	–	–	–

2.1.1. PSA technology to separate CO_2 from BFG

PSA, or vacuum pressure swing adsorption, is one approach that is routinely used to upgrade BFG. This method works by removing the CO_2 from the BFG and then recycling the CO_2-depleted BFG back into the blast furnace [27,28]. The Linde Group has developed a PSA system that features a unit capacity of up to 300,000 Nm^3/h and the ability to achieve a product purity of 95 vol% [29]. The pressure used in their PSA ranges from 7 bar to 35 bar, with a minimum CO_2 feed-gas content of around 10 vol%. According to the literature [30,31], the estimated cost of recovering the CO_2 from BFG containing 30–40% CO_2 and 10–20% N_2 is approximately $38/ton ($41.9/tonne) CO_2 (all dollar values in this paper are expressed in US $). This figure includes the cost of compressing the CO_2 to 120 bar. The cost in this study should be relatively lower than $38/ton ($41.9/tonne) CO_2 because the CO_2 recovered will be used directly for CSR without requiring compression. By comparison, the JFE steel developing PSA process, which uses zeolite as an adsorbent, costs $41/ton ($45.2 /tonne) CO_2 [32]. However, JFE's process is capable of purities as high as 99% [32].

2.1.2. MEA technology to separate CO_2 from BFG

Chemical absorption technology is the most mature commercialized technology for CO_2 capture, especially for NG and syngas sweetening. However, the two main drawbacks to these approaches are their high rate of equipment corrosion—specifically amine degradation by O_2, hence their higher absorbent makeup rates—and their high energy costs, which is due to the high temperature required for absorbent regeneration [31]. The regeneration of MEA during the stripper process usually accounts 70–80% of the CO_2 extraction process' entire operating costs [33]. Nonetheless, MEA has been demonstrated to be a good choice for separating CO_2 from gases [34], as it favors higher pressures and lower temperatures (35–50 °C) for CO_2 absorption and lower pressures and higher temperatures (around 120 °C) for CO_2 desorption in the stripper. MEA has also demonstrated high absorption and CO_2 production rates for BFG's specific gas composition, which contains higher concentrations of CO and H_2 than traditional post-combustion flue gas [35]. The use of MEA absorption can produce recovery rates ranging from 67.8% to 98.4% due to different concentrations of MEA in solution [36]. Separation costs are approximately $71.7/ton (ton = 2000 lbs) ($79.0/tonne, tonne = 1000 kg) CO_2 when using BFG containing 30–40% CO_2 [31].

2.1.3. Membrane technology to separate CO_2 from BFG

The main advantages of membrane technologies are their low capital investment, good space efficiency, ability to be scaled-up, minimal associated hardware, flexibility, and minimum utility requirements [37]. On the other hand, they also have a few disadvantages, including the need for clean feed (particulates and, in most cases, entrained liquids must be removed) [37], and a tradeoff between permeance and selectivity, which can make it difficult to achieve both high yield and high purity vis-à-vis the recovered products from a systems perspective. Permeance and selectivity are particularly important for BFG. A simulation based on a binary gas (ideal) mixture (CO_2 with one of BFG's other constituent gases, i.e., H_2, N_2, or CO) revealed an estimated total CO_2 recovery cost, including the cost of CO_2 compressed to 110 bar, ranging between 15.0 and 17.5€/tonnes CO_2 (18.1–21.1$/tonne CO_2) [32]. However, the cost of recovering CO_2 from the BFG real mixture was not documented in this paper [32]. A more relevant study by Ramírez-Santos et al.[38] found that a commercialized industrial-scale blast furnace flue gas membrane separation process (from MTR Inc.) was able to recover up to 90% CO_2 with 95% purity and a cost range of 23–33€/ton CO_2 (28.2–40.5$/tonne CO_2).

The above three methods have all been commercialized. For the purposes of our study, we assume that the cost estimates of the aforementioned studies are directly comparable (i.e., that they have similar enough assumptions, boundary definitions, conditions, and methods) and can be taken at face value such that the cost of CO_2 recovery increases in the order of membrane, PSA, and MEA recovery methods. Since the purity and recovery rate are not a primary focus in this study, the relatively higher purity obtainable via MEA or PSA is not necessary from a systems perspective. Hence, the membrane method was selected for CO_2 recovery, as it appeared to meet the process needs at the lowest cost when taking the reported costs in the literature at face value.

2.2. Methane reforming

2.2.1. Methane conversion process validation

In the third step of the process, the recovered CO_2 and the sweetened COG are fed into a methane-reforming reactor, which is placed inside a furnace and maintained at a high temperature. In the reformer, the methane in the COG is reformed into synthesis gas, and the thiophene and carbon sulfide in the COG is reformed into H_2S; this process has been demonstrated at this temperature at the lab scale by Zhang et al. [39] and Cao et al. [19]. Zhang et al. [39] used a CDR reactor, which is a continuous-flow quartz reactor that is packed with a coal char catalyst, and a mixed-gas residence time of 3 s. A platinum–rhodium thermocouple is installed in the centre of the catalyst bed to detect the temperature, which is increased up to a maximum temperature of 1200 °C using electricity. However, quartz-flow reactors are not traditionally used in industrial applications; rather, stainless steel furnaces are most commonly used in these settings. Specifically, stainless steel 310 is optimal for constructing furnaces due to its very high temperature rating and ability to withstand temperatures of up to 1100 °C. The CDR process has a higher methane conversion rate than NG + CO_2 dry reforming due to its high H_2 content. The proposed method enables CDR to achieve up to 100% methane reformation at high temperatures (1100 °C), without being significantly affected by the carbon formation phenomenon. Indeed, the conversion rate is much higher than the NG + CO_2 dry reforming method, which achieves nearly 90% methane conversion [40] but has a significant carbonation effect.

The CDR was modeled using the RGIBBS reactor module in Aspen Plus (which assumes both chemical and phase equilibria are achieved), with the results showing that the organic sulfur was almost entirely converted to H_2S. To validate the RGIBBS model, the simulation conditions were set to the exact same gas composition, operation pressure, and temperatures used in [41]. As such, the CDR experiment was conducted at temperatures of 800 °C, 900 °C, and 1000 °C with a Ni/γAl_2O_3 catalyst (with 5 wt% Ni) in a fixed-bed quartz reactor under atmospheric pressure. The volumetric hourly space velocity (VHSV) was 0.75 L gas per gram of catalyst per hour (L $g^{-1}h^{-1}$) and was adjusted by adding or reducing the amount of catalyst. The results showed that that the conversion rate was highest at the lowest used VHSV, which was 0.75 L $g^{-1}h^{-1}$. Thus, in this study, a VHSV of 0.75 L $g^{-1}h^{-1}$ will be used. Furthermore, the experiment defined the gas composition

Table 2
Validation of CDR simulation using RGIBBS model.

	Experiment conversion rate (%) [41]		RGIBBS conversion rate (%)		Error (%)	
	CO_2	CH_4	CO_2	CH_4	CO_2	CH_4
800 °C	95	85	93.2	88.25	−1.89	3.82
900 °C	96.9	95.6	98.32	94.838	1.465	−0.80
1000 °C	100	100	99.51	97.64	−0.49	−2.36

as 54% H_2, 23% CH_4, and 23% CO_2, but neglected other components, such as H_2O, N_2, C_2H_2, and C_2H_6, among others. Their experiment reached equilibrium within 60 min. As temperature increased, the equilibrium time decreased from around 70 min to 20 min. The comparison of the CH_4 and CO_2 conversion is detailed in Table 2.

As Table 2 indicates, the error between the experimental results and the Aspen Plus simulation results was less than 4% for all of the three different temperature cases. This is an acceptable level of error for a first stage techno-economic analysis. In addition, the CH_4 and CO_2 conversion rates from the RGIBBS model were slightly lower than those observed in the experiment, meaning the simulation results will be on the whole more conservative. The exceptions to this trend were the CH_4 conversion rate at 800 °C and the CO_2 conversion rate at 900 °C. Overall, the results suggest that RGIBBS can be used to simulate the CDR process.

Carbon deposition happens at low temperatures in the CDR process, and the CH_4 conversion rate is lower at the relatively low temperature of 800 °C. As such, some researchers might argue that CDR at high temperatures could achieve up to 100% CH_4 conversion. However, achieving these extremely high temperatures (1000 °C) would require more expensive reactor material. As such, Koo et al. [42] studied the viability of using combined CO_2 and steam reforming (CSR) of methane in COG. Their results demonstrated that high CH_4 conversion can be achieved by using a Ca-promoted 10Ni/$MgAl_2O_4$ catalyst for COG reforming, and that this approach offers superior coke formation resistance to those that do not use a Ca addition. Specifically, the CH_4 conversion rates ranged from 83.7% to 91.3% at 900 °C, with a fixed CH_4: H_2O: CO_2: H_2: CO: N_2 mole ratio of 1: 1.2: 0.4: 2: 0.3: 0.3, respectively. However, they did not study the composition effects on the conversion. Jang et al. [21] examined whether the CSR of methane effectively reduces carbon deposition when the mole ratio of (CO_2 + H_2O)/CH_4 is higher than 1.2 and Ni-MgO-$Ce_{0.8}Zr_{0.2}O_2$ is used as a catalyst. Their results indicated that the CH_4 conversion rate could reach up to 99.8% at 800 °C and a (CO_2 + H_2O)/CH_4 mole ratio of 2.9, which they confirmed using a Gibbs free energy minimization based equilibrium simulation (the same idea as an RGIBBS model in Aspen Plus). The RGIBBS model based CH_4 conversion rate in this work is 97.8% with (CO_2 + H_2O)/CH_4 mole ratio of 2.8 at 800 °C. This rate is a little bit lower than those documented in the literature due to the relatively lower (CO_2 + H_2O)/CH_4 mole ratio. Hence, the use of RGIBBS in Aspen Plus can be considered representative for CSR simulations.

2.2.2. CSR heating utility chosen

In this process, the CSR unit requires the largest amount of heat possible, and there are two obvious continuous energy sources that can be used to satisfy this need: BFG and COG. Another conventional material that can be used to generate heat is NG. In addition, the purge stream (PURGE1 in Fig. 2) could also be a potential heating utility given the considerable amount of energy it contains. However, since the pressure of the purge stream is very high, it was decided that it would be much better to generate power using a gas turbine instead of simply releasing the pressure without energy recovery and combusting it to provide heat for the CSR process. The LHV of the purge gas is 7515 kJ/m^3 at 15 °C, and its H_2 content is greater than 50 mol.%. This purge gas belongs to the classification of high hydrogen gaseous fuels which can be handled with existing commercial turbines [43]. such as the GE model 6B.03 gas turbine [44]. Hence this purge gas is designed to generate electricity in a gas turbine.

BFG has a very low heating value. Therefore, before using it as a heating utility for CSR, it is crucial to ensure that the BFG can be combusted at temperatures greater than 800 °C in order to heat the CSR. A study by Ji-Won Moon et al. [45] also demonstrated that BFG combustion could reach up to 1193 °C under stoichiometric conditions. For comparison purposes, BFG, COG, and NG combustion were simulated in Aspen Plus using the RSTOIC combustion model and 20% more air than in the stoichiometric condition is provided. Table 3 shows that combustion temperature of all three gases are very high. The BFG combustion temperature is higher in the present study due to the use of a slightly higher air/BFG input temperature and its slightly higher HHV. Nonetheless, it is safe to say that NG, BFG, and COG are qualified heating utility candidates for a CSR unit.

However, the use of each utility affects certain variables, such as the production rate of MeOH, the reduction of direct CO_2 emissions, and the operation costs. The following compares the relative benefits and drawbacks associated with each heating utility:

a. NG

Natural gas has a higher heating value than BFG and COG. If heating is provided by combusted NG, then H_2-rich COG can be used completely for methanol synthesis, while BFG could still be used further downstream in the steel manufacturing process to provide heat for things like galvanizing. In addition, the use of NG would achieve the highest level of MeOH production, as it would provide enough heat to convert all of the COG. The drawbacks to using NG as a heating source is that there would be utility costs and increased fossil fuel consumption associated with its use.

b. COG

COG has a moderate HHV. If the raw COG is free, the utility cost for this CSR unit would be zero. Although COG is originally used to generate electricity, the amount it generates is ultimately replaced by electricity purchased from the market. In this case, about 20% of the COG will be required to heat up the CSR unit, while the remaining 80% will be used for MeOH synthesis. The use of COG as a heating utility will result in the lowest CO_2 emissions of the three heating utilities (Table 3), and it also has the lowest capital costs, and utility costs due to the relatively smaller amounts required. However, the use of COG will reduce MeOH production by about 20% compared to NG/BFG. Since it is not obvious whether the use of COG as a heating utility provides significant benefits, further detailed calculations are computed in later sections.

c. BFG

BFG has a very low HHV compared to NG and COG, and it produces the highest CO_2 emissions when used for CSR heating. In addition, if BFG is used as a heating utility for CSR, it becomes necessary to find another heating source to replace it for downstream steel

Table 3
CSR utility comparison.

	High heating value (MJ/kg)	Temperature of combustion at 20% excess air (°C)	Price ($/GJ)	Flow rate (kg/kg COG)	CO_2 emission factor (kg/kJ)
BFG	2.64	1269	0	3.12	247.90
COG	32.53	1991	0	0.20	36.01
NG	55.57	1825	1.61	0.15	49.59

manufacturing. Therefore, any calculations of CO_2 emissions associated with BFG must also take into account the CO_2 produced by this additional heating source. For example, if NG is used in downstream to replace the BFG being used for CSR, the utility cost and MeOH production rate would be the same as just using NG for CSR in the first place. On the other hand, if BFG is considered a free heating source, and its use will not affect the downstream process, then the utility cost for the CSR unit would be zero. However, the use of BFG may lead to higher CO_2 emissions than the use of COG. Conversely, if BFG's replacement in the downstream process is less carbon intense and has a lower utility cost than NG, then BFG might be a cheaper and more environmental friendly option than NG.

Since it is not obvious whether COG is the best available heating utility, a thorough comparison is needed. This comparison is provided in Sections 3.2 and 3.3, wherein the system design and optimization, TCI, and TOPC, among other features, are compared in detail.

2.3. COG desulphurization

The conditions required for MeOH synthesis are stringent, especially regarding catalyst deactivation due to sulphur compounds. Thus, it is important to remove sulphur compounds from COG-converted syngas. Commercialized plants have found that, as a rule, the total concentration of sulphur compounds in syngas should be less than 0.1 ppmv [17,46]. In general, the COG emitted from coke ovens is high in H_2S, COS, CS_2, and C_4H_4S. Fortunately, there are numerous available technologies for removing H_2S, COS, and CS_2 that are already very mature. For example, physical adsorption, chemical absorption, and wet oxidization are commonly employed to remove H_2S. However, it is much more difficult to remove C_4H_4S using these methods, largely due to being a stable heterocyclic compound. As such, the commercial desulphurization process is very complicated. A representative commercialized method is shown in Fig. 1.

As Fig. 1 shows, the high H_2S content in the COG is mostly removed via wet desulphurization, which reduces the total sulphur content to less than 20 mg/m^3. Next, the COG is compressed to 2.5 MPa and heated up to 300 °C in order to conduct the first stage of hydrodesulfurization, which mainly converts organic sulphur compounds to H_2S. At the same time, unsaturated hydrocarbons (HC_A) are also converted to saturated hydrocarbons. After this stage, a catalyst is used to further reduce the converted H_2S to less than 1 mg/m^3. Following this step, a relatively more expensive catalyst is used to conduct a second stage of hydrodesulfurization wherein the remaining organic sulphur compounds (especially C_4H_4S) are converted to H_2S and unsaturated HC_A is converted to saturated HC_As. The CH_4 in the COG is then reformed into H_2 and CO using a catalyst partial oxidization unit, with oxygen added from air separation unit, and with CO_2 from coal gasification being added to the process to adjust the H_2/CO mole ratio. At

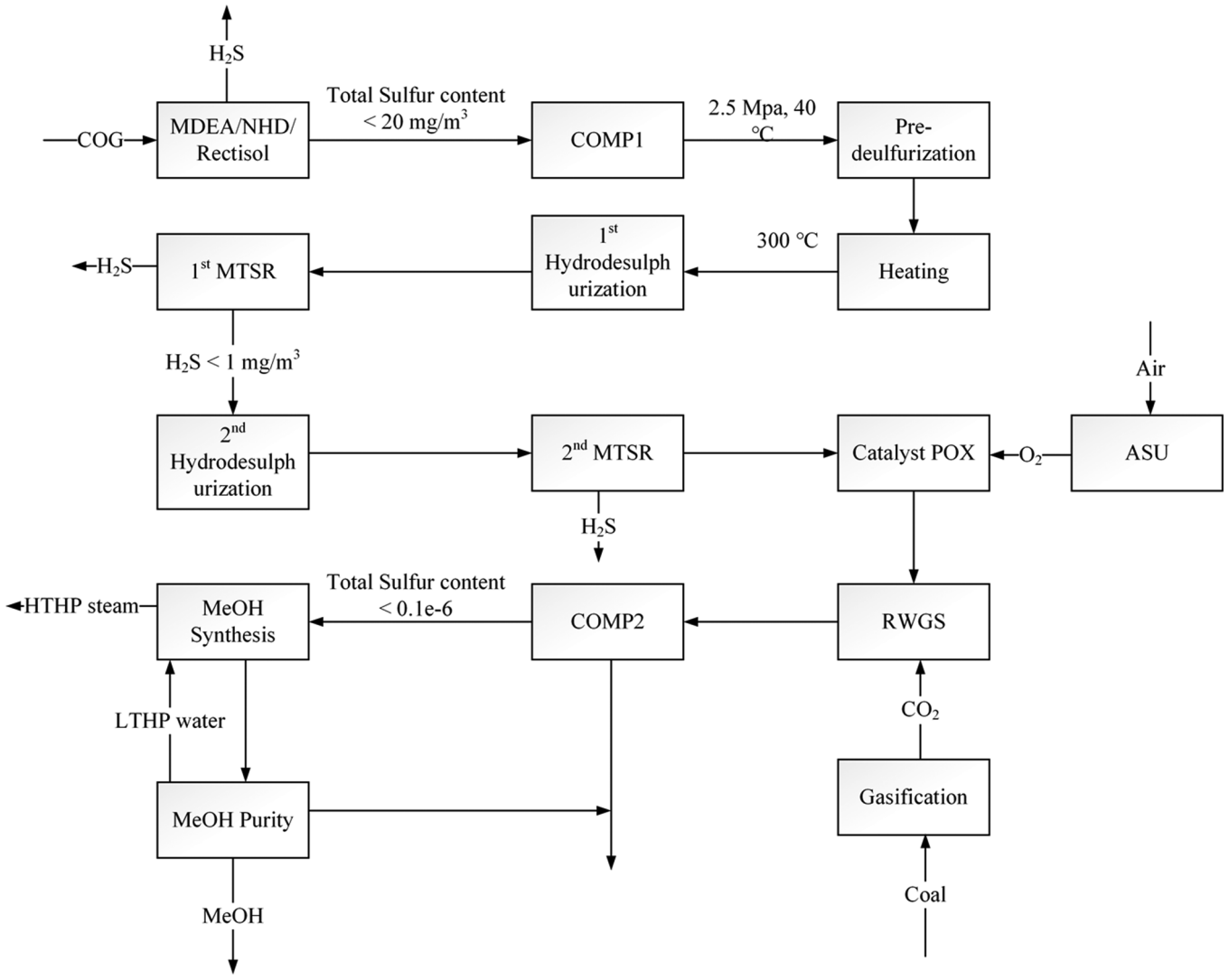

Fig. 1. Typical commercialized COG to MeOH process (Ref.: [17]).

last, the syngas is converted into MeOH using the typical catalyst, pressure, and temperature.

In this paper, a shorter and more effective desulphurization method is proposed, namely, CDR/CSR. This method allows both methane and organic sulphur compounds to be converted at the same time, while also minimizing the carbon formation/catalyst deactivation effect. As Bermúdez et al. [41] noted, Ni/γAl_2O_3 is used as a catalyst during CDR. Al_2O_3 is mainly used as a support, and the catalyst effect is mainly provided by the metal, in this case, Ni. Catalyst deactivation largely occurs due to carbon deposits created by methane decomposition, which can block the reactants' access to the active center, while another common cause is the sintering of nickel particles on the catalyst surface [41]. It is believed [47,48] that hydrocarbons dissociate to produce highly reactive monatomic carbon on the surface of the nickel-based catalyst; once the gasification of the monatomic carbon rate becomes lower than its formation, the excess monatomic carbon will grow and form nickel carbide (the growth of carbon whiskers). However, if the gas contains H_2S, carbon whiskers will not grow because the H_2S will adsorb in the nickel surface. Trimm [47] and Rostrup-Nielsen [48] both attempted to determine how much H_2S is needed to prevent carbon deposit. Each found that carbon formation remained close to the equilibrium point when (H_2S/H_2) was in the range of 0.5–27 $\times$ 10^{-6}, with few normal carbon whiskers being observed at H_2S/H_2 at 0.5 $\times$ 10^{-6}. Although carbon formation can be inhibited by increasing the H_2S content in the gas, excessive levels of H_2S can also deactivate the catalyst by occupying the hollow site on Ni.

While a different catalyst is used for CSR in this work, Ni is still responsible for producing the main catalyst effect. Consequently, it is reasonable to expect that H_2S will have the same effect on a Ni-MgO-$Ce_{0.8}Zr_{0.2}O_2$ catalyst. In addition, Rectisol is used to reduce the levels of the H_2S and COS (if any) in the COG to lower than 0.1 ppmv [49], while the organic sulphur in the sweet COG is converted to H_2S during the CSR with the nickel catalyst [50]. The H_2S/H_2 ratio is less than 27 $\times$ 10^{-6}, which means that catalyst deactivation can be restricted. Thus, this process enables hydrodesulfurization and the various stages of catalytic H_2S removal to be shortened to one middle-temperature Fe_2O_3 catalytic H_2S removal step after CSR. Furthermore, the MeOH production process can also be shortened, as shown in the design depicted in Fig. 2.

2.4. MeOH synthesis and composition effect

Various experiments using mature MeOH synthesis processes have shown that H_2O will be produced during MeOH synthesis when it is absent in the feed gas [51]. Conversely, the production or consumption of CO_2 is entirely dependent on the composition of the syngas [24]. In the case of the pure H_2 and CO used for methanol synthesis, water is needed to initiate the reaction and to enhance the methanol synthesis rate. However, the final MeOH production rate can be inhibited if the water content in the syngas is increased too much [52]. In contrast, the H_2O and the MeOH production rate increase alongside CO_2 [51]. It is commonly believed that a CO_2/H_2 mixture will facilitate a decent rate of MeOH synthesis, while a CO/H_2 mixture will produce a very slow rate of synthesis. Thus, either CO_2 or H_2O needs to be added to the syngas.

Water-gas shift (WGS) has proven to be an effective method for adjusting the S parameter in order to maximize MeOH production. There are two types of WGS: high-temperature WGS and low-temperature WGS [51]. The equilibrium constant for WGS increases as temperature decreases. In this paper, low-temperature WGS is needed to enhance the forward WGS, and a CO_2 removal step is also required to remove excess CO_2 in order to achieve an optimal R ratio [53]. However, the above-described CSR process allows the S parameter to be adjusted by changing the ratios among the CO_2, CH_4, and H_2O in the CSR unit, which eliminates the need for WGS.

2.5. System design and optimization

According to the above discussion, two design choices are possible: one that utilizes WGS/RWGS, as shown in Supplimentary material Fig. S1; and another that does not use WGS/RWGS, as shown in Fig. 2. Both designs are modeled in Aspen Plus v10 using the PR-BM physical property package for the gas-related units and STEAMNBS for all water streams/operations.

As described above, the additional CO_2 is recovered from BFG, and the COG is sweetened via the Rectisol process to remove H_2S. The mixture of sweet COG, steam, and CO_2 is then injected into the CSR reactor, where methane and organic sulphur are converted into H_2S. The syngas from CSR is in turn used to preheat the raw gas mixture. Next, the syngas, which is still at a high temperature, must be cooled to 300 °C for the H_2S removal process. At the same time, the high-pressure water, which is used as a coolant for methanol synthesis, has to be heated to 240 °C. Thus, there may be heat exchange between these two streams, though the heat from the syngas stream is not great enough to heat the coolant to the required temperature. To remedy this, additional heat can be provided by the flue gas that is emitted from the gas turbine. The reactor effluent is then cooled to 300 °C and used in the adsorbent-based MTSR process. A relatively cheaper catalyst (Fe_2O_3), which is a commercially used catalyst in the MTSR unit [17], is used to remove H_2S produced in CSR unit. Furthermore, a ZnO catalyst-based MTSR unit is also used to strictly control the H_2S content in the syngas to less than 0.1 PPMV [17]. The H_2S can be further processed to produce solid sulphur via a commercialized Claus process. However, this is outside the scope of this research.

The cleaned syngas is then cooled and fed into a multistage compressor to be compressed to 52 bar. The kinetic functions for MeOH synthesis are partial-pressure based [23]; that is, higher pressure is preferred to lower pressure. However, the use of pressures that are too high will result in high capital costs for the compressors and high utility costs for electricity. The pressure effect has been widely studied [23,24], and this study uses pressures that are consistent with those used in the commercialized MeOH synthesis process [23]. Furthermore, compressor efficiency (0.72) is set to the default, and air is used as the inter-stage coolant. After further temperature adjustment, the syngas is fed into the MeOH synthesis unit, which is temperature controlled using boiling water. The methanol synthesis unit (SYN-MEOH) uses the RPLUG model and features a reactor with co-current thermal fluid. A design spec specifies the input coolant (high-pressure water) amount, which restricts phase changes to those via evaporation in order to maintain the reactor's temperature. The MeOH synthesis kinetics were taken from Abrol et al. [23]. The product is cooled and flashed, with some of the unconverted gas being recycled back into the synthesis unit and the remainder being purged for combustion in order to avoid accumulation (such as the inert N_2). The purged gas (PURGE1) is combusted with air that has been compressed to an identical pressure, which is controlled by a calculator block. In addition, the gas turbine's maximum temperature is controlled to 1260 °C [3] by adding excess air. The heat in the flue gas out of gas turbine is used to heat the high-pressure water to be used in the boiling-water shell-and-tube MeOH synthesis unit. The product stream is further flashed and distilled to achieve the desired purity (97.8 wt%) via the design specs. The unconverted gas from the second flash drum is then combusted, and the heat from this combustion is used to generate steam utility. The key stream conditions of Fig. 2 are shown in Table 4.

After CO_2 recovery, the remaining BFG (Upgraded BFG: mostly CO and N_2) can be used for heat in downstream steel manufacturing processes in the same manner as the status quo without reducing its heating ability. Alternatively, the CO can also be extracted from the upgraded BFG via temperature swing adsorption (TSA). According to Ghanbari et al. [11], it is possible to extract up to 99 vol% of CO using this method. The high purity CO can then be recycled back into the blast furnace (BF) to help reduce the coke requirement. However, the

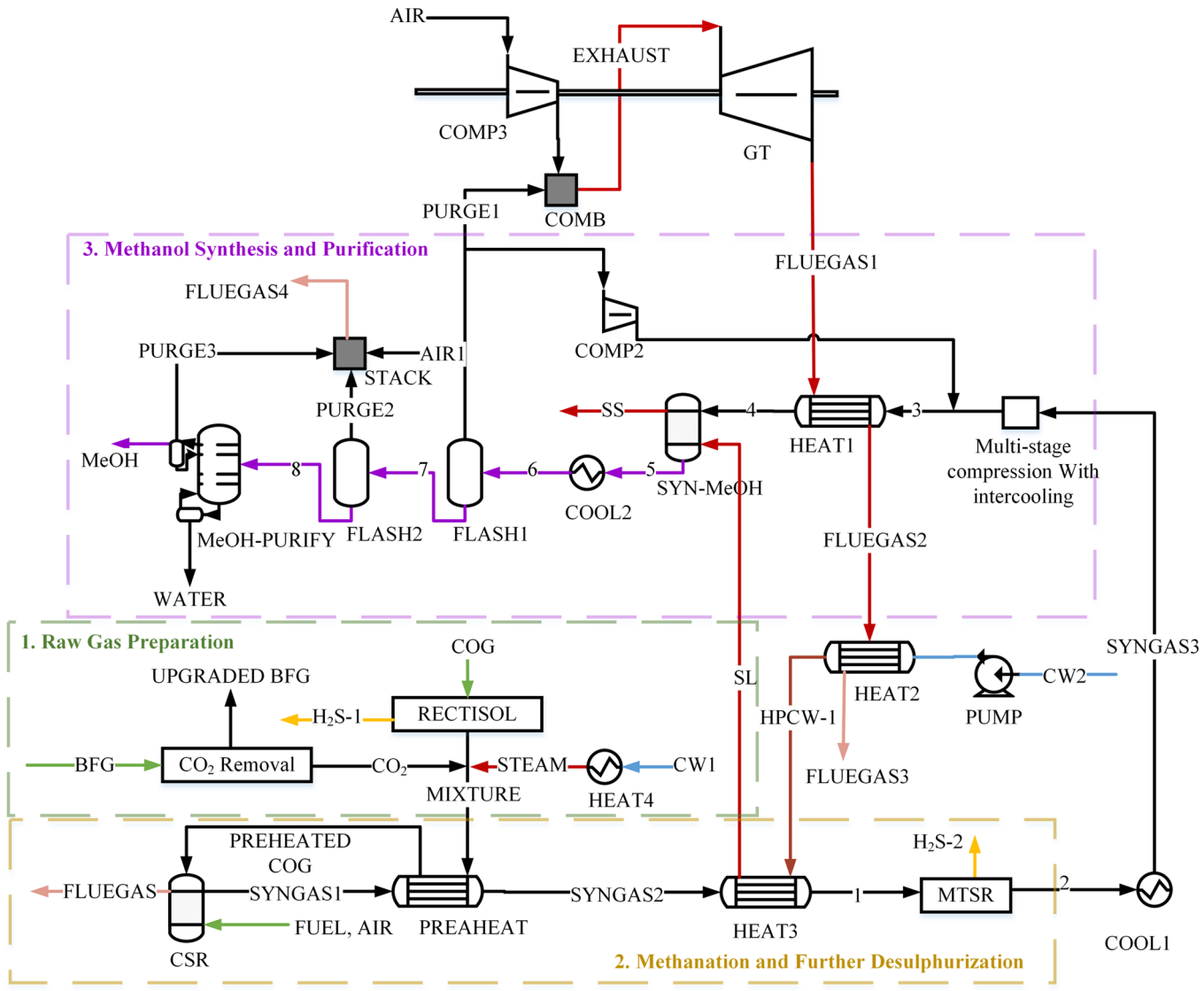

Fig. 2. The proposed COG + BFG to methanol process using CSR for methane reforming and organic sulfur handling.

Table 4
Key stream conditions based on Fig. 2 (NG/BFG used as heating utility for the CSR).

	Temperature (°C)	Pressure (bar)	Flow rate (kg/kg MeOH)	HHV (MJ/kg)
COG	35	1.45	0.75	39.07
CO_2	38	1.3	0.75	0
STEAM	220	1	0.47	0
SYNGAS1	800	1	1.97	17.69
4	240	51.95	6.46	13.88
PURGE1	45	49.90	0.56	11.98
EXHAUST	1260	49.4	4.54	0.23
FLUEGAS1	615	1.1	4.54	0
FLUEGAS4	150	1.05	0.16	0
PURGE2	43	1.01	0.06	5.85
FLUEGAS3	150	1.03	4.54	0
5	241	50.95	6.74	13.46
WATER	101	1.06	0.04	0
MEOH	56	1.01	1.02	23.57

investigation of these options is out of the scope of this study.

In order to maximize MeOH production, the system optimization tests considered the flow rates of the feed stream BFG and COG, the steam to the LTWGS (if applicable), the amount of CO_2 removed (if applicable), and the integration of heating and cooling utilities. The heating utility from flue gas and MeOH exothermic reaction are used to generate high-pressure steam, while the power generated by the gas turbine is internally used for compressors and pumps. Heat that cannot be used in this process is used to generate steam utilities with various pressure levels, with heating being provided by NG. However, as specified above, the proposed CSR unit can be heated using NG, COG, or BFG.

2.6. Economic analysis

All of the economic analysis in this work is based on a plant that is the size of AMD, which means that all of the COG produced at AMD's plant will be considered usable for MeOH production. A capital cost analysis was performed using Aspen Economics v10 (AEv10) and equipment cost equations taken from Seider et al. [54] and Towler et al. [55]. Associated utility costs were calculated using Aspen Economics v10. For the Rectisol process, fixed capital costs and operation costs are linearly correlated to amount of recovered H_2S [22]. Similarly, the CO_2 recovered from the BFG is linearly correlated to the total amount of CO_2 recovered. This relationship was detailed in Section 2.1. All costs are converted to 2018 via CEPCI. Detailed calculation methods for the equipment are shown in Table 5.

Table 5
Equipment purchase costs and calculation methods for all cases.

	Equipment type	Equipment cost ($)[1]	Reference
HEAT4	Fired heater for steam boiler	241,300	[54]
PREHEAT	HX-Plate and frame	450,200	[54]
DRYREFORM	Box type furnace, 316S	3,170,800	Aspen Economizer
HEAT3	Floating head shell and tube[2]	385,100	[55]
MTH2SR	Vertical, cs[3] pressure vessel	43,300	[55]
COOL1	Floating head shell and tube	184,900	[55]
COMP1	Centrifugal compressors[4]	11,249,400	[54,55]
PUMP1	Single-stage centrifugal pumps	11,800	[55]
HEAT2	Floating head shell and tube	41,500	[55]
HEAT1	Floating head shell and tube	44,800	[55]
SYN-MEOH	Fixed tube, float head, u-tube HX	2,689,400	Aspen Economizer
COOL2	Floating head shell and tube	503,600	[55]
FLASH1	Vertical, cs pressure vessel	73,200	[55]
COMP2	Centrifugal compressors + MOTOR	1,657,500	[55]
FLASH2	Vertical, cs pressure vessel	75,200	[55]
MEOH-PURIFY	Distillation column[5]	265,900	Aspen Economizer
STACK	Fired heaters for steam boiler	73,000	[54]
COMP3	Centrifugal compressors	9,414,200	[55]
GT	Gas turbine with a combustion chamber	11,117,900	Aspen Economizer

Note:
[1] The equipment costs are based on using NG as a utility, without WGS.
[2] Heat exchange area derived from Aspen Plus.
[3] cs means carbon steel.
[4] The compressor is driven partially by GT and partially by motor.
[5] The cost includs distillation tower, condenser, reboiler and reflux pump.

The catalysts used in the process are also estimated. Ni-MgO-$Ce_{0.8}Zr_{0.2}O_2$ was used as a catalyst in CSR [21] and was prepared using a one-step co-precipitation method. In accordance with Jang's study [21], stoichiometric quantities of $Ni(NO_3)_2{\cdot}6H_2O$, $Mg(NO_3)_2{\cdot}6H_2O$, $Ce(NO_3)_3{\cdot}6H_2O$, and ZrO_2 were purchased for catalyst preparation and sized up for their study.

The prices of the catalysts are based on the upper bounds of the listed prices. Most of the commercialized catalysts for MeOH synthesis have a lifetime of 1–5 years [56]. We assume that the copper-based catalyst has a lifetime of 1 year, and assume that the catalyst lifetime for the CSR unit is the same as MTH2SR, which is 4000 h due to sulfur deactivation. Since all of these catalysts can be regenerated after their lifetime, the initial catalyst costs can be included as part of the fixed capital cost.

Fe_2O_3 was used as a desulfurization catalyst for the middle-temperature sulfur-removal unit. This catalyst costs between $600 and $1000/tonne with a purity of 99.9% [61]. Supposing the size of the MTSR is linearly correlated to the amount of H_2S to be removed, the industrial sizes provided by Li [17] would require 158.4 m^3 of catalyst for 7.1 kg H_2S/h of sulfur removal. The catalyst lifetime is about 4000 hrs. In this study, the H_2S flow rate after CSR was about 13.7 kg H_2S/h. Hence, the catalyst occupied about 304.0 m^3. The catalyst density was 5.24 g/cm^3, assuming a bed voidage of 0.1. The total catalyst required for this process was about 2867.7 tonne/yr, with a maximum cost of 2.8 million $/yr.

The copper-based catalyst is most commonly used for the MeOH synthesis process. According to Lee [56], the composition of this catalyst is CuO: ZnO: Al_2O_3: SiO_2 at 55:36:8:1, respectively (page 90). The packed-bed particle density for this study was 1775 kg/m^3. The reactor was designed to be the same size as a commercialized 200 ktonne/year MeOH synthesis reactor, which contains 6713 tubes measuring 6 m in length and 3.8 cm (1.5 in.) in diameter [66]. Bed voidage is 0.1. Thus, the total reaction volume was 41.11 m^3 and the catalyst amount was 73 tonne. Industrial-grade prices for the catalysts are shown in Table 6.

The raw material and utility prices used are shown in the Table 7:

The purpose of this work is to consider a retrofit process to an existing steel manufacturing process. COG and BFG are considered free since they are internal streams. For the utilities used within the system, the Aspen Economizer default price are used.

The net present value (NPV) is used to measure the profitability of this MeOH process. A cash flow analysis is applied since this process has a saleable product of MeOH subject to taxation when gross income is positive. The depreciable percentage is calculated based on the total capital investment as suggested in Seider et al. [54], which is also provided in the supporting information Table S1. A conservative loan lifetime (10 years) is assumed considering our proposed process is new. Detailed cash flow parameters are shown in Table 8.

Total fixed capital investment (TFCI) is calculated based on the equipment purchase cost (Table 5) and the other associated costs, such as shipping, installation, construction, contractor engineering, piping, land, royalties, start-up, and depreciation. The associated costs are calculated using the same method that was documented in the Supporting Information of Deng and Adams' [3] previous paper. The same manner, total production cost (TPC), which includes operation costs, maintenance costs, operating overhead cost, property taxes and insurance, and general expenses, is also calculated using the method detailed by Deng and Adams [3]. For conveniences purposes, both TFCI and TPC calculation methods are shown in the Supplimentary material Tables S1 and S2 respectively.

In addition, for conservative purposes, for cases in which the amount of electricity generated is less than the amount of electricity generated by COG combustion in the status quo case, it is assumed that difference in electricity is purchased from the grid at the industrial electricity price and this is counted as a production cost. The net effect is that the COG + BFG to MeOH retrofit cases can result in either reduced or increased CO_2 emissions compared to status quo depending on the carbon intensity of the local power grid. Likewise, the carbon credit/tax is counted as either a cost (in the case of higher carbon emissions compared to the status quo) or revenue that is untaxable (in the case of lower carbon emissions). The tax loss carry forward is also applied in the cash flow calculation. The payback period is counted from the first year until cumulative present value is positive.

With regards to CO_2 emissions, the proposed MeOH synthesis process not only accounts for the amount of carbon in the COG, but it also accounts for the carbon footprint created by the utilities that are used in the process. The cost of CO_2 avoided (CCA) in this process is calculated in the same manner detailed in [3]. Briefly, CCA is calculated as the amount of NPV gained divided by amount of CO_2 emission reduced:

$$\mathrm{CCA} = \frac{NPV_{SQ} - NPV_{MeOH,without\ CO_2\ credit}}{(CO_2\ emission\ in\ status\ quo - CO_2\ emission\ in\ MeOH) \times plant\ lifetime}\ (\$/\mathrm{tonne}CO_2\mathrm{e}) \quad (1)$$

where subscripts SQ and MeOH indicate status quo and the proposed MeOH production process. The status quo is our comparison base, which meansNPV_{SQ}: =0.

3. Results and discussion

3.1. CSR based methane reforming and sulfur removal

The CSR units not only convert 97.8% methane, but they also converted organic sulfur into H_2S. The R ratio is adjusted via manipulate the CO_2, steam and methane molar ratio. The detailed results and analysis of CO_2 and steam injection molar ratio to MeOH production rate are shown in the following section. In addition, for transparency and reproducibility purposes, the Aspen Plus simulation files, MATLAB code, and Microsoft Excel files used in the analysis are uploaded in the Living Archive for Process Systems Engineering repository (http://PSEcommunity.org/LAPSE:2019.0444).

Table 6
Catalyst price from Alibaba used in all cases.

	Price	Unit	Purity (%)	Reference
$Ni(NO_3)_2{\cdot}6H_2O$	100–5000	$/tonne	98	[57]
$Mg(NO_3)_2{\cdot}6H_2O$	200–300	$/tonne	> 98	[58]
$Ce(NO_3)_3{\cdot}6H_2O$	3–20	$/kg	95.95–99.99	[59]
ZrO_2	20–50	$/kg	99.99	[60]
Fe_2O_3	600–1000	$/tonne	99.9	[61]
CuO	8950–9600	$/tonne	96–98	[62]
ZnO	150–300	$/tonne	95	[63]
Al_2O_3	660–830	$/tonne	93	[64]
SiO_2	1–100	$/ kg	99.8	[65]

Table 7
Base case raw material and utility prices.

	Price	Reference
COG ($/kg)	0	
BFG ($/kg)	0	
NG ($/GJ)	1.61	Aspen Economizer
Middle pressure steam generated ($/GJ)	2.19	Aspen Economizer
Cold water ($/$m^3$)	0.02	[54]
High pressure steam generated ($/GJ)	2.49	Aspen Economizer
Middle pressure steam ($/GJ)	2.2	Aspen Economizer

Table 8
Base case cash flow calculation parameters.

Parameters	Value	References
Depreciable percentage (%)	88	[54]
Depreciation time (years)	7	[54]
TFCI paid by loan (%)	50	[67]
TFCI paid by equity (%)	50	[67]
Loan interest rate (%)	9.5	[67]
Loan lifetime (years)	10	
Equity interest rate (%)	15	[3]
Plant lifetime (years)	30	[3]
Inflation rate (%)	2.5	[54]

3.2. Process comparison

First, the four different processes, namely, the COG utility based process without WGS (uCOG), the BFG utility based process without WGS (uBFG), the NG utility based process without WGS (uNG), and the NG utility based process with WGS (uNG-WGS), need to be optimized and compared under these conditions so that one can be selected. The processes were optimized by varying the purge gas ratio, and the feed flow rate of steam and CO_2 to CSR. The sensitivity analysis of the purge ratio was varied from 0.08 to 0.11. As the purge ratio decreases from a higher number, the efficieny and methanol production rate increase rapidly, until 0.1, as shown in Fig. 3. Below 0.1, these terms increase slowly, indicating significant diminishing returns. When the purge gas ratio is below 0.08, a massive system re-design is needed. The gas turbine which produces electricity from purge gas can no longer be used because the purge stream must be entirely used for heat needs in the balance-of-plant. This causes major design changes to the heat and power network, and is less efficient. Note that the heat exchanger network has to be redesigned at each point as complete system wide heat exchange and utilities are considered. Therefore, we chose the 0.1 inflection point as the optimum.

The optimized flow rates were determined using optimization and sensitivity analysis methods in Aspen Plus. Fig. 4 shows the relationship between the variables of steam and CO_2 flow rate, and how they affect the MeOH production flow rate.

Along with H_2O, CO_2 is a necessary carbon resource to reduce the H_2 ratio in the syngas. As described in Section 2.2.1, H_2O is added to help increase the conversion rate of CH_4. If H_2O is not added, solid carbon will form when the CO_2 flow rate is lower than 300 kmol/h. This carbonation will not only deactivate the catalyst, but it will also reduce the carbon efficiency (defined as the number carbon atoms in the methanol divided by the number of carbon atoms in the input stream BFG and COG). In the present system, no carbon deposition will occur with a higher H_2O mole flow rate, but the R ratio will be much higher than required 2.04. This means that maximum MeOH production will likely not be achieved by decreasing the CO_2 flow rate and increasing the H_2O flow rate. Hence, the CO_2 flow rate should be higher than 300 kmol/h. Fig. 4 shows that, as the CO_2 flow rate increases from 300 to 450 kmol/h, MeOH production increases and then decreases. When the H_2O flow rate is increased, MeOH production increases sharply to the maximum before slowly decreasing. The red point marked in the figure denotes the point of maximum MeOH production. At this point, the CSR reforming unit has an input gas content consisting of CH_4: CO_2: H_2O: CO: N_2: H_2: O_2: C_2H_2: HC_A with mole ratios of 1: 1.16: 1.8: 0.20: 0.41: 2.26: 0.03: 0.08: 0.17, respectively. Under this optimized CSR reforming condition, the mole fraction of the syngas mixture entering the MeOH synthesis unit (in stream SYNGAS6) contains 53.22%, 18.80%, 11.36%, and 0.23% of H_2, CO, CO_2, and H_2O, respectively. Furthermore, the H_2: CO mole ratio is 2.83, and the S parameter is equal to 1.39.

For the process that includes the WGS reaction and an additional CO_2 removal process (shown in Appendix Fig. 1), the optimized CH_4: CO_2: H_2O: CO: N_2: H_2: O_2: C_2H_2: CH_A mole ratio for the CSR unit is equal to 1: 1.33: 1.69: 0.20: 0.41: 2.26: 0.03: 0.08: 0.16, respectively. After the CO_2 has been removed from the SYN-MEOH input stream, the mole fraction of the main reaction components, H_2, CO, CO_2, and H_2O, is adjusted to 55.17%, 20.71%, 5.91%, and 0.10%, respectively, for MeOH synthesis. The H_2: CO mole ratio is decreased to 2.66, while the S parameter is increased from 1.39 to 1.85. The following economic analyses are based on the corresponding optimized conditions for maximizing MeOH production.

3.2.1. Energy conversion analysis and results

Throughout the process, waste thermal energy is recovered either by the generation of utility steam (which in our analysis is credited as a saleable by-product) or as electricity in a gas turbine. Some thermal energy is lost as heat in the flue gas or as pressure drop in the various process units. The overall Sankey energy flow diagram that represents the version of the COG + BFG to MeOH process using NG as the heating utility in the CSR without WGS (the uNG case) is shown in Fig. 5. The Sankey diagrams for the other process variants are quite similar and so are not shown. The uBFG and uCOG cases look very similar except the Natural Gas box is relabeled BFG for the uBFG case and the Natural Gas box does not exist for uCOG case, with similar numbers throughout.

For the uNG case, the total energy flow into the system is about 282 MW_{HHV}. This is the sum of the HHV of the COG and natural gas feeds, the electric power input from the grid, the energy associated with the captured CO_2 plus the HHV of the small amount of H_2 and CO captured

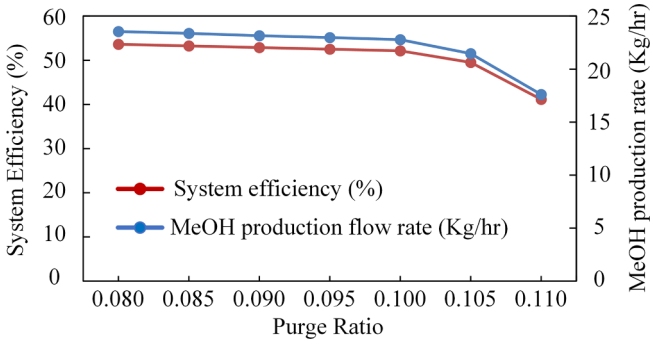

Fig. 3. Sensitivity analysis of purge ratio effect on system efficiency and methanol production rate.

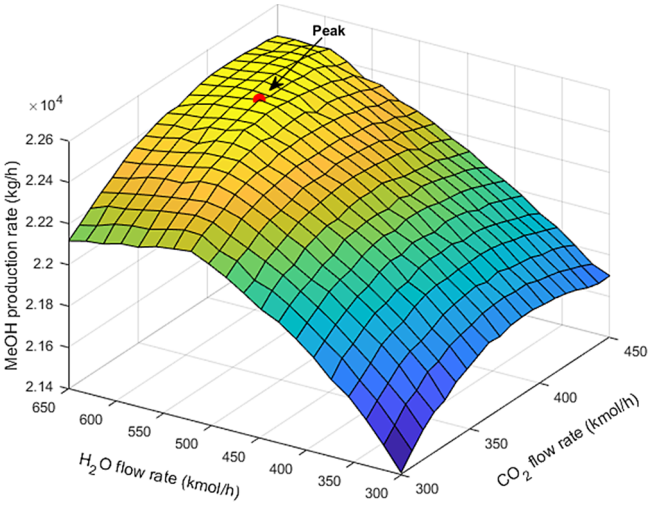

Fig. 4. Sensitivity analysis of MeOH production rate with CO_2 and H_2O flow rate changes: without WGS.

along with it, and the specific heat of feed water which is slightly above ambient temperature. About 86% of this energy is retained in the syngas after the syngas preparation step, which includes the sulphur removal, methane reforming, and syngas compression steps. Only a small amount of energy is lost during syngas preparation as waste in the form of pressure losses, thermal losses through the stack, or lost in the energy content of the captured sulfur (in an amount of about 2% of the system feed), with the majority (14.1 MW) of waste heat recovered as steam for sale.

In the MeOH synthesis process about 54% of the energy in the syngas is converted to methanol. Only a small amount of energy is lost during methanol purification, resulting in a total of 52% of the system input energy recovered in the form of methanol. The total waste energy, which includes the energy lost in the flue stack, pressure drops in the reactor and other system components, air cooling in the multistage compressor, and waste water, adds up to about 15% of the total system input. The remaining energy is captured and either converted to electricity and heat (which is recycled internally to the syngas preparation step) or saleable steam. A net 33% of the original energy content of the system input is converted to saleable steam.

In this paper we define the system efficiency for each system as the total amount of energy of the primary products divided by total amount of energy input into the system:

$$\eta_{sys} = \frac{E_{MeOH,HHV} + E_{Electricity,net\_output}}{E_{COG,HHV} + E_{NG,HHV} + E_{CO_2,HHV} + E_{electricity,input} + E_{H_2O,specific\ heat}} \quad (2)$$

In the above equation, η_{sys} denotes the system efficiency, $E_{MeOH,HHV}$ denotes the amount of energy fixed in product MeOH (HHV basis), and $E_{Electricity,net\_output}$ is the net electricity produced by the system. Note that $E_{Electricity,net\_output}$ is zero for all of the COG + BFG to MeOH systems in this work because they have a net consumption of electricity rather than production. It is included for comparison purposes with previously-published COG-to-electricity production systems as described in the next section. Also, note that $E_{CO_2,HHV}$ is small because only the small amounts of H_2 and CO captured along with CO_2 have a heating value.

We also define the thermal efficiency η_{therm}similarly:

$$\eta_{therm} = \frac{E_{MeOH,HHV} + E_{Electricity,net\_output} + E_{Steam}}{E_{COG,HHV} + E_{NG,HHV} + E_{CO_2,HHV} + E_{electricity,input} + E_{H_2O,specific\ heat}} \quad (3)$$

which includes the energy of the saleable steam produced as a by-product E_{Steam} (in terms of latent heat content). For example, in Fig. 5, η_{sys} is about 54 $\%_{HHV}$ and η_{therm} is about 87 $\%_{HHV}$.

We define the system exergy efficiency (ψ_{sys})and thermal exergy efficiency (ψ_{therm}) analogously:

$$\psi_{sys} = \frac{Ex_{MeOH} + Ex_{Electricity,net\_output}}{Ex_{COG} + Ex_{NG} + Ex_{CO_2} + Ex_{electricity,input} + E_{H_2O,specific\ heat}} \quad (4)$$

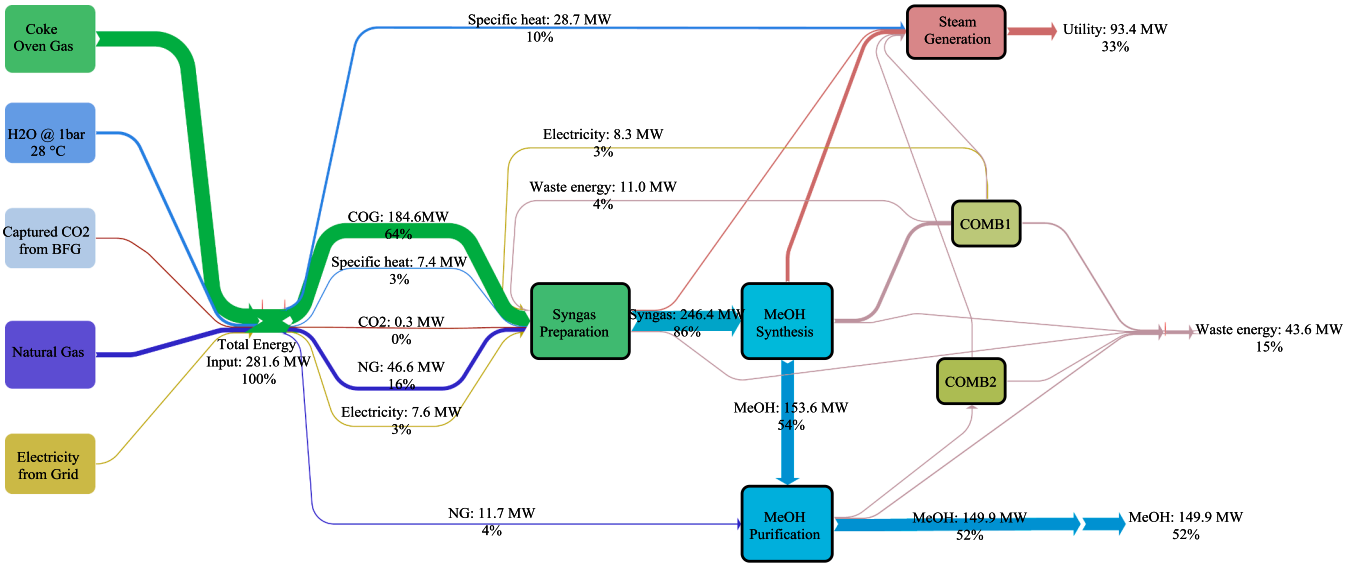

Fig. 5. Sankey energy flow diagram for the COG + BFG to MeOH process with NG as heating source (without WGS) for CSR. The stream energy values are the sum of the higher heating value of the stream (for combustible streams), electric power (for electricity streams), potential energy content (for streams above atmospheric pressure), and latent/specific heats above ambient temperature. The four left side boxes represent all the raw material and utility that goes into the system. The boxes in this diagram correspond with the process units in Fig. 2. Syngas Preparation includes: RECTISOL, CO2 Removal, CSR, PREHEAT, HEAT4, HEAT3, MTSR, COOL1, and Multi-stage compression with intercooling; MeOH Synthesis box includes: SYN-MeOH, COOL2, and FLASH1; MeOH Purification boxy includes: FLASH2 and MeOH-PURIFY; COMB1 box includes: COMB, COMP3, GT, HEAT1, and HEAT2; The COMB2 box includes: STACK; The Steam Generation box includes all of the process-to-process heat exchangers (or heat exchangers embedded within other equipment, such as the methanol synthesis reactor) for all the units and water that are used to produce steam, this includes: CW1, HEAT1, HEAT2, HEAT3, SYN-MeOH, COOL1, STACK, and COOL2.

$$\psi_{therm} = \frac{Ex_{MeOH} + Ex_{Electricity,net\_output} + Ex_{Steam}}{Ex_{COG} + Ex_{NG} + Ex_{CO_2} + Ex_{electricity,input} + E_{H_2O,specific\ heat}} \quad (5)$$

Where Ex is the exergy of the associated stream. For this analysis, we use the following molar chemical exergies relative to atmospheric conditions (25 °C, 1 bar, 60% relative humidity) [68]: methanol, 720 kJ/mol; hydrogen, 236.1 kJ/mol; methane, 831.2 kJ/mol; ethane, 1500 kJ/mol; carbon dioxide, 20 kJ/mol; carbon monoxide, 274.7 kJ/mol; liquid water, 1.3 kJ/mol; water vapour, 9.5 kJ/mol. For the steam and electricity streams, we use the exergy grade function approach:

$$Ex = E\ R \quad (6)$$

Where E is the energy content of the stream and R is the exergy grade function. For electricity, $R = 1$, and for steam pressures of 40 bar, and 9 bar, $R = 0.43$, and 0.33, respectively [69]. The resulting system exergy and thermal exergy efficiencies of the uNG process are 61.2% and 65.9%, respectively.

3.2.2. Economic analysis results

TPC, TFCI, NPV, payback period, and CO_2 emission reduction, among others, were selected as the main criteria to be considered when choosing among the four processes. As Fig. 6 shows, TPC consists of seven main components: utility, operations, maintenance, operation overhead, property taxes and insurance, depreciation, and general expenses. Maintenance costs were the greatest expense in all four cases, mainly due to high total depreciable costs. Furthermore, the process that uses BFG/NG as heating utility had a relatively higher utility cost than the process that uses COG. In addition, processes that incorporate WGS and CO_2 removal will have higher maintenance and utility costs than those that do not. Detailed percentages for each cost category are shown in Figs. S1–S4 in the Supplimentary material.

Table 9 provides a further detailed process comparison. As can be seen, NG/BFG is the most economical and environmental friendly heating utility, and it also produces the lowest CCA. Despite this, it should be noted that the MeOH production rate could be further increased by adding a WGS reaction process and fixing more CO_2 in the MeOH. However, the added capital costs and utility costs from such additions would outweigh the potential benefits of additional MeOH production in the Ontario case. Specifically, the inclusion of a WGS process would extend the time required to see a return on the initial investment.

The methanol production processes are considerably more efficient than their electricity counterparts, with a thermal efficiency of around 85%. The difference in efficiencies between the methanol synthesis process variants is slight. Using water gas shift gives a small efficiency improvement but it is not worth the higher cost. These efficiencies are much higher than the status quo case of 15% and the CCPP case of 31%. This indicates that the proposed methanol processes do a good job of capturing and using waste heat for a saleable product. From an exergy perspective, the process using uCOG as the CSR heating utility has the highest thermal exergy, while using uBFG/uNG as the CSR heating utility has the lowest thermal exergy among methanol synthesis process. Note that high exergy efficiency does not necessary correlate with a more profitable process. On the contrary, it seems that the lower the exergy efficiency, the higher the NPV for the MeOH production system. Similarly, a direct comparison between the methanol synthesis processes and electricity production ones is not very meaningful since they produce unlike products. Instead, the comparative value between processes comes down to economic and environmental terms.

A plant of this size can produce about 145–184 ktonne of MeOH annually. Table 9 assumes that BFG will be replaced by NG in the downstream process. If surplus BFG is used for MeOH production, the downstream process will not be affected, even without other energy resource replacement. Given this, the most economical method would be to use BFG as a heating utility in CSR.

Compared to uCOG/uNG/uBFG, the uNG-WGS process had a much higher MeOH conversion rate due to S parameter adjustment; however, the use of WGS and subsequent CO_2 removal led to the lowest carbon efficiency. Without WGS and CO_2 removal, COG + BFG to MeOH has a carbon efficiency of 72%.

The proposed methanol production process was compared with the traditional method (Fig. 1), a capacity of 200 ktonne/year of MeOH plant. The total equipment purchasing cost, COG flow rate, and actual MeOH production rate from the cited paper [70] are used. The total fixed capital investment and total production cost are calculated the same way as in this paper. The NPV analysis is converted to Ontario's situation using PPP for the purpose of comparison. The utility cost is assumed to be the same as our proposed process. The CO_2 emission reduction is unknown hence no CO_2 credit is accounted. The results shows (Table 9) that our proposed process has a much higher MeOH conversion rate (1.34 kg MeOH/kg COG) compared to the traditional process (0.98 kg MeOH/kg COG), and the traditional process has a longer payback period compared to our proposed process. Overall, the traditional process has lower NPV than our proposed uNG and uBFG process. MeOH production is more economical and environmentally friendly than both the status quo and the previously studied valorisation choice of CCPP. Despite requiring a fixed capital investment 2.8

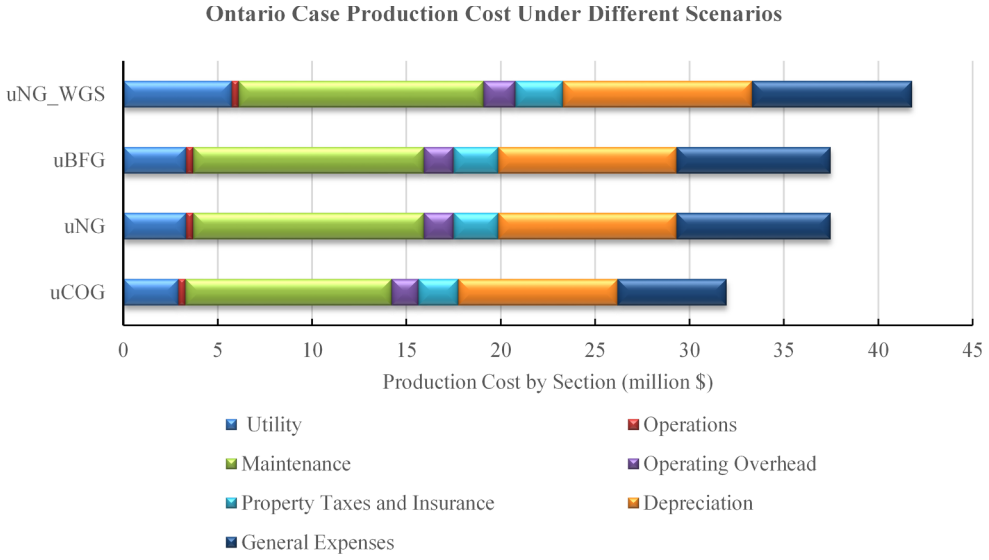

Fig. 6. TPC of AMD by section, Ontario case in 2018.

Table 9
System comparison (Ontario 2018) with base case parameters. See text for efficiency definitions.

	Status quo[a]	CCPP[b]	Proposed COG + BFG to MeOH				Typical COG to MeOH
			uCOG	uNG	uBFG[d]	uNG-WGS	
System efficiency (%HHV)	15	31	54.2	52.3	52.3	53.4	–
Thermal efficiency (%HHV)	15	31	87.5	84.8	84.8	86.0	–
System exergy efficiency (%)	–	36.7	61.9	61.2	61.2	62.4	–
Thermal exergy efficiency (%)	–	36.7	66.6	65.9	65.9	67.2	–
Additional CO_2 from BFG (kg CO_2/kg MeOH)			0.68	0.73	0.73	0.82	–
MeOH conversion rate (kg MeOH /kg COG)			1.09	1.34	1.34	1.38	0.98
Carbon efficiency (%)			74.4	72.0	72.0	69.8	–
MeOH production rate (ktonne/year)			145	179	179	184	197
Total Production cost rate ($/tonne MeOH)			260	246	246	264	294
Fixed capital investment ($M[e])	0.00	61	150	168	168	179	134
Total CO_2 emissions reduction (ktonne /year)	0.00	11	240	228	228	272	–
NPV ($M)	0.00	−7	−2	54	54	40	24
NPV without carbon credit ($M)	0.00	−9	−30	28	28	8	24
Payback period (years)	0.00	–	–	8	8	12	13
CCA ($/tonne$CO_2$e)		26.16	4.28	−4.24	−4.24	−0.99	–

[a] :Status quo represents the AMD, Ontario's present scenario. Which they combust COG by low pressure steam turbine to generate electricity;
[b] :CCPP is the scenario that proposed in the former paper [3]. It proposed a combined cycle power plant that uses the same amount of COG as status quo to produce electricity.
[d] :Assumes the use of BFG will be replaced by NG in the downstream process.
[e] :$M: million $.

times higher than CCPP, the production of MeOH can produce $54 million in NPV, the MeOH process consumes additional 246 ktonne of CO_2 and fix it into 179 ktonne of MeOH annually. It results in reducing 228 ktonne of CO_2 emissions compared to the status quo, which is a 4.56% gate-to-gate reduction in GHG emissions for the whole AMD plant (the plant emits about 5 million tonnes of CO_2 annually).

3.3. Application of this retrofit in other geological locations

As previously discussed, the process with uNG/uBFG as heating utility for CSR unit shows that a COG + BFG to MeOH retrofit could get an extra $54 million in NPV when applied in the Ontario case. However, the effects are different if applied in other countries. Electricity (x_{Elec}) prices, electricity carbon intensity (ω_{CO_2}), MeOH market price (x_{MeOH}), location effects (purchasing power parity, or PPP), carbon taxes (T_{CO_2}), and income tax are all factors which impact both the economic and environmental bottom lines. Table 10 lists the five locations examined in this study, along with their location-related parameters.

Since the results show that either using BFG or NG as heating utility will be the optimal choice for the COG + BFG to MeOH process, the location-based sensitivity analysis considers only cases which use NG as heating utility (the uNG design).

The results of the sensitivity analysis are summarized in Fig. 7, which shows "price maps" for each of the five geographical locations. The price maps show which retrofit decision results in the highest NPV: either the construction of the COG + BFG to Methanol retrofit, the construction of the COG combined cycle power plant retrofit, or the status quo (do nothing/business as usual case). Solid lines show the boundaries of these regions using current carbon taxes for that location, and the dashed lines show the boundaries of the regions when the carbon tax is increased to $50/tonne. For context, historical market conditions are shown as circles, in which the average industrial electricity price and methanol price for a given year are shown in 2018 dollars using the inflation rate in each location [85–89]. For example, in the Finland case, if the average lifetime electricity and methanol prices are the same as they were in 2016, it would be better not to build either retrofit (i.e. the status quo case, with NPV of zero, has the highest NPV). But if they were the same as in 2010, it would be best to build the CCPP plant, and if the prices were the same as they were in 2008, it would be best to build the COG + BFG to Methanol retrofit.

Fig. 7 shows that the carbon tax has bigger effect for locations that have high electricity carbon intensity such as USA, Mexico and China. For the Ontario case, when carbon tax increases from present carbon tax which is about 13.53 $/ton to 50 $/ton, the decision region boundaries shift down somewhat, with almost no shifting to the left because its power grid has such a low carbon intensity. The historical data shows that the prices experienced during 9 years out of the last 13 years in Ontario would be favorable for building the MeOH plant, and this number increases to 11/13 years when carbon tax increases. Table 11 also shows that the NPV of MeOH plant is $54 million while for CCPP plant is $3 million at recent (2018) conditions. Though the payback period is relatively long (8 years), the amount of CO_2 emission reduced is 228 ktonne/year. For the USA, when carbon tax increases to 50 $/tonne, the NPV_{CCPP} shifts from negative to positive due to the relatively high carbon intensity of the US grid. So in the USA case, the CCPP plant should only considered with much higher carbon taxes.

For Finland, only six historical points are located in the Build MeOH plant region, and all of those are very close to the decision boundary. The remaining historical points are well within the status quo and Build CPPP decision regions. Therefore, it is not clear what decision is better for them. For Mexico, most of the historical points are well within the Build Methanol boundary, although the CCPP plant becomes more favorable with higher carbon taxes. Either way though, both processes are quite profitable at current conditions. For China, both CCPP and Methanol retrofit options are profitable under current conditions while historically speaking, building the COG + BFG to MeOH plant is more profitable. CCPP becomes favorable under higher carbon taxes, and

Table 10
Location parameters at 2018.

	Ontario	USA	Finland	Mexico	China	Reference
PPP	1.25	1	0.88	9.04	3.54	[71]
Tax ($/tonne)	13.5	0	29.3	3.7	0	[3]
$X_{electricity}$ (LCU[a] ¢/kWh)	11.63	6.93	6.67	14.29	52.61	[72–77]
ω_{CO_2}(g/kWh)	40	588	285	856	1064	[3]
X_{MeOH} ($/tonne)	495.5	495.5	474.1	495.5	475.4	[78]
Income tax (%)	39.5	25.7	20	30	25	[79–83]
Exchange rate (LCD to USD)	1.30	1	0.85	19.23	6.62	[84]

[a] :LCU = local currency unit (Canada in CAD, USA in USD, Finland in Euro, Mexico in MXN, and China in RMB).

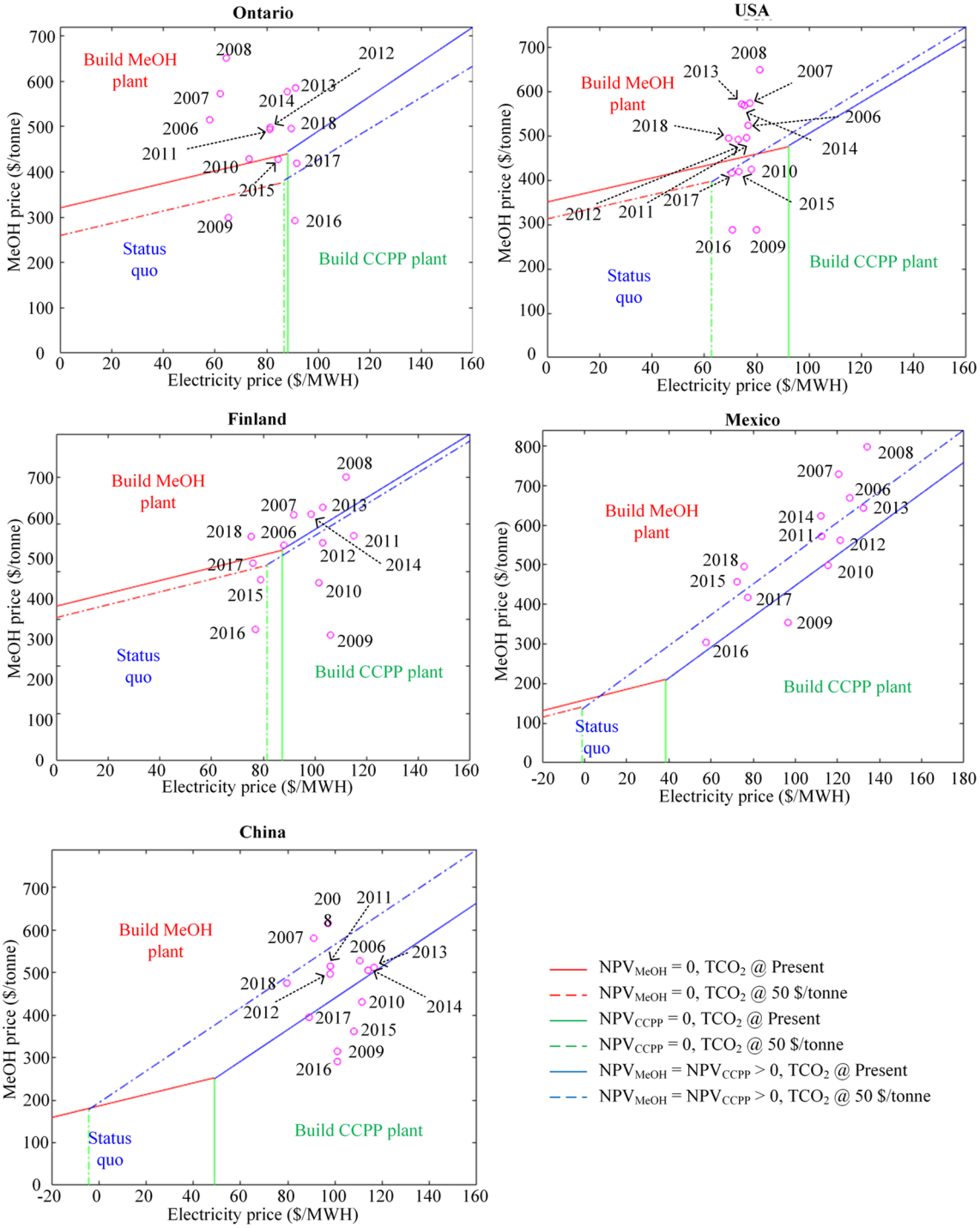

Fig. 7. Price maps showing which decision results in the highest NPV based on the market conditions (namely the lifetime average electricity and methanol prices) for each of the five geographical locations of interest. Solid lines are the boundaries that separate the regions using the current carbon taxes for that region. Dashed lines are the boundaries that separate the regions when the carbon tax is increased to $50/tonne. Circles are historical average market conditions by year, converted to 2018 dollars, and are provided for context.

because the COG + BFG to MeOH case for China actually reduce less CO_2 emissions than the status quo, CCPP is more environmental friendly for China. However, despite this, there is a very strong business case for the COG + BFG to Methanol retrofit under current market conditions in both Mexico and China.

In order to explore the uncertainties in other key parameters, a sensitivity analysis was conducted based on the Ontario 2018 uNG case (which we call the base case for sensitivity analysis purposes). Thirteen parameters were each individually varied from the base case, with all else kept at their base case values, resulting in the tornado plot shown in Fig. 8.

The tornado plot indicates that about ± 19% MeOH price change will cause more than 150% of NPV increase or decrease. About ± 1.5 percentage pointsof inflation rate change will cause about 30% NPV change. An electricity price change of ± 50 $/MWh will cause an NPV change of about 102%.The electricity carbon intensity and plant lifetime has relatively low impact on the NPV. (For example, when increasing plant lifetime from 30 to 40 years, the NPV almost stays the

Table 11
NPV of MeOH and CCPP of different locations based on location parameters in 2018.

	Ontario	USA	Finland	Mexico	China
Best variants of the COG + BFG to Methanol concept					
Payback period (yrs)	8	10	11	2	2
CO_2 reduction (ktonne/yr)	220	102	167	45	0.4
CCA ($/t$CO_2$e)	−4	−18	−2	−172	−16454
NPV ($M)	54	57	56	233	194
NPV without carbon credit ($M)	28	57	12	232	194
Best variants of the COG to CCPP concept					
Payback period (yrs)	22	–	–	2	2
CO_2 reduction (ktonne/yr)	11	165	80	241	299
CCA ($/t$CO_2$e)	−6	12	21	−12	−9
NPV ($M)	3	−57	−30	93	77
NPV without carbon credit ($M)	2	−57	−51	85	77
Final recommendations by region	Build MeOH Plant	Build MeOH Plant	Inconclusive	Build MeOH Plant	Build MeOH Plant

same). Debt-to-equity ratio changes of ± 43% will cause about 12% of NPV change. A carbon tax increase of 2.7 times will cause about 130% NPV increase. Overall, this indicates that market prices and inflation tends to have a much bigger impact on the bottom line than financing details and grid intensities.

4. Conclusions

We presented a new process for converting COG and BFG to methanol that also addresses the removal of thiophene and other sulfur compounds. The proposed process drastically shortens the desulphurization process through its use of high temperature (800 °C) CO_2 steam reforming with a Ni-MgO-$Ce_{0.8}Zr_{0.2}O_2$ catalyst. In addition, this method allows the molar ratio of (H_2-CO_2)/(CO + CO_2) to be adjusted by varying the CO_2 content and steam input flow rate. Significantly, the proposed COG + BFG to MeOH process is capable of producing about 179 ktonne of MeOH annually.

In terms of environmental impact, the proposed method consumes about 0.75 kg of COG and additional 0.73 kg of CO_2 from BFG per kg of methanol produced. In total, a carbon efficiency of 72% was achieved. Furthermore, the feasibility study conducted for AMD demonstrated that the process is efficient and results in a net CO_2 emissions reduction of 228 ktonne/yr (about 4.6% of net CO_2 emission reduction) and fix up to 246 ktonne of CO_2 into MeOH annually.

From an energy conversion aspect, CCPP has higher system efficiency than staus-quo, while COG + BFG to MeOH has the highest system efficiency among the three. About 52% of the energy in the feed is converted to MeOH, regardless of the configuration options. The energy thermal recovered in the MeOH production system (including utility recovery) adds up to 85%. This is because waste heat is very effectively used for medium pressure steam production. The thermal exergy efficiency of a processes does not necessarily have a positive correlation with thermal efficiency, and the highest thermal efficiency is not necessary the most profitable process either.

Economically, the TFCI for Ontario would be $150 million with COG as heating utility, and $168 million with BFG/NG as heating utility. TFCI is the highest when WGS is included, totalling $179 million. The payback period is 8 years when NG/BFG is used as a heating utility for Ontario. Compared to COG, BFG, and NG, the use of NG/BFG as a heating utility for CSR will yield the highest NPV for Ontario at $54 million. This is much higher than the NPV yielded by CCPP. Although the inclusion of WGS reaction produces the largest reduction in CO_2 emissions, it produces smaller economic gains compared to processes without WGS. Ultimately, the findings of this study indicate that under no circumstances is COG the best heating utility option. Compared to the status quo and the previously proposed CCPP process, generating MeOH via COG + BFG appears to be a superior option for Ontario from both an economic and environmental perspective.

Indeed, it would be highly profitable to apply this MeOH retrofit to plants Mexico and China. For Cases in which the CCA is strongly negative, such as Mexico, at 2018, it could be a potential suitable CO_2 mitigation method without requiring much policy incentives. Applications in Ontario and USA are also promising, although to a lesser degree. However, it is not recommended that Finland invest in this retrofit due to its long payback period. Ultimately, though, because of the uncertainties in future market conditions and carbon taxes (which were shown to be some of the largest influences on profitability), it is not strictly clear which design choices will be the best in any given scenario.

Although this analysis focused on steel manufacturing, there are

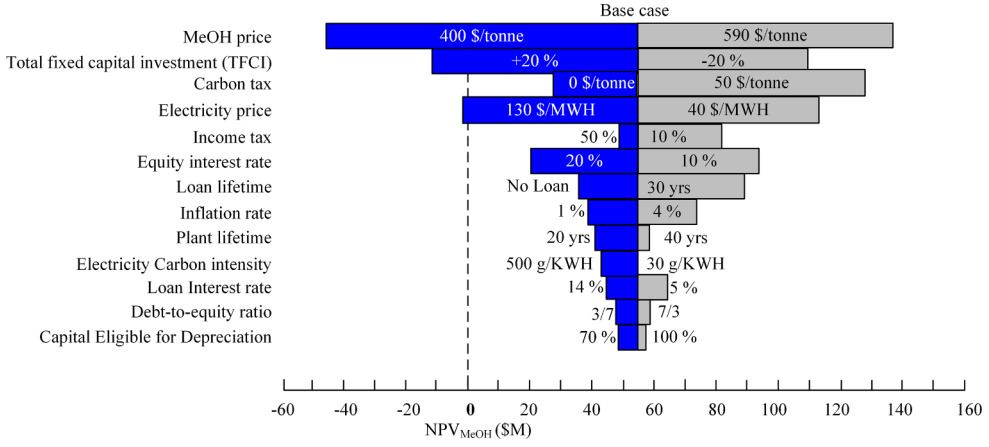

Fig. 8. NPV_{MeOH} changes with uncertainties vary in certain ranges based on 2018 Ontario case.

other applications of this proposed COG + BFG to MeOH process. For example, there exist many plants which make coke from coal for purposes other than steel making. Their by-product COG utilization could also follow this retrofit route, except that the CO_2 input source might be captured CO_2 from a power plant or a cement making plant. Further, if one considers MeOH as a CO_2 storage mechanism (for example, converting the methanol into a stable solid product instead of a fuel), this route provides a potential CO_2 capture and storage mechanism in and of itself.

CRediT authorship contribution statement

Lingyan Deng: Conceptualization, Methodology, Software, Formal analysis, Investigation, Writing - original draft, Visualization. **Thomas A. Adams II:** Writing - review & editing, Supervision, Funding acquisition.

Declaration of Competing Interest

The authors declare that they have no known competing financial interests or personal relationships that could have appeared to influence the work reported in this paper.

Acknowledgements

This work was supported by the Ontario Research Fund-Research Excellence Project [RE09-058], and McMaster Advanced Control Consortium, McMaster University, Canada. We are grateful for their funding. The collaborations and data from Ian Shaw and David Meredith (AMD) and helpful conversations with Dr. Farhang Farahani (McMaster) are gratefully acknowledged.

Appendix A. Supplementary data

Supplementary data to this article can be found online at https://doi.org/10.1016/j.enconman.2019.112315.

References

[1] Worldsteel. Sustainable Steel: Indicators 2017 and the future, https://www.worldsteel.org/en/dam/jcr:938bf06f-764e-441c-874a-057932e06dba/Sust_Steel_2017_update0408.pdf; 2017 [accessed March, 2018].
[2] A. Purvis. Steel and CO2 – a global perspecive, IEA wordshop 20th, https://www.iea.org/media/workshops/2017/ieaglobalironsteeltechnologyroadmap/ISTRM_Session1_A._PURVIS_241117.pdf; 2017 [accessed March, 2018].
[3] Deng LY, Adams II TA. Optimization of coke oven gas desulphurization and combined cycle power plant electricity generation. Ind Eng Chem Res 2018;57(38):12816–28. https://doi.org/10.1021/acs.iecr.8b00246.
[4] Deng LY, Adams TA. Methanol production from coke oven gas and blast furnace gas. Comput Aided Chem Eng 2018;44:163–8. https://doi.org/10.1016/B978-0-444-64241-7.50022-7. Elsevier.
[5] Pérez-Fortes Mar, et al. Methanol synthesis using captured CO_2 as raw material: techno-economic and environmental assessment. Appl Energy 2016;161:718–32. https://doi.org/10.1016/j.apenergy.2015.07.067.
[6] Bocin-Dumitriu A, Pérez-Fortes M, Tzimas E, Sveen T. Carbon capture and utilisation workshop. Background and proceedings. Scientific and policy report by the Joint Research Centre of the European Commission, European Commission, European Union, http://publications.jrc.ec.europa.eu/repository/handle/JRC86324; 2013 [accessed June 16th, 2019].
[7] Kim SH, Kim MS, Kim YT, Kwak GJ, Kim JY. Techno-economic evaluation of the integrated polygeneration system of methanol, power and heat production from coke oven gas. Energy Convers Manage 2019;182:240–50. https://doi.org/10.1016/j.enconman.2018.12.037.
[8] Wu Xiang, Rong Wu, Sufang Wu. Kinetic study of reactive sorption-enhanced reforming of coke oven gas for hydrogen production. J Nat Gas Sci Eng 2015;27:1432–7. https://doi.org/10.1016/j.jngse.2015.10.007.
[9] Bermúdez JM, Ferrera-Lorenzo N, Luque S, Arenillas A, Menéndez JA. New process for producing methanol from coke oven gas by means of CO_2 reforming. comparison with conventional process. Fuel Process Technol 2013;115:215–21. https://doi.org/10.1016/j.fuproc.2013.06.006.
[10] Hernández Borja, Martín Mariano. Optimal process operation for biogas reforming to methanol: effects of dry reforming and biogas composition. Ind Eng Chem Res 2016. https://doi.org/10.1021/acs.iecr.6b01044.
[11] Yi Qun, Gong Min-Hui, Huang Yi, Feng Jie, Hao Yan-Hong, Zhang Ji-Long, Li Wen-Ying. Process development of coke oven gas to methanol integrated with CO2 recycle for satisfactory techno-economic performance. Energy 2016;112:618–28. https://doi.org/10.1016/j.energy.2016.06.111.
[12] Ghanbari H, Saxén H, Grossmann IE. Optimal design and operation of a steel plant integrated with a polygeneration system. AIChE J 2013;59(10):3659–70. https://doi.org/10.1002/aic.14098.
[13] Ghanbari H, Pettersson F, Saxen H. Sustainable development of primary steelmaking under novel blast furnace operation and injection of different reducing agents. Chem Eng Sci 2015;129:208–22. https://doi.org/10.1016/j.ces.2015.01.069.
[14] Zhao ZC, Ding YY. Desulphurization and purification technology for coke oven gas synthesis into syngas. Ind Technol 2015;20:40.
[15] Chen AP. Analysis on the purification technology of coke-oven gas to methanol. Sci-Tech Inf Dev Econ 2009;29:214–5.
[16] Wu CM. Study on methanol production technology from coke oven gas. Gas Heat. 2008;1:36–42.
[17] Li JN. 焦炉煤气制甲醇生产中干法脱硫工艺的改进. The process improvements of dry desulphurization in the production of coke-oven gas-to-methanol. Sci-Tech Inf Dev Econ 2009;19(16):180–2. http://www.cqvip.com/qk/97443x/200916/30868207.html.
[18] Field E, Oldach CS. Conversion of organic sulfur to hydrogen sulphide for analyisis. Ind Eng Chem, Anal Ed 1946;18:668. https://doi.org/10.1021/i560159a004.
[19] Cao HC, Bei KL, PW, Zhang GZ, Zhang YF. 焦炉煤气制甲醇工艺中的净化脱硫探讨. Discussion of the Desulphurization Process for Coke Oven Gas Synthesis to Methanol. Symposium on Methanol and Its Downstream Products New Technologies. 2007. https://wenku.baidu.com/view/b5daee0abed5b9f3f90f1ccf.html.
[20] Bermúdez JM, Fidalgo B, Arenillas A, Menéndez JA. Dry reforming of coke oven gases over activated carbon to produce syngas for methanol synthesis. Fuel 2010;89(10):2897–902. https://doi.org/10.1016/j.fuel.2010.01.014.
[21] Jang Won-Jun, Jeong Dae-Woon, Shim Jae-Oh, Kim Hak-Min, Roh Hyun-Seog, Son In Hyuk, Lee Seung Jae. Combined steam and carbon dioxide reforming of methane and side reactions: thermodynamic equilibrium analysis and experimental application. Appl Energy 2016;173:80–91. https://doi.org/10.1016/j.apenergy.2016.04.006.
[22] Dalrymple Dennis A, Trofe Timothy W, Evans James M. Liquid redox sulfur recovery options, costs, and environmental considerations. Environ Prog 1989;8(4):217–22. https://doi.org/10.1002/ep.3300080412.
[23] Abrol S, Hilton CM. Modeling, simulation and advanced control of methanol production from variable synthesis gas feed. Comput Chem Eng 2012;40:117–31. https://doi.org/10.1016/j.compchemeng.2012.02.005.
[24] Lee Sunggyu. Methanol synthesis technology. Florida: CRC Press. Inc.; 1989.
[25] Yang ZB, Ding WZh, Zhang YY, Lu XG, Zhang YW, Shen PJ. Catalytic partial oxidation of coke oven gas to syngas in an oxygen permeation membrane reactor combined with NiO/MgO catalyst. Int J Hydrogen Energy 2010;35(12):6239–47. https://doi.org/10.1016/j.ijhydene.2009.07.103.
[26] Uribe-Soto W, Portha JF, Commenge JM, Falk L. A review of thermochemical processes and technologies to use steelworks off-gases. Renew Sustain Energy Rev 2017;74:809–23. https://doi.org/10.1016/j.rser.2017.03.008.
[27] Qiao Z, She XF, Wang JS, Xue QG. Current State of Gas Resource Utilization and Countermeasures of Energy Saving for Integrated Iron and Steel Works in China. Adv Mater Res 2014;849:165–9. https://doi.org/10.4028/www.scientific.net/AMR.849.165. Trans Tech Publications.
[28] Hell H, Helle M, Saxen H, Pettersson F. Optimization of top gas recycling conditions under high oxygen enrichment in the blast furnace. ISIJ Int 2010;50(7):931–8. https://doi.org/10.2355/isijinternational.50.931.
[29] The Linde Group. Carbon dioxide recovery and removal. https://www.linde-engineering.com/en/process_plants/adsorption-and-membrane-plants/carbon_dioxide_recovery_removal/index.html; 2018 [accessed Nov., 2018].
[30] Kim H, Lee J, Lee S, Lee IB, Park J, Han J. Economic process design for separation of CO2 from the off-gas in ironmaking and steelmaking plants. Energy 2015;88:756–64. https://doi.org/10.1016/j.energy.2015.05.093.
[31] Ramírez-Santos ÁA, Castel C, Favre E. A review of gas separation technologies within emission reduction programs in the iron and steel sector: current application and development perspectives. Sep Purif Technol 2018. https://doi.org/10.1016/j.seppur.2017.11.063.
[32] Lie JA, Vassbotn T, Hagg MB, Grainger D, Kim TJ, Mejdell T. Optimization of a membrane process for CO2 capture in the steelmaking industry. Int J Greenhouse Gas Control 2007;1(3):309–17. https://doi.org/10.1016/S1750-5836(07)00069-2.
[33] Tobiesen FA, Svendsen HF, Mejdell T. Modeling of blast furnace CO2 capture using amine absorbents. Ind Eng Chem Res 2007;46(23):7811–9. https://doi.org/10.1021/ie061556j.
[34] Aaron D, Tsouris C. Separation of CO2 from flue gas: a review. Sep Sci Technol 2005;40(1-3):321–48. https://doi.org/10.1081/SS-200042244.
[35] Goto K, Okabe H, Chowdhury FA, Shimizu S, Fujioka Y, Onoda M. Development of novel absorbents for CO2 capture from blast furnace gas. Int J Greenhouse Gas Control 2011;5(5):1214–9. https://doi.org/10.1016/j.ijggc.2011.06.006.
[36] Choi WJ, Seo JB, Jang SY, Jung JH, Oh KJ. Removal characteristics of CO2 using aqueous MEA/AMP solutions in the absorption and regeneration process. J Environ Sci 2009;21(7):907–13. https://doi.org/10.1016/S1001-0742(08)62360-8.
[37] Kohl AL, Nielsen R. Gas Purification. Elsevier; 1997.
[38] Ramírez-Santos ÁA, Castel C, Favre E. Utilization of blast furnace flue gas: opportunities and challenges for polymeric membrane gas separation processes. J Membr Sci 2017;526:191–204. https://doi.org/10.1016/j.memsci.2016.12.033.
[39] Zhang G, Dong Y, Feng M, Zhang Y, Zhao W, Cao HC. CO2 reforming of CH4 in coke oven gas to syngas over coal char catalyst. Chem Eng J 2010;156(3):519–23.

https://doi.org/10.1016/j.cej.2009.04.005.
[40] Hoseinzade L, Adams II TA. Modeling and simulation of an integrated steam reforming and nuclear heat system. Int J Hydrogen Energy 2017;42(39):25048–62. https://doi.org/10.1016/j.ijhydene.2017.08.031.
[41] Bermúdez JM, Fidalgo B, Arenillas A, Menerdez JA. CO2 reforming of coke oven gas over a Ni/γAl2O3 catalyst to produce syngas for methanol synthesis. Fuel 2012;94:197–203. https://doi.org/10.1016/j.fuel.2011.10.033.
[42] Koo KY, Lee JH, Jung UH, Kim SH, Yoon WL. Combined H_2O and CO_2 reforming of coke oven gas over Ca-promoted Ni/$MgAl_2O_4$ catalyst for direct reduced iron production. Fuel 2015;153:303–9. https://doi.org/10.1016/j.fuel.2015.03.007.
[43] Jones R, Goldmeer J, Monatti B, 2011. Addressing Gas Turbine Fuel Flexibility, GE Energy Report GER4601 rev. B, October 29, 2012, http://www.ge-energy.com/content/multimedia/_files/downloads/Fuel%20Flexibility%20White%20Paper.pdf.
[44] 6B.03 Gas Turbine. GE power. https://www.ge.com/power/gas/gas-turbines/6b-03. 2019.
[45] Moon JW, Kim SJ, Sasaki Y. Effect of preheated top gas and air on blast furnace top gas combustion. ISIJ Int 2014;54(1):63–71. https://doi.org/10.2355/isijinternational.54.63.
[46] Chen AP. 焦炉煤气制甲醇净化工艺分析. Analysis on the purification technology of coke-oven gas to methanol. Sci-Tech Inf Dev Econ 2009;19(21):214–6. http://xueshu.baidu.com/usercenter/paper/show?paperid=2c07ae613090ec50d5710fca569cbfd0&site=xueshu_se.
[47] Trimm DL. Catalysts for the control of coking during steam reforming. Catal Today 1999;49(1-3):3–10. https://doi.org/10.1016/S0920-5861(98)00401-5.
[48] Rostrup-Nielsen JR. Sulfur-passivated nickel catalysts for carbon-free steam reforming of methane. J Catal 1984;85(1):31–43. https://doi.org/10.1016/0021-9517(84)90107-6.
[49] Hochgesand G. Rectisol and purisol. Ind Eng Chem 1970;62(7):37–43.
[50] Elgin II JC. Pure sulfur compounds in hydrocarbon materials in contact with nicel catalysts. Ind Eng Chem 1930;22(12):1290–3. https://doi.org/10.1021/ie50252a012.
[51] Liu G, Willcox D, Garland M, Kung HH. The rate of methanol production on a copper-zinc oxide catalyst: the dependence on the feed composition. J Catal 1984;90(1):139–46. https://doi.org/10.1016/0021-9517(84)90094-0.
[52] Yang Y, Mims CA, Mei DH, Peden CHF, Campbell CT. Mechanistic studies of methanol synthesis over Cu from CO/CO2/H2/H2O mixtures: the source of C in methanol and the role of water. J Catal 2013;298:10–7. https://doi.org/10.1016/j.jcat.2012.10.028.
[53] Hamelinck CN, Faaij APC. Future prospects for production of methanol and hydrogen from biomass. J Power Sources 2002;111(1):1–22. https://doi.org/10.1016/S0378-7753(02)00220-3.
[54] Seider WD, Seader JD, Lewin DR, Widagdo S. Product and process design principles: synthesis, analysis, and evaluation. Chapter 23. Annual Costs, Earnings, and Profitability Analysis. 3rd ed. New York: Wiley; 2010.
[55] Towler G, Sinnott RK. Chemical engineering design: principles, practice and economics of plant and process design. Chapter 7. Capital cost estimation. 2nd ed. Elsevier; 2012. p. 307–51.
[56] Lee Sunggyu. Methanol synthesis technology. Chapter 8. Catalytic activity and life. CRC Press; 1989.
[57] Alibaba. 98% Nickel nitrate hexahydrate Ni(NO3)2.6H2O. https://www.alibaba.com/product-detail/98-Nickel-nitrate-hexahydrate-Ni-NO3_507738630.html?spm=a2700.7724838.2017115.10.17a57c6aemnyHu&s=p; 2018 [accessed Oct. 9th, 2018].
[58] Alibaba. Magnesium Nitrate Hexahydrate 98% 99% Mg(NO3)2.6H2O Manufacturer Price. https://www.alibaba.com/product-detail/Magnesium-Nitrate-Hexahydrate-98-99-Mg_60404962193.html?spm=a2700.7724838.2017115.1.7fea3691lRhDg1&s=p; 2018 [accessed Oct. 9th, 2018].
[59] Alibaba. Cerium Nitrate Ce(NO3)3.6H2O. https://www.alibaba.com/product-detail/Cerium-Nitrate-Ce-NO3-3-6H2O_60795755062.html?spm=a2700.7724838.2017115.1.4e2a46b4Nre28A&s=p; 2018 [accessed Oct. 9th, 2018].
[60] Alibaba. hard coating material zro2 supplier. https://www.alibaba.com/product-detail/hard-coating-material-zro2-supplier_60797105002.html?spm=a2700.7724838.2017115.21.551d6163VZAxAc&s=p; 2018 [accessed Oct. 9th, 2018].
[61] Alibaba. Ferric Oxide FE2O3 Desulfurization Catalyst. https://www.alibaba.com/product-detail/Ferric-Oxide-FE2O3-Desulfurization-Catalyst_60780101912.html?spm=a2700.7724838.2017115.11.605115c3qq1Ueb&s=p; 2018 [accessed Sep. 27th, 2018].
[62] Alibaba. copper oxide catalyst CUO raw material copper oxide powder. https://www.alibaba.com/product-detail/copper-oxide-catalyst-CUO-raw-material_60735971031.html?spm=a2700.7724838.2017115.1.2238590ba72ECk&s=p; 2018 [accessed Sep. 27th, 2018].
[63] Alibaba. zno desulfurization catalyst used in oil refinery. https://www.alibaba.com/product-detail/zno-desulfurization-catalyst-used-in-oil_60804559218.html?spm=a2700.7724838.2017115.1.72545c96TAc52x; 2018 [accessed Sep. 27th, 2018].
[64] Alibaba. AL2O3 Adsorbents Activated Alumina Catalyst Desiccant. https://www.alibaba.com/product-detail/AL2O3-Adsorbents-Activated-Alumina-Catalyst-Desiccant_60834778470.html?spm=a2700.7724838.2017115.1.494f6cdfXQlv1h&s=p; 2018 [accessed Sep. 27th, 2018].
[65] Alibaba. SiO2 powder CAS:14808-60-7 high purity Nano Silicon Oxide Powder for chemical catalyst. https://www.alibaba.com/product-detail/SiO2-powder-CAS-14808-60-7_60585046958.html?spm=a2700.7724838.2017115.20.57441b7dXdAOw3&s=p; 2018 [accessed Sep. 27th, 2018].
[66] Ying WY, Fang DY, Zhu BC, Sun SL. Simulation of methanol synthesis converter. J East China Univ Sci Technol 2000;26:5–9. https://doi.org/10.14135/j.cnki.1006-3080.2000.01.002.
[67] P. Worhach, J. Haslbeck, Recommended Project Finance Structures for the Economic Analysis of Fossil-Based Energy Projects, DOE/NETL-401/090808, September 8, 2008.
[68] Demirel Y. Nonequilibrium Thermodynamics: Transport and Rate Processes in Physical Chemical, and Biological Systems, 3rd ed. Chapter 4 – Using the Second Law: Thermodynamic Analysis. Amsterdam: Elsevier; 2014.
[69] Dincer I, Rosen MA. Exergy: Energy, Environment, and Sustainable Development. 1st ed. Oxford: Elsevier; 2007.
[70] Luo WJ, Liu XJ, Li YL, Zhang LG. Technical and economic evaluation and production practices on coke oven gas to methanol. Coal Econ Res 2012;32:52–5. https://doi.org/10.13202/j.cnki.cer.2012.08.029.
[71] The World Bank, PPP conversion factor, GDP (LCU per international $), https://data.worldbank.org/indicator/PA.NUS.PPP; 2017 [accessed June 2nd, 2019].
[72] Average weighted hourly electricity price in Ontario from 2004 to 2018 (in Canadian dollar cents per kilowatt hour), https://www.statista.com/statistics/483230/ontario-yearly-average-electricity-market-price/; 2018 [accessed May 22nd, 2019].
[73] Global Adjustment for Mid-sized and Large Businesses, http://www.ieso.ca/en/Learn/Electricity-Pricing/Global-Adjustment-for-Mid-sized-and-Large-Businesses; 2018 [accessed May 22nd, 2019].
[74] [Data] Average U.S. retail prices of electricity between 1998 and 2018, by sector (in cents per kilowatt hour), https://www.statista.com/statistics/200197/average-retail-price-of-electricity-in-the-us-by-sector-since-1998/; 2018 [accessed May 23rd, 2019].
[75] Prices of electricity for industry in Finland from 1995 to 2017 (in euro cents), https://www.statista.com/statistics/595853/electricity-industry-price-finland/; 2018 [accessed May 21st, 2019].
[76] Precios medios de energía eléctrica por tipo de tarifa, https://datos.gob.mx/busca/dataset/precios-medios-de-energia-electrica-por-tipo-de-tarifa?fbclid=IwAR12XrfUdQMVV4ENQxlNmXX7xNEYgo4zAxONNfuIQOfMjbDteR9c5S5dR7E; 2018 [accessed May 22nd, 2019].
[77] The most updated Chinese national electricity sale price report, http://www.sohu.com/a/271827080_146940; 2018 [accessed May 22nd, 2019].
[78] Methanex, 2018, Methanex posts regional contract methanol prices for North America, Europe and Asia, https://www.methanex.com/our-business/pricing; 2018 [accessed April, 2018].
[79] Corporation tax rates, https://www.canada.ca/en/revenue-agency/services/tax/businesses/topics/corporations/corporation-tax-rates.html; 2018 [accessed June 12th, 2019].
[80] Kyle Pomerleau, The United States' Corporate Income Tax Rate is Now More in Line with those levied by other Major Nations. https://taxfoundation.org/us-corporate-income-tax-more-competitive/; 2018 [accessed June 12th, 2019].
[81] Finland Corporate Tax Rate, https://tradingeconomics.com/finland/corporate-tax-rate; 2018 [accessed June 12th, 2019].
[82] Mexico Corporate Tax Rate, https://tradingeconomics.com/mexico/corporate-tax-rate; 2018 [accessed June 12th, 2019].
[83] China Corporate Tax Rate, https://tradingeconomics.com/china/corporate-tax-rate; 2018 [accessed June 12th, 2019].
[84] Yearly Average rates. Historical exchange rates, https://www.ofx.com/en-ca/forex-news/historical-exchange-rates/yearly-average-rates/; 2018 [accessed May 23rd, 2019].
[85] Inflation calculator, https://inflationcalculator.ca/ontario/; 2018 [accessed June 5th, 2019].
[86] US Inflation Calculator, https://www.usinflationcalculator.com/; 2018 [accessed June 5th, 2019].
[87] Inflation calculator for Finland, https://www.worlddata.info/europe/finland/inflation-rates.php.
[88] Calculate Price change due to inflation for custom period, https://www.statbureau.org/en/mexico/inflation-calculators?dateBack=2017-12-1&dateTo=2018-7-1&amount=75.76; 2018 [accessed June 5th, 2019].
[89] Inflation calculator-Chinese Renminbi, https://www.inflationtool.com/chinese-renminbi?amount=388&year1=2017&year2=201; 2018 [accessed June 5th, 2019].

Supplementary material

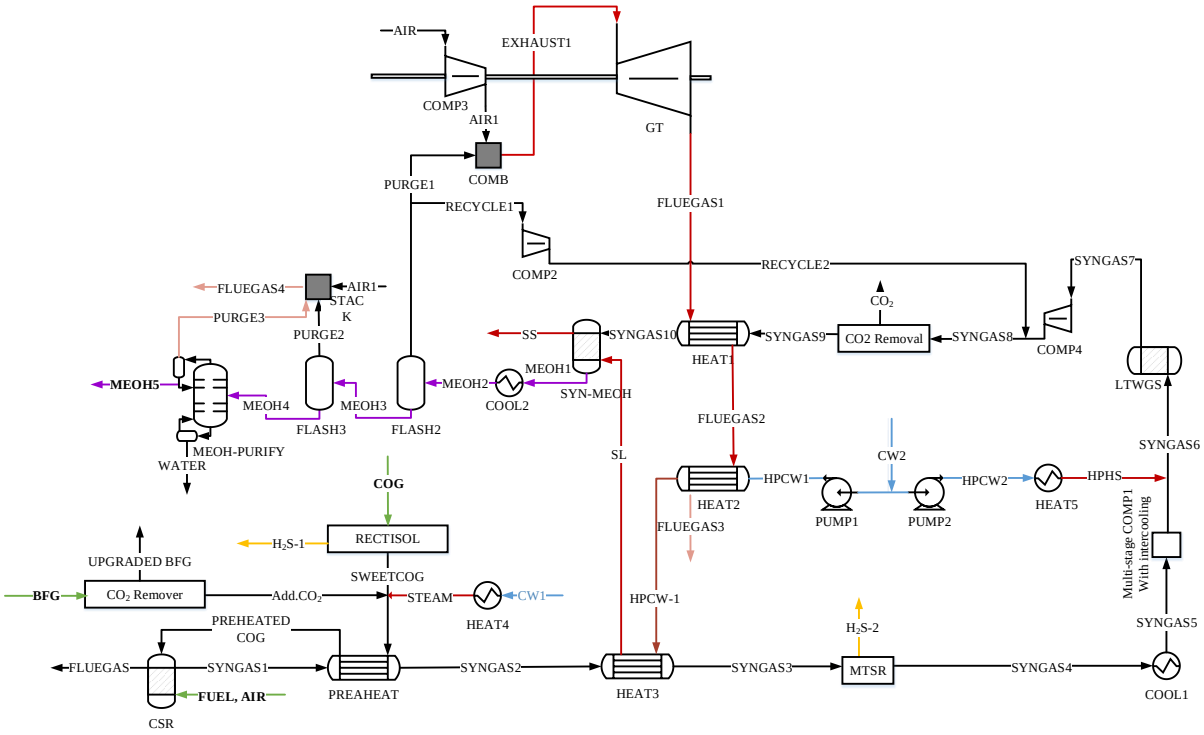

Figure S1. Proposed COG+BFG to MeOH with WGS.

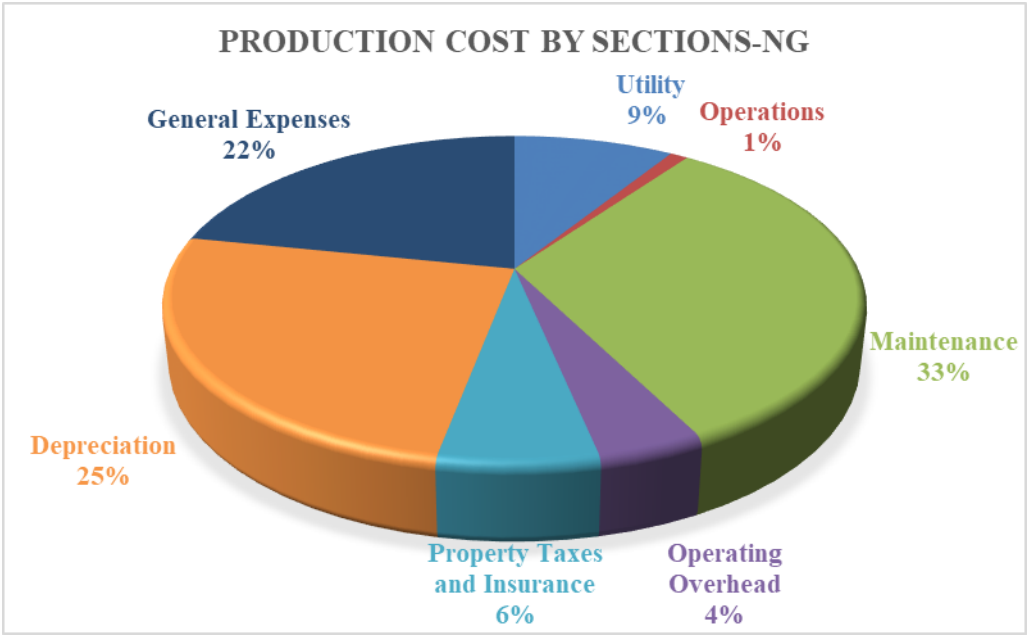

Figure S2. Production cost share with NG/BFG as heating utility, Ontario 2018 case.

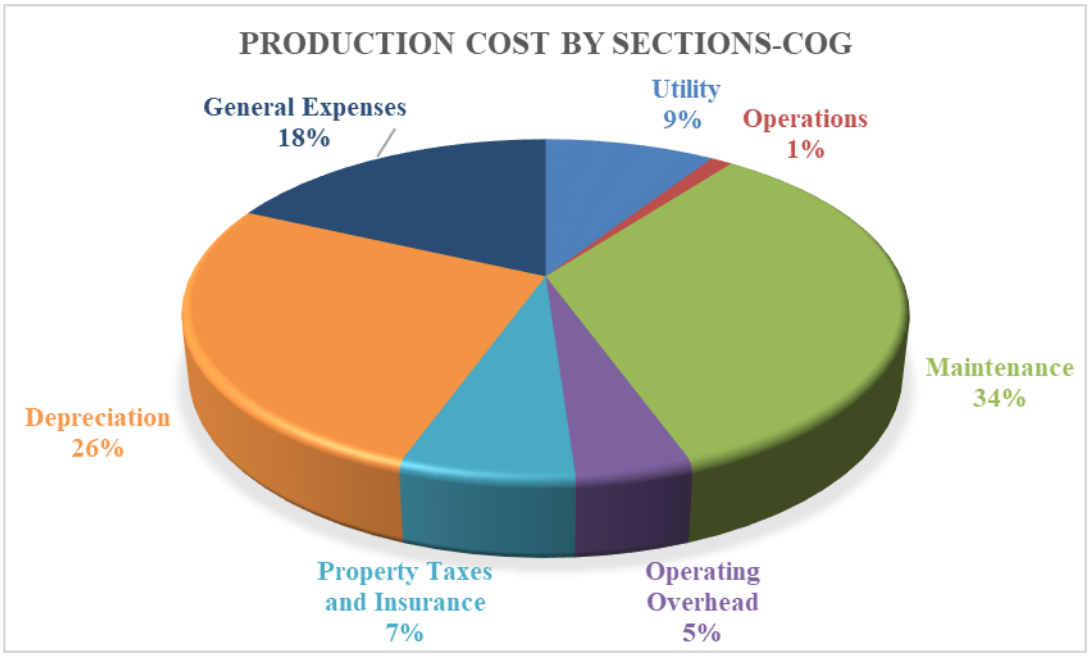

Figure S3. Production cost share with COG as heating utility, Ontario 2018 Case.

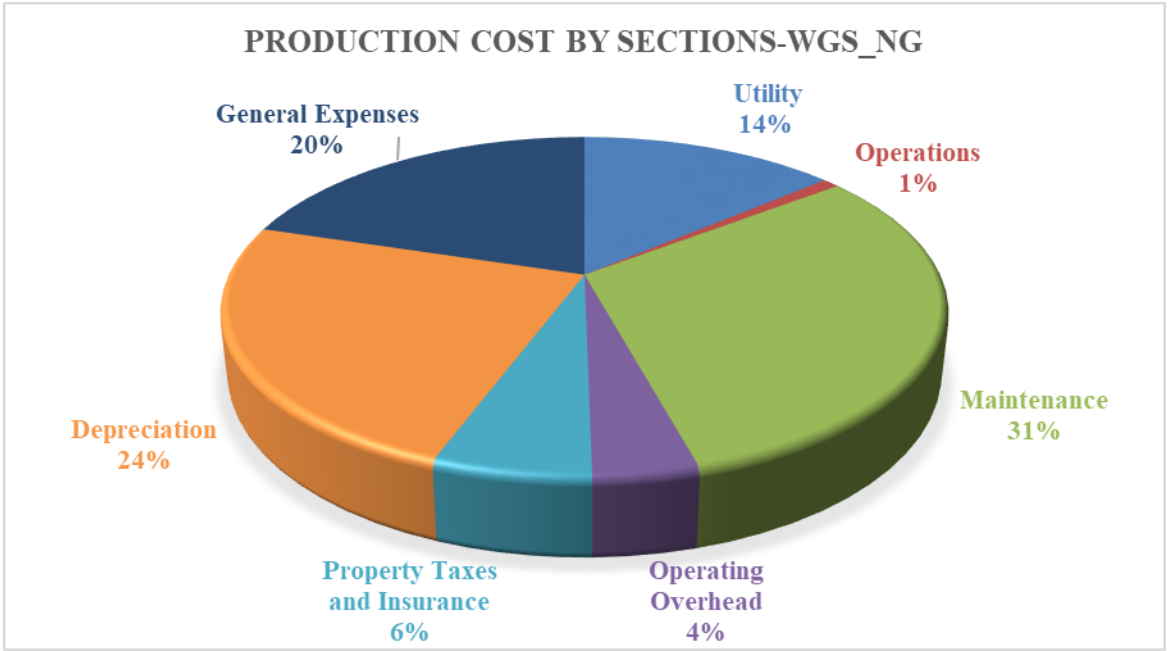

Figure S4. Production cost share with NG as heating utility with WGS, Ontario 2018 case.

Table S1. Factors for total capital investment calculation [54].

F.O.B. (Purchase) Costs	C_{fob}	Historical charts
Installation Costs	C_{inst}	$0.714*C_{fob}$
Construction Costs (Incl. Labor)	C_{cons}	$0.63*C_{fob}$
Total Direct Costs	C_{TDC}	$C_{TDC}=C_{fob} + C_{inst} + C_{cons}$
Shipping (Incl. Insurance & Tax)	C_{ship}	$0.08*C_{fob}$

Construction Overhead	C_{over}	$0.571*C_{fob}$
Contractor Engineering	C_{engn}	$0.296*C_{fob}$
Contingencies	C_{slop}	$0.15 - 0.35*C_{fob}$
Total Indirect Costs	C_{TIC}	$C_{TIC}=C_{ship}+C_{over}+C_{engn}+C_{slop}$
Total Depreciable Capital	C_{dep}	$C_{dep}=C_{TDC}+C_{TIC}$
Land (Pure Real Estate)	C_{land}	$0.02*C_{dep}$
Royalties	C_{royle}	$0.02*C_{dep}$
Startup Costs	C_{strt}	$0.02\text{-}0.3*C_{dep}$ (often 0.1)
Fixed Capital Investment	C_{FCI}	$C_{FCI}=C_{dep}+C_{land}+C_{royle}+C_{strt}$
Cash Reserves	C_{cash}	8.33% of total annual expense
Inventory	C_{inv}	1.92% of annual tangible sales
Accounts Receivable	C_{recy}	8.33% of total annual revenue
Accounts Payable	C_{payb}	8.33% of annual tangible expenses
Total Working Capital	C_{wc}	sum of this section $0.7\text{-}0.89*(C_{fob}+C_{ship})$
Total Capital Investment	C_{TCI}	(total FCI and working capital) $C_{TCI} = C_{FCI}+C_{WC}$

Table S2. Factors for total production cost calculation [54].

Annual operation (hr) 8000			
Operations (labor-related)			*463800*
Direct wages and benefits (DW&B)	35	$/hr	*280000*
Direct salaries and benefits	15	% of DW&B	*42000*
Operating supplies and services	6	% of DW&B	*16800*
Technical assistance to manufacturing			*60000*
Control laboratory			*65000*
Maintenance (M)			
Wages and benefits (MW&B)	13	% of C_{TDC}	
Fluid handling process	3.5	% of C_{TDC}	
Salaries and benefits	25	% of MW&B	

Materials and services	100	% of MW&B
Maintenance overhead	5	% of MW&B
Operating overhead		
General plant overhead	7.1	% of M&O-SW&B
Mechanical department services	2.4	% of M&O-SW&B
Employee relations department	5.9	% of M&O-SW&B
Business services	7.4	% of M&O-SW&B
Property taxes and insurance	2	% of C_{TDC}
Depreciation		
Direct plant	8	% of (C_{TDC}-1.18 C_{alloc})
Allocated plant	6	% of 1.18 C_{alloc}
Cost of Manufacture (COM)	the sum of the above from DW&B	
General Expenses		
Selling (or transfer) expense	3	% of sales
Direct research	4.8	% of sales
Allocated research	0.5	% of sales
Administrative expense	2	% of sales
Management incentive compensation	1.25	% of sales
Total general expenses (GE)		
Total Production cost (C)	TPC = COM+GE	

Chapter 4 Comparison of Steel Manufacturing Off-gas Utilization Methods via Life Cycle Analysis

This work is a continuous study of the previous two projects (CCPP, CBMeOH). The system boundaries, location chosen are in consistent with previous work.

The content of this chapter has been submitted for peer review in the Journal of Cleaner Production

Lingyan Deng, and Thomas A. Adams II. *Comparison of Steel Manufacturing Off-Gas Utilization Methods via Life Cycle Analysis*. Journal of Cleaner Production. Submitted March 20, 2020.

Comparison of Steel Manufacturing Off-Gas Utilization Methods via Life Cycle Analysis

Lingyan Deng and Thomas A. Adams II*

Department of Chemical Engineering, McMaster University, 1280 Main St. West, Hamilton, Ontario L8S 4L7, Canada

**Corresponding author. Tel.:+1 905 525 9140 ext.24782 E-Mail address: tadams@mcmaster.ca*

Abstract

This study utilizes life cycle analysis to compare three steel manufacturing off-gas utilization systems: a status quo system, which produces electricity via a low-pressure steam turbine; a combined cycle power plant (CCPP) system, which produces electricity using gas and steam turbines; and a methanol (MeOH) system, which converts coke oven gas (COG) and blast furnace gas (BFG) into MeOH (CBMeOH). This research seeks to compare the environmental impacts of each system based on equivalent raw material inputs. Since the systems have different products, system expansion is used to ensure that they have the same outputs and are therefore comparable. The system boundary consists of a combination of cradle-to-gate and gate-to-gate boundaries. The environmental effects of each system are compared at five locations—Ontario, the USA, Finland, Mexico, and China—using TRACI, CML-IA baseline, ReCiPe2016, and IMPACT2002+ in SimaPro v9. The results show that in Ontario, Finland, and China, CBMeOH systems had the lowest environmental impact, while the CCPP system had the lowest impact in the USA and Mexico. The status quo system had the greatest environmental impact for all of the studied locations, except for the USA. This environmental assessment, combined with previous economic analysis, demonstrates that the CBMeOH system is the optimal choice in Ontario, and China. In the USA, plants might be better off adopting CCPP systems when carbon taxes reach $50/tonne. For Mexico, the CCPP system is the most environmentally friendly choice, while the CBMeOH system is the most profitable. Finally, the results indicate that status quo systems are not recommended in Mexico or China in any foreseeable circumstance.

Keywords: coke oven gas, blast furnace gas, life cycle analysis, combined cycle power plant, methanol production.

1. Introduction

Steel manufacturing off-gas mainly consists of coke oven gas (COG), blast furnace gas (BFG), and basic oxygen furnace gas (BOFG). COG and BFG are continuously produced throughout the manufacturing process, while BOFG is only produced intermittently. COG has relatively greater higher heating value (HHV) compared to BFG and BOFG, while BFG is produced in the greatest quantities. In general, the life cycle of COG and BFG during the steelmaking process consists of four main stages [1]. First, they are used for constant consumption in various milling processes, such as sintering, coking, and blast furnace processing. Second, the surplus gas from these processes is then stored in gas holders for future use. Third, if the quantity of surplus gas is large enough, it will be used to produce electricity via a built-in power plant. Finally, any remaining gas is burned and emitted into the atmosphere, which is an undesirable outcome. The four stages of off-gas utilization methods might not be the best option, as they result in high CO_2 emissions and low energy recovery efficiency. Given this, considerable research on steel manufacturing off-gas valorization has been conducted to develop more effective methods of reducing CO_2 emissions and increasing energy recovery efficiencies. As noted by Deng and Adams, steel manufacturing off-gass is most commonly used to generate electricity via combined cycle power plants (CCPP) and for methanol (MeOH) synthesis [2] [3]. Deng and Adams analyzed the economic feasibility and CO_2 emissions of these two systems, and found that, due to a variety of factors, it was economically advantageous to build CCPP and MeOH plants in some countries, but not in others. This was demonstrated in a prior study by Deng et al.[3] wherein coke oven gas (COG) and blast furnace gas (BFG) were used to synthesize MeOH (called the CBMeOH process). As their results showed, lower MeOH market prices do not necessarily result in lower net present value (NPV) because NPV is impacted by lots of other factors, such as electricity price, carbon tax, electricity carbon intensity, power purchasing parity, and income tax. For example, although China has lower MeOH prices than the USA, retrofitting plants with CBMeOH systems will yield a much higher NPV within a Chinese setting. However, this study only consisted of a gate-to-gate analysis, which meant that it had some deficiencies. For example, it did not consider the related upstream carbon

footprint. Additionally, since the products of each system were different, it was not possible to compare them directly. Finally, it did not consider other categories of environmental impact aside from greenhouse gas (GHG) emissions. Hence, it is desirable to do a thorough life cycle analysis (LCA).

The literature contains numerous LCAs of power co-production in steel plants and methanol production from COG. For example, Li et al. [1] conducted an LCA of a steel plant that had been outfitted with a combined cycle power plant. Specifically, they compared the results of a gate-to-gate LCA for this system to those of a coal-powered system that produces the same amount of electricity and steel off-gas, which is burned without energy recovery. The LCAs in this study were conducted using eBalance software, which is produced in China and uses data that is specific to a Chinese context. The results showed that, in producing the same amount of electricity, the steel plant with the combined cycle power plant used 54% less energy and emitted 29% less CO_2 than the other coal-powered system. Li's et al.'s LCA showed that building a CCPP plant in China would help to reduce CO_2 emissions. However, they did not factor in equivalent amounts of electricity from China's electricity grid. In addition, Li et al.'s LCA lacked data regarding other environmental effect, such as acidification and eutrophication.

Several research groups have also conducted LCAs of methanol production from coal, COG, and NG [4-6]. Both Lee et al. [4] and Chen et al. [6] found that using COG to produce MeOH is cleaner than using coal, with NG being the cleanest option of the three. Similarly, Li et al. [5] performed LCAs for methanol production from coal gasification and coal-coking-produced COG, and found that the COG method was much cleaner than coal gasification. Other research groups, such as Ou et al. [7], have performed LCAs on the conversion of steel mill off-gas to ethanol via fermentation, and compared them to LCAs of traditional petroleum gasoline to ethanol conversion. As their results show, fermentation is capable of reducing GHG emmisions by approximately 50%, and requires significantly less fossil fuel consumption (0.51-0.74 MJ fossil fuel/MJ ethanol) than the conventional method (1.34 MJ fossil fuel/MJ ethanol). The above-mentioned COG-to-MeOH process [4-6] uses the traditional

method, which acquires the additional CO_2 required for adjusting the H_2/CO mole ratio via coal gasification or CO_2 recycled from the MeOH synthesis process. However, in this work, BFG is used as an additional CO_2 source, which is a novel contribution. In addition, the proposed CBMeOH system's desulphurization process is much shorter than the traditional two-stage hydrodesulfurization process [3]. While prior studies have conducted LCAs of methanol production from COG [4-6], this is the first work to conduct an LCA of a CBMeOH plant.

Although the findings of the prior studies indicate that the production of electricity or methanol using off-gas from steel production is cleaner than traditional methods, it is unknown whether these processes are more environmental friendly given equivalent amounts of off-gas. To the best of our knowledge, no one has ever conducted LCA comparisons of the status quo, CCPP, and CBMeOH systems with equal levels of COG. Furthermore, the impact of factors such as the acquisition of raw materials, transportation distances, and traditional methanol production processes all vary based on the location of the plant. Thus, this research uses LCAs to understand the environmental impact of the status quo, CCPP, and CBMeOH systems in five locations: Ontario, the USA, Finland, Mexico, and China.

2. Systems Description and Methods

The status quo system used in this research is based on the off-gas utilization method used by ArcelorMittal Dofasco (AMD), located in Ontario, Canada. AMD's approach to off-gas utilization involves combusting the COG in order to boil low-pressure water into steam, which is then fed into the low-pressure steam turbine to generate electricity. Electricity is the only product of the status quo system.

The CCPP system uses the same amount of COG as the status quo system for electricity generation. However, instead of combusting the COG directly, the CCPP system uses MDEA desulphurization to remove bulk H_2S. In this process, the COG is compressed before being fed into the MDEA absorber to produce sweet COG, which leaves the stripper at about 16 bar, and with a sulfur content reduced to

less than 1 ppmv. Next, the sweet COG is fed into a combustor to react with compressed air, creating combusted high-pressure exhaust gas which is passed through a gas turbine to generate electricity. After passing through the gas turbine, the exhaust gas still contains a high amount of thermal energy (temperature around 650 ℃), which is subsequently recovered using process water and low-, intermediate-, and high-pressure steam turbines. This process allows for a maximum amount of energy to be recovered. Optimizing the volume of process water is critical, as it enables the NPV of the CCPP system to be maximized. The results show that the CCPP system produces over twice as much overall electricity as the status quo system. As with the status quo system, electricity is the only product of the CCPP system.

The CBMeOH system uses the same amount of COG as the status quo and CCPP systems. However, unlike the status quo and CCPP systems, the CBMeOH system also uses BFG as raw material. Furthermore, the CBMeOH system also requires the COG to undergo fine desulphurization. Instead of the two-stage hydro desulphurization process used in the commercialized method, the CBMeOH system uses an energy-intensive CO_2 and steam reforming (CSR) process that not only cracks the methane in the COG into H_2 and CO, but that also breaks and converts the thiophene into H_2S. Following this CSR process, the converted H_2S is removed using a middle-temperature sulfur-removal process. The CO_2 recovered from the BFG via Rectisol is used as an additional carbon source, with the volume being adjusted to convert the methane in the COG, as well as to adjust the $(H_2-CO_2)/(CO+CO_2)$ molar ratio. Next, prepared syngas is supplied to a typical boiling water reactor for MeOH synthesis. Most of the unconverted syngas is recycled to the MeOH synthesis reactor, while the remainder is combusted and used in a gas turbine to produce electricity. The thermal energy created by the exhaust gas exiting the turbine is further used to preheat the water used in the boiling reactor for MeOH synthesis, and to control the reaction temperature. In this system, the remaining BFG (mainly CO, H_2, and N_2) contains a large amoung of energy, and is capable of providing the same amount of heat downstream as the status quo method. The major product of this system is MeOH, but

it is also capable of recovering some heat. However, the CBMeOH system is reliant on electricity from the grid, as it only produces a small amount on its own.

The different products produced by the three systems poses a challenge, as a comparison of their relative environmental impacts requires the same outputs. This issue is addressed by using system expansion, which is detailed in Section 2.1. In addition, SimaPro V9 is used to conduct the life cycle analyses and comparisons of the environmental effects of the status-quo, CCPP, and CBMeOH systems. The LCA methods utilized in this work are in accordance with ISO 14040, which contains four main steps: goal and scope definition, inventory analysis, impact assessment, and interpretation.

2.1.Goal and Scope Definition

The goal of this study is to use LCA to compare the environmental effects of three different systems available to steel manufacturers. These results will expand upon the findings of previous economic analyses, and help steel plant operators select the most optimal off-gas utilization method. As such, this work's main target audience is steel manufacturers. The functional units used in all three systems are the combined co-products of 1 MWh of electricity and 1.37 MWh of heat.

The system boundary of this work is a combination of 'cradle-to-gate' and 'gate-to-gate' boundaries. Since the aim of this work is to analyze retrofitting options for AMD's off-gas utilization systems, the upstream production of raw material, COG, and BFG is irrelevant. Consequently, the mining and transportation of coal, the making of coke, the removal of tar, benzene, ammonia, and other compounds from COG, and the BFG produced by the steel plant will all be considered the same for all three scenarios. In this respect, a gate-to-gate boundary is sufficient. However, further traceback is required with respect to NG, electricity, oxygen, steel, solvent, and catalyst, as each of the three systems uses different amounts of these utilities and materials. Therefore, a cradle-to-gate boundary is also needed in order to consider these pathways.

Another issue that must be considered when drawing the system's boundary is where the system ends, and what falls inside or outside of the boundary. The status quo and CCPP system only use COG

from steel manufacturing, while the CBMeOH system uses both COG and BFG. Additionally, the three systems have different products: the status-quo and CCPP systems produce electricity only, while the CBMeOH system produces MeOH and heat, but no electricity output. In order to conduct a fair comparison, it is critical to consider the same amounts of raw COG and BFG, and the same products for each system. In this study, both COG and BFG are taken into consideration, and the considered products are the amount of electricity and heat produced by the status quo system with an expansion. The detailed system boundaries are illustrated in Figures 1 to 3. The inputs for the status quo system (Figure 1) mainly consist of COG, water, and air, with BFG serving as the system expansion material, while the outputs include electricity, heat, and emissions into the atmosphere.

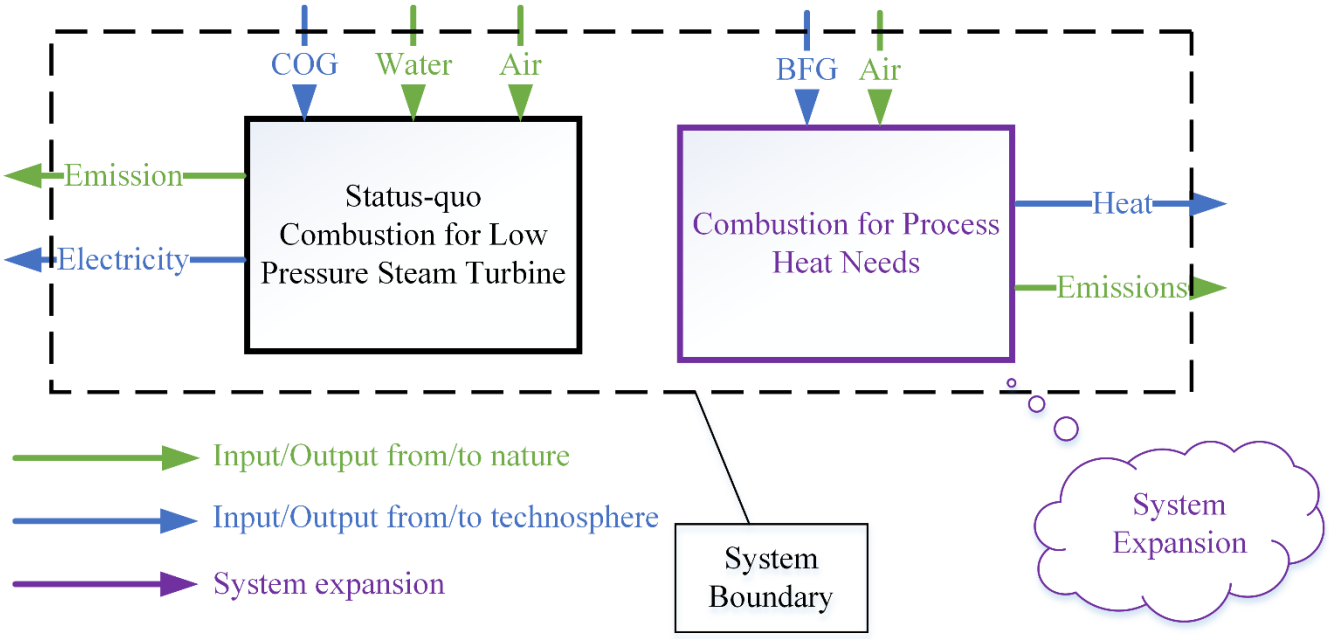

Figure 1. Status-quo COG utilization boundary

As shown in Figure 2, desulphurization is one of the major processes in a CCPP system. The major raw materials used in the CCPP system are COG and BFG, with NG serving as the heating utility for the desulphurization process. The cradle-to-gate environmental effects of NG and steel are represented by the dashed box. The Claus process is a waste treatment process. As can be seen in Figure 2, the upstream environmental effects of the oxygen supplied in this process are also included.

Compared to the COG flow rate, only a very small amount of makeup MDEA is used as solvent in COG desulphurization (less than 1 % of total COG input). Thus, no further tracing back is considered. System expansion that combusts the same amount of BFG used as a carbon source in CBMeOH was also used. This system expansion is shown in purple in Figure 2. The major products of the CCPP system are electricity and heat.

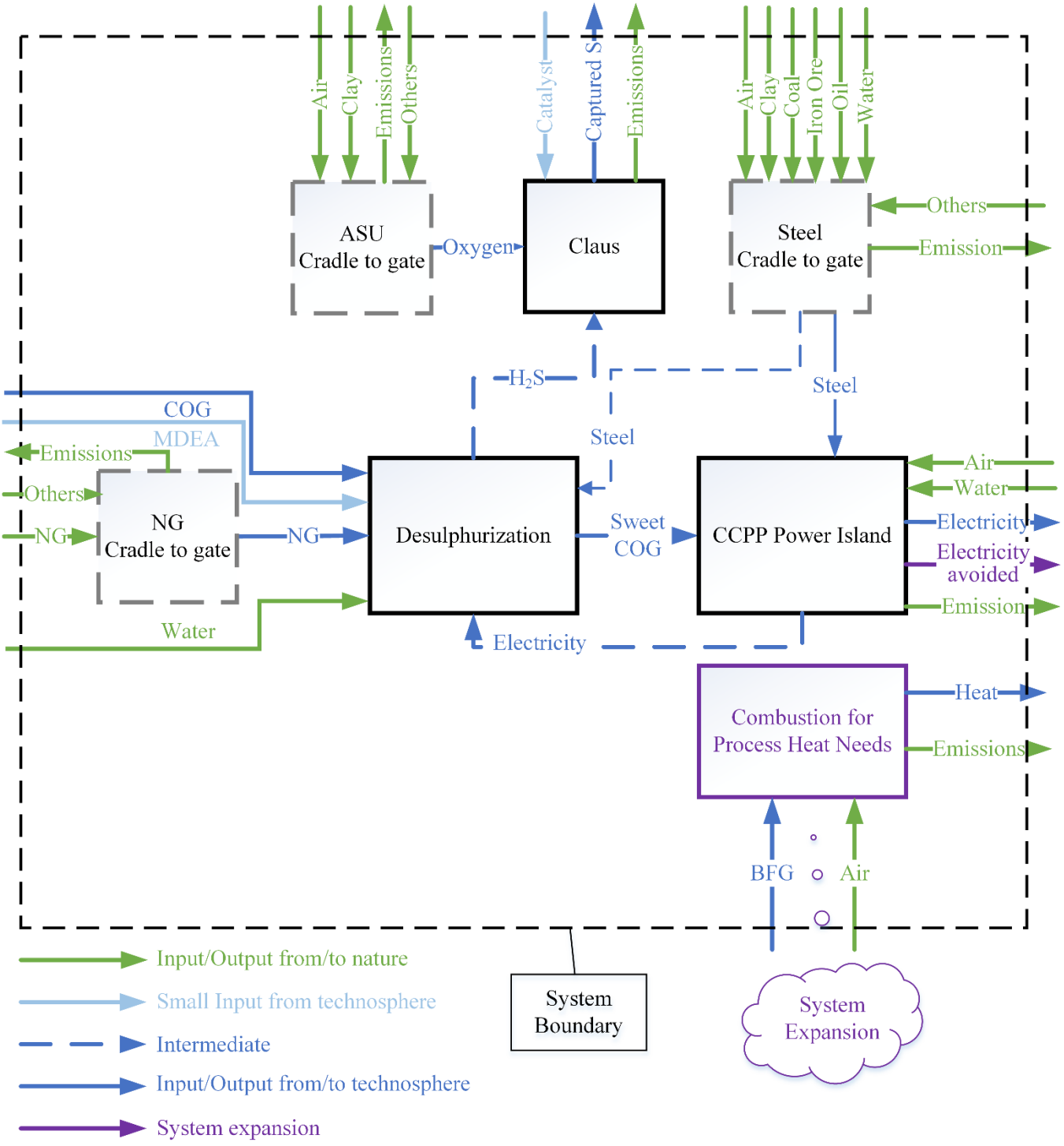

Figure 2. CCPP System boundary.

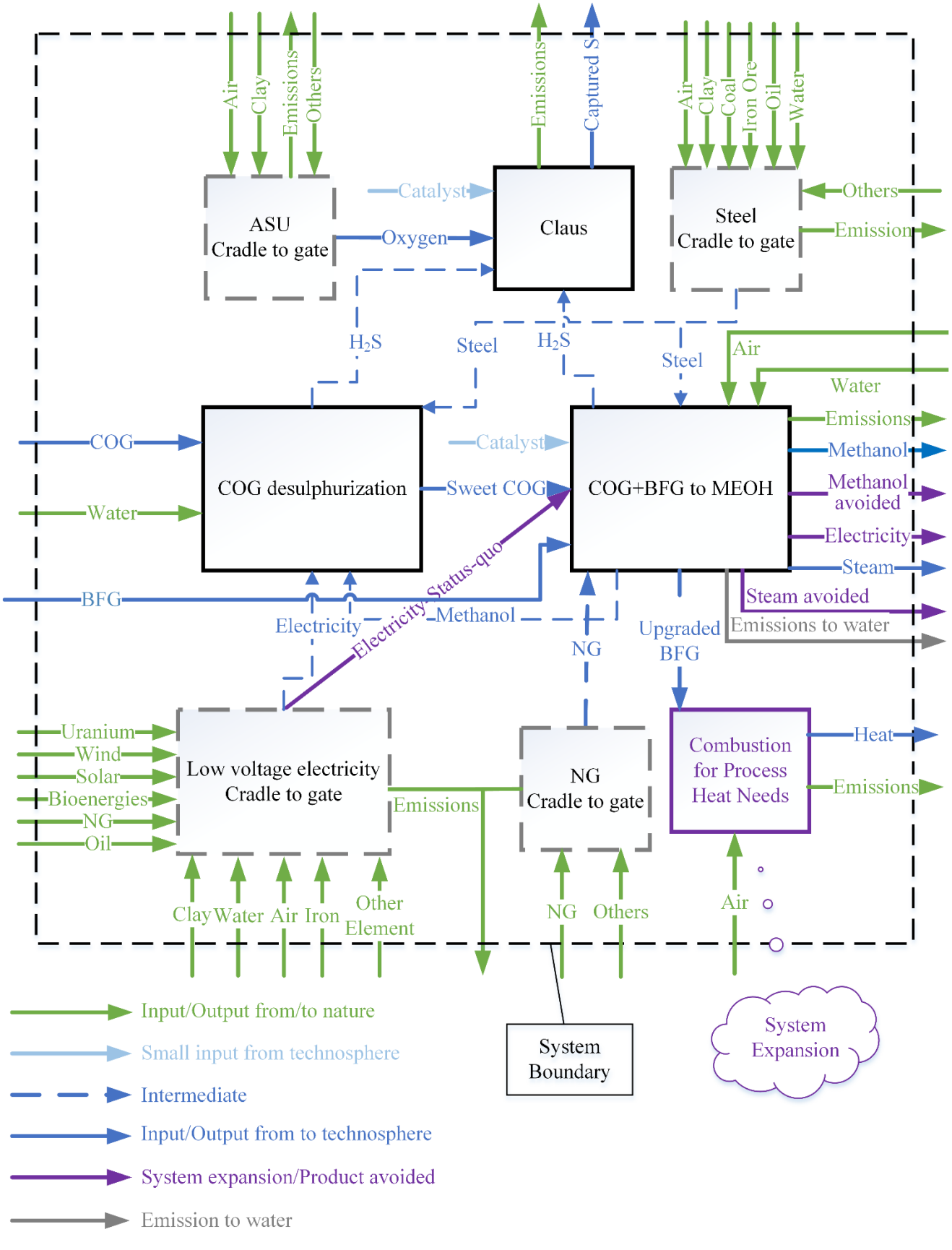

Figure 3. COG + BFG to MeOH system boundaries

The major inputs for the CBMeOH system are COG, BFG, air, water, NG, and electricity. The solvent used in the Rectisol process (methanol) is an intermediate of the system's products, while NG serves as the heating utility for the reboiler and process steam. The cradle-to-gate environmental impacts of steel, oxygen, NG, and electricity are also considered. As with the CCPP system, system expansion is used to enable an adequate comparison between the CBMeOH system and the status quo system. The same amount of electricity is consumed from what is assumed to be the local grid, and the same amount of methanol and steam is assumed to be produced as product avoided. Even though the CBMeOH system uses BFG as a carbon source, the heat rate of the remaining BFG remains the same as the original BFG, as up to 97.6 wt.% purity of CO_2 is removed from it. The other 2.4 wt.% mainly consists of H_2O in the removed CO_2 stream [3]. Hence, the upgraded BFG can still provide the same amount of heat when combusted in the downstream process. The major output of the CBMeOH system is electricity and heat.

The use of system expansion ensures that the three systems produce the same amount of COG and BFG from steel manufacturing, and the same products, namely, electricity and heat. Thus, the three systems are now comparable.

2.2. Life Cycle Inventory

The process data inputs and outputs for each system were consistent with those used in our prior work. Input and output data not included in the previous model, such as the cradle-to-gate impacts of NG, steel, electricity, and traditional MeOH, were obtained from the Ecoinvent v3.5 database in order to ensure the highest possible level of accuracy. The ISO 14040 standard allows a cutoff for material or energy flow, in this work, we assume that if the flow is smaller than 1% of the total input, is the flow will not be considered when evaluating the system, as the environmental impact of these streams is minimal [8]. In total, less than 5% of the input was unaccounted for.

In this work, the total catalyst used in the reactors for the CBMeOH process was less than half of the total fixed capital equipment [3], which in in turn is a trivially small percentage of the total mass consumed by the system over its lifetime (about 0.035%). As such, the effects of catalyst manufacturing are not accounted for in this analysis. The total amount of solvent required for the Rectisol process is also small, since it is continually regenerated, and the MeOH that is produced during the process can be used for the relatively small amount of makeup solvent required. Hence, the environmental impacts of the solvents in the Rectisol process are considered to be intermediate, and are calculated according to linear correlation to the process described by Sun et al. [9]

The difference between the three systems is largely related to the equipment used in each. For example, the status-quo system only requires a combustor, a pump, a heat exchanger, a steam turbine, and a condenser. In contrast, as described in a previous paper, the CCPP system requires six heat exchangers, three steam turbines, three pumps, one gas turbine, three compressors, two distillation columns, one reboiler, and two condensers. The CBMeOH process uses two distillation columns, one reboiler, two condensers, one CSR, one MeOH synthesis reactor, two flash drums, four compressors, one gas turbine, one stack, and eight heat exchangers. The environmental effects associated with the equipment used in these processes are modeled in a first-order model, which only considers the production and transportation of materials.

A Claus process is used in both the CCPP and CBMeOH processes for treating H_2S waste. The main inputs for the Claus process are oxygen, sour gas, and boiler feed water, while the products are solid sulfur, low-pressure steam, high-pressure steam, and tail gas. The materials and energy required for the furnace, reheating, and condenser utility were calculated using a linear correlation, which was detailed in a previous study by our group [10].

The wastewater from the CBMeOH plant contains trace amount of CO, CH_4, C_2H_2, H_2S, CH_4O, C_2H_4, SO_2, C_2H_6O, and $C_2H_4O_2$. Those organic and sulfide components‘ environmental impact are considered as emissions to water.

The electricity used in steel manufacturing is a mixture of medium-voltage and low-voltage electricity [11]. For simplification and conservation, this study assumes that all electricity used is low voltage. However, the emissions and losses associated with the conversion from medium- to low-voltage electric power are also considered.

Databases were carefully chosen in order to obtain the most representative information on heat avoided, NG, and methanol avoided for each location. With respect to heat avoided, due to lack of more representative data, the European database (RER) was selected for all locations except for China, as the global database offered the most representative data for this location. For NG and methanol avoided, the USLCI database was selected for Ontario, USA, and Mexico. For Finland, the RER database was used for NG avoided, while global market data was used for methanol avoided. For China, global market data was used for NG avoided, while methanol avoided data was obtained from the literature. In fact, IKE (Short name of Integrated Knowledge of our Environment) has developed life cycle analysis software, known as eBalance, which is based on Chinese data and normalization references. eBalance features a China-based life cycle database for methanol production [12] specifically. However, the data are not publically accessible. According to the literature, 58% of China's methanol supply is derived from coal-to-methanol (CTM), of which 17% comes from COG-to-methanol (COGTM), and 14% is produced via NG-to-methanol (NGTM). The remaining 11% is generated due to the coproduction of ammonia and methanol (CAM) [5], most of which is the result of coal conversion [13]. The rate of methanol to ammonia is adjustable and varies from plant to plant. For example, Li et al. [14] indicate that 4.5 million tonnes of methanol are produced for every 4.5 million tonnes of ammonia that are produced. Thus, according to Li et al., the methanol to ammonia ratio (MTA) is 1:1, though it can be as low as 0.201 [15]. In general, the environmental impact allocation in the CAM system is either based on mass or energy. As such, methanol produced via the CAM system will have a relatively lower environmental impact than methanol produced by the CTM method, as part of the burden is taken up by ammonia. There is no database regarding ammonia

produced from coal, nor is there any literature regarding LCAs of the coproduction of ammonia and methanol from coal. This could be an interesting subject of study for future work. For now, however, we assume that the 11% of methanol produced via the CAM system has the same environmental impact as the methanol produced via the CTM system. Although Li et. al.'s [5] study on the cradle-to-gate life cycles of coal-to-methanol (CTM) and coke-oven-gas-to-methanol (COGTM) provides with detailed data on these methods, it does not provide data for the NG-to-methanol (NGTM) method. For this reason, Chen et al.'s [6] data was used for the NGTM method, as it was the most accurate data available.

Based on the above discussion, the following assumptions were made with respect to data utilization:

1. It is assumed that there are no upstream environmental effects assigned to the raw material COG and BFG.
2. The Rectisol process for BFG washing mainly removes CO_2 and H_2S in the stream. Given that the change of energy in the upgraded BFG stream is negligible, we assume that the upgraded BFG in the CBMeOH system can produce the same amount of heat as the status quo and CCPP processes.
3. It is assumed that the retrofitted CCPP and CBMeOH plants are mainly constructed of steel. As such, the cement required for construction is not considered. Since the status quo system already exists in the plant, no construction is required. Hence, we assume that there is no construction footprint for the status quo system.
4. The weight of the construction materials used for the CCPP and CBMeOH plants is less than 0.03 wt.% and 0.07 wt.% of the total COG and BFG inputs over the process lifetime of 30 years. According to ISSO 1440, these materials can be discounted, as they account for less than 1% of the total input. However, we consider the cradle-to-gate environmental impact of the required construction material, as it is one of the main areas of difference between the three studied systems.

5. The CBMeOH system requires the following amounts of catalyst each year: 73 tonnes for MeOH synthesis, 16.2 tonnes for the CSR unit, and 2867.7 tonnes for MTSR [3]. Assuming the catalyst is regenerable, the total weight required would be approximately 3 ktonnes over a plant lifetime of 30 years, or about 12.32 kg/h, which accounts for 0.7% of the CBMeOH system's total input. According to ISSO 1440, the cradle-to-gate environmental effects of the required catalyst can be neglected; however, we still account for their transportation footprint.
6. The makeup of the MDEA solvent is 7.03E-6 kg/kg COG. Thus, the effects related to the production and transportation of MEDA are neglected.
7. In order to compare the three systems, the extra electricity produced by the CCPP system is subtracted from electricity avoided from the grid, while the extra methanol produced by the CBMeOH system is subtracted from methanol avoided. The electricity avoided data uses the specific location's low-voltage national wide electricity grid mix except Ontario uses Ontario's provincial electricity grid value other than Canada's national electricity grid value.
8. The electricity utility for each location are using each location's low-voltage mixture of electricity grid.
9. Although the COG and BFG are produced on site, the transportation of the process water that is required for the systems must be considered. However, as AMD is located on the shore of Lake Ontario, it can reasonably be assumed that the transportation impact for process water is zero. Given this, it is assumed that the steel plants in the other locations are located close to water resources as well.
10. The USLCI database is used for NG as utility and methanol avoided for the North American locations (Ontario, USA, and Mexico).
11. For Finland, the RER database is used for NG utility, while global data is used for methanol avoided.

12. For China, global data is used for NG as utility, while methanol avoided LCI data is obtained from two papers: CTM and COGTM from Changhang Li et al. [5], and NGTM from Chen et al. [6].
13. CAM in China comes from coal sources. The environmental impact of methanol in this process is assumed to be the same as in CTM.
14. Steel is assumed to be the main material required to construct the desulphurization, CCPP, COG desulphurization, and COG+BFG to MEOH plants. Thus, the cement required for the construction of these plants is not considered.
15. Combustion mainly provides heat for downstream processes, and it is assumed that the combustion chamber already exists in the steel plant. Hence the construction of the combustion chamber is not considered.

The detailed input and output data for each of the three systems are shown in Table 2. The input and output data listed in the table are directly related to the three systems (gate-to-gate), and do not consider any upstream factors. This means that the heat from NG, electricity, methanol avoided, and transportation are based on the cut-off data in the database. No details regarding the production of electricity are provided.

Table 2. Flow of elements into and out of the system boundaries based on functional units of 1MWh of electricity and 1.37 MWh of heat.

	Status quo	CCPP	CBMeOH	Unit
System Input				
COG	624	624	624	kg
BFG	0	0	2088	kg
Air	17791	17791	3413	kg
One-time process water for power generation (Recyclable)	1.67×10^{-5}	1.67×10^{-5}	0	m^3
Electricity from grid	0	0	1.34	MWh

Electricity from internal	0	0.13	0.86	MWh
Water for solvent	0	0.006	0	m^3
Heat from NG	0	23.5	40.7	MWh
MeOH from internal	0	0	0.42	kg
Refrigerant	0	0	0.062	MWh
Steel	0	0.35	0.79	kg
Steel transport, freight, Ontario	0	0.53	1.18	tkm
Catalyst transport, freight, Ontario	0	0	4.12×10^{-5}	tkm
Water for synthesis	0	0	0.4	m^3
Water for cooling	0		13.48	m^3
MDEA make up	0	0.004	0	kg
System Output				
Electricity product	**1**	**1**	0	MWh
Electricity to internal	0	0.133	0.86	MWh
MeOH	0	0	835	kg
System expansion				
Input				
BFG	2088	2088	0	kg
MeOH avoided	0	0	835	kg
Heat avoided from the process	0	0.37	2.31	MWh
Electricity avoided	0	1.04	0	MWh
Output				
Heat from BFG combustion	**1.37**	**1.37**	**1.37**	MWh
Electricity product, the same as status quo	0	0	**1**	MWh

Emissions to air				
Sulfur dioxide	13.69	0.71	3.50×10^{-6}	kg
CO_2 from process	995	995	402	kg
CO_2 from BFG as source	1368	1368	756	kg
Hydrogen	0	0	0.012	kg
Water	0	0	287	kg
Nitric oxide	0	0	4.22	kg
Nitrogen dioxide	0	0	0.14	kg
Emissions to water				
Methanol	0	0	0.001	kg
Ethanol	0	0	6.2×10^{-7}	kg
Methyl formate	0	0	4.0×10^{-9}	kg
Waste treatment: Clause process				
ACID INPUT				
O_2 (99.44 wt.% purity)	0	3.4	3.7	kg
Boiling feed water	0	22.3	24.7	kg
H_2S content in acid gas	0	7	7.7	kg
CO_2 content in ACID gas	0	13	14.4	kg
N_2 content in ACID gas	0	3.2	3.5	kg
CH_4 content in ACID gas	0	3.1×10^{-6}	3.4×10^{-6}	kg
Total heat required (heater) (NG for temp. >200C)	0	2.6	2.9	kwh
Total heat required(utility) (NG)	0	0.17	0.2	kg
Total heat removed (utility) (steam 45 bar)	0	22.3	24.7	kg
Total heat removed (condenser) （steam)	0	18.1	20	kwh

Output				
solid sulfur	0	6.4	7.13	kg
tail gas H_2S content	0	0.17	0.19	kg
Sour water total (H_2S content)	0	0.0002	0.0002	kg
Sour water total (NH_3 content)	0	0.0002	0.0002	kg
Sour water total (CO_2 content)	0	0.006	0.006	kg
Sour water total (SO_2 content)	0	5.7×10^{-14}	6.3×10^{-14}	kg
Sour water total (COS content)	0	1.2×10^{-7}	1.3×10^{-7}	kg
Sour water total (CH_4 content)	0	1.1×10^{-6}	1.2×10^{-6}	kg
Sour water electricity required	0	1.8×10^{-5}	2.0×10^{-5}	kwh

Table 2 shows the raw materials and elements from the environment and energy inputs from the technosphere required for each of the three systems. Each data column lists the gate-to-gate flows of the corresponding boxes in the system boundary figures. For example, the column, 'Status Quo,' represents the input/output of the 'Status-quo combustion' box in *Figure 1*; the column, 'CBMeOH,' represents the input/output of the boxes, 'COG desulphurization' and 'COG+BFG to MeOH,' in *Figure 3*; and the column, 'CCPP,' represent the boxes, 'Desulphurization' and 'CCPP,' in *Figure 2*. All five locations have the same data: for every 1 MWh of electricity produced, the system consumes about 624 kg of COG. For the CBMeOH process, 1.34 MWH of electricity and 2.2 kg of NG as heating utility are required. The fresh water requirements for the status quo and CCPP systems are very small, as the process water can be recycled. The other notable number relates to heat output. After applying the system expansion, the major output of the three systems are electricity and heat. The heat output here represents heat from BFG combustion, which is one of the products of system expansion. The emission from BFG combustion is CO_2; no other emissions are included. With respect to direct emissions into the atmosphere, the CBMeOH system produces almost no SO_2; however, it does emit some SO_2 into the waterways via wastewater from the MeOH purification process. The status quo and

CCPP systems release approximately the same amount of CO_2 into the atmosphere because they combust the same amounts of COG and BFG within their system boundaries. The emission of ethyne, hydrogen sulfide, carbon disulfide, thiophene, methanol, ethene, ethane, ethanol, monoethanolamine, methyl formade, methane, and dimethyl ether to air and water as predicted by simulation were only trace amounts, which are not listed in the table. However, those computed values are still available in the source files uploaded to LAPSE: http://psecommunity.org/LAPSE:2020.0267 .

2.3. Life Cycle Impact Assessment Method

This work utilizes two environmental assessment tools: TRACI 2.1 v1.05/US-Canadian 2008, and CML-IA EU25+3, 2000. TRACI includes categories such as ozone depletion, global warming, smog, acidification, eutrophication, carcinogenic, non-carcinogenic, respiratory effects, ecotoxicity, and fossil fuel depletion. CML's categories include abiotic depletion, abiotic depletion (fossil fuels), global warming, ozone layer depletion, human toxicity, freshwater aquatic ecotoxicity, marine aquatic ecotoxicity, terrestrial ecotoxicity, photochemical oxidation, acidification, and eutrophication. Although these tools have overlapping categories, there are variations between how they are measured. One example of this difference can be observed in how they respectively treat the global warming category. In TRACI, 1 kg of CH_4 is equivalent to 25 kg of CO_2, whereas the CML tool considers 1 kg CH_4 as being equal to 28 kg of CO_2. These figures are current as of TRACI and CML's most recent updates, which occurred in March 2012 (IPCC report 2007) and September 2016 (IPCC report 2013), respectively. In addition, while CML considers more variables in relation to global warming, TRACI assesses more variables relating to ozone depletion. Thus, it is possible that the analysis results will be slightly different depending on the chosen method. Although TRACI's GHG data is outdated compared to CML's, it was selected because it is based on North American data. In contrast, the CML tool is based on European data. Since the four of the five locations in this study are located in either North America or Europe, TRACI and CML are appropriate tools for use in this study.

Though both TRACI and CML provide each system's midpoint emissions, the damage to the environment caused by those emissions is still unknown. Therefore, other methods that are capable of converting these emissions into damages are required. One selected endpoint method, ReCiPe2016, uses 17 categories to assess a system's midpoint impacts, which can then be converted into three damage categories at its endpoints [16]:

1. Human health: particulate matter, tropical Ozone formation, ionizing radiation, stratospheric Ozone depletion, human toxicity, human toxicity, global warming, water use.
2. Ecosystem: global warming, water use, freshwater ecotoxicity, freshwater eutrophication, tropical Ozone formation, terrestrial ecotoxicity, terrestrial acidification, land use/transformation, marine ecotoxicity, marine eutrophication.
3. Resources: mineral resources, fossil resources.

ReCiPe2016 allows users to choose from three time horizons: 20 years (I: individual), 100 years (H: hierarchies), and 100,000 years or infinite (E: Egalitarian) [16]. According to the ISO 14040 series, weighting is not allowed if the results will be used to compare (competing) products, and if they will be presented to the public. However, ReCiPe2016 allows for a triangle analysis between two products (or system in this work), which helps to eliminate the subjectivity that comes with weighting factors for each type of damage. While ReCiPe2016 uses IPCC report 5, which is the most recent, it should be noted that its midpoint-level characterization factor for the global warming effect is different from that used in CML. For instance, ReCiPe2016 classifies 1 kg of CH_4 as being equivalent to 34 kg CO_2 over a 100-year time horizon, which is much higher than CML's 28 kg CO_2 equivalent [16].

The other selected endpoint method, IMPACT 2002+, assigns 17 variables to one or more damage categories. IMPACT 2002+ is a combination of four methods: IMPACT 2002, Eco-indicator 99, CML and IPCC. The unit of all normalization is based on the number of equivalent persons affected during one year per unit of emission in Europe (persons × year/$unit_{emission}$). This method categorizes the impact into four damage groups [17]:

1. Human health: effects include human toxicity, respiratory effects, ionizing radiation, ozone layer depletion, photochemical oxidation, water turbined, water withdrawal, and water consumption.
2. Ecosystem quality: effects include ozone layer depletion, photochemical oxidation, aquatic ecotoxicity, terrestrial ecotoxicity, aquatic acidification, aquatic eutrophication, terrestrial acid, land occupation, water turbined, water withdrawal, and water consumption.
3. Climate change: global warming is the only effect considered in this category.
4. Resources: includes non-renewable energy and mineral extraction.

Normalization relates the magnitude of the calculated impact scores to a common reference, namely, the impact of society's production/consumption activities. As a result, LCA methods are able to provide a better understanding of how the product system under study impacts the reference system [18]. IMPACT 2002+ is a European method, while ReCiPe2016 is a global method. As such, both tools have their respective pros and cons. Thus, this work uses ReCiPe 2016, IMPACT 2002+, TRACI, and CML, as it was decided that this would provide the most robust analysis.

3. Results and Discussion

Since the CBMeOH system is the most complex of the three systems under review, it is worthwhile to examine which of its process stages has the greatest environmental impact. Figure 4 presents the emissions impact of the CBMeOH system producting the functional unit (1MWh of electricity and 1.37 MWh of heat) in stacked columns. In this figure, 'Desulphurization' represents the COG desulphurization process using Rectisol, and 'Electricity Product' refers to the output of the system expansion. Since the CBMeOH process does not produce electricity, the environmental impact from the electricity required from the grid is denoted as 'Electricity from Grid'. 'Steel' represents the environmental impact from the steel used to construct the CBMeOH synthesis system. This category does not account for the Rectisol washing process. 'Electricity for CBMeOH' denotes the total net electricity consumed throughout the CBMeOH process. 'NG for CSR' represents the heating utility

effect of the CSR units used in the CBMeOH process. ‘Heat for Reboiler’ indicates the amount of heat required for the MeOH purification process via NG. ‘Steel transport’ and ‘Catalyst transport’ capture the environmental impact of transporting these materials from their production sites to the plant. For these categories, transportation is assumed to be within the country. ‘Heat Avoided’ denotes the amount of heat that is recovered during the CBMeOH process. This requires another system expansion stream in order to ensure that the product is the same as that of the status quo system. Similarly, ‘Methanol Avoided’ refers to the amount of methanol that is recovered during the CBMeOH process. Although methanol is the main product of the CBMeOH system, the status quo and CCPP systems do not produce any. Hence, the amount of MeOH produced is subtracted using product avoided. ‘Claus process’ denotes the waste treatment process. ‘Heat from BFG’ refers to another system expansion that mainly accounts for CO_2 emissions created by the combustion of upgraded BFG in order to provide heat. The red ‘Sum’ dot in each column represents the total process flow emissions.

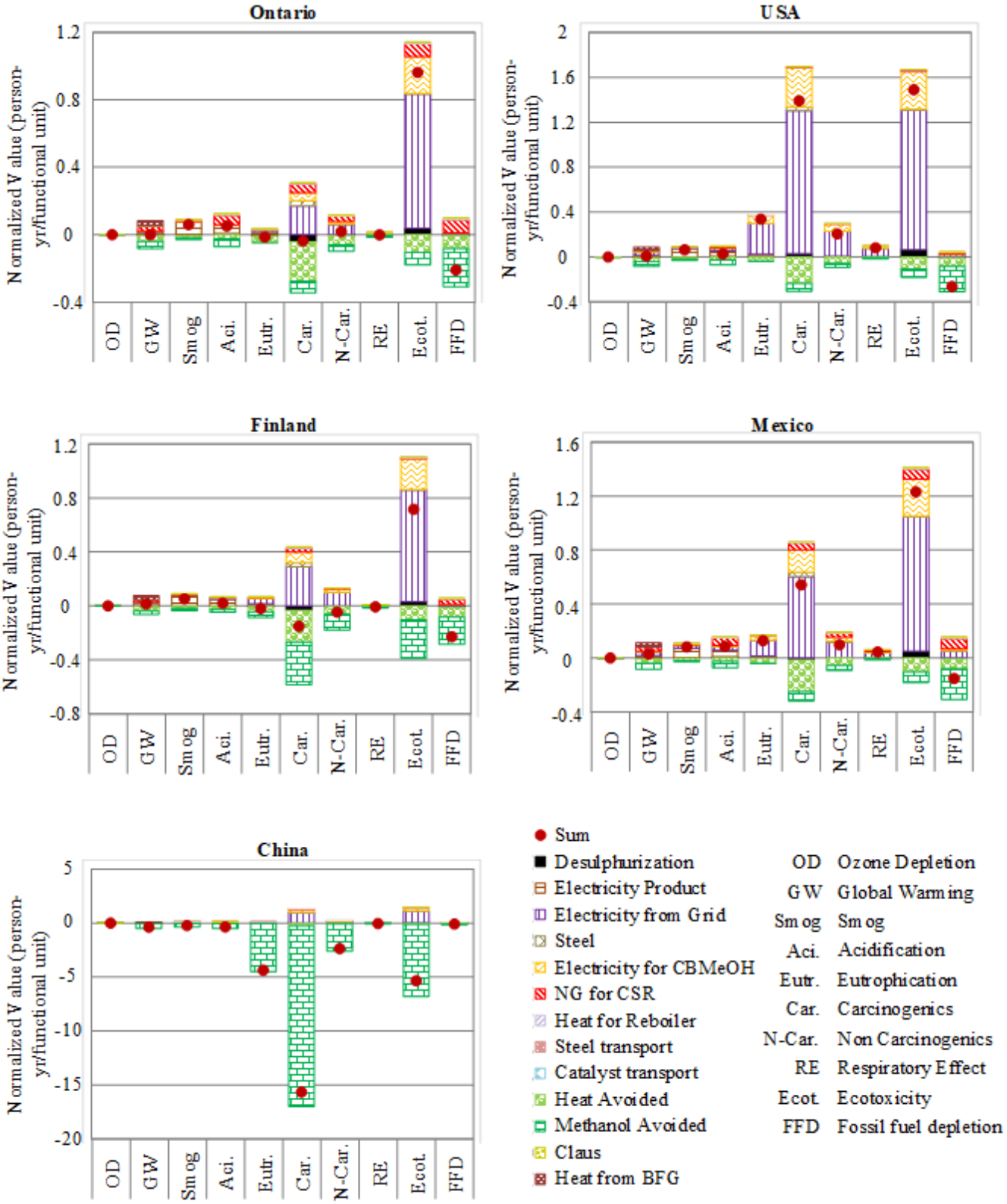

Figure 4. CBMeOH process emission contributions with NG as a heating utility: TRACI.

It is obvious from *Figure 4* that, except for China, accounting for Heat Avoided and Methanol Avoided reduced major environmental impacts at all locations. One likely reason why similar effects were observed at these locations is that data for Heat Avoided was acquired from the RER database for each one. For Methanol Avoided, data for Ontario, the USA, and Mexico were obtained from the USLCI database, which is specific to an American context. In the USA, methanol is mainly produced via NG [19]; as such, USLCI uses NG for 100% of methanol production. In contrast, 69% of methanol in China is produced from coal, which is also the most environmentally damaging method [6]. Consequently, the environment impact of methanol production in China is significantly higher than in the USA. As illustrated in *Figure 4*, the negative effect of Methanol Avoided in China's case is obviously higher than in the North American countries. Methanol Avoided data for Finland was acquired using the global database; these results indicated that methanol production in the Finnish context produced a greater environmental impact than in North America, but less than in China.

Smog, Acidification, Global Warming, and Eutrophication are the main environmental effects produced when the CBMeOH system generates the same amount of electricity as the status quo system, which is the effect of Electricity Product. The other big effect produced by the CBMeOH system relates to the use of NG as a heating utility for the CSR unit. The utilization of Electricity from the Grid mainly impacts carcinogenics, respiratory effects, and ecotoxicity. The effects related to the fabrication and transportation of construction materials are trivial compared to the above categories.

The Desulphurization effect was more pronounced in Ontario and Finland than in the other three countries. Figure 4 also shows different impacts of NG utilization, Methanol Avoided, and Heat Avoided for all five locations. As discussed above, data for Ontario, the USA, and Mexico were obtained from the USLCI database, which indicated that NG, Methanol Avoided, and Heat Avoided all had similar trends across these three locations. The big difference affecting the stacked columns comes from electricity utilization. In the USA and Mexico, up to 65% and 79% of electricity is produced using fossil fuels [20], [21]; in contrast, only about 6.7% of Ontario's electricity is produced

using fossil fuels, with the remainder being produced via nuclear energy (58.4%), hydro (23.9%), wind (8%), and solar PV (2.3%) [22]. Hence, the USA and Mexico's Electricity from Grid has a much higher impact on all categories than Ontario, especially regarding the effects on eutrophication, carcinogenics, non-carcinogenics, respiratory effects, ecotoxicity, and ozone depletion. In Finland, about 40% of Electricity from Grid is produced using fossil fuels [23]. Thus, the biggest impact of Electricity from Grid can be seen between Ontario and the USA/Mexico. Although up to 70% of of China's electricity is produced from fossil fuels [24], the effects related to Methanol Avoided are much higher than those related to electricity consumption or production. Hence, Electricity from Grid has a relatively lower environmental impact for China.

3.1. System Comparison

The system comparisons from the TRACI analysis are shown in Figure 5. As can be seen, with the exception of ozone depletion, the CBMeOH process had a negative effect on all categories for the Chinese case, making it the most environmentally friendly process for this context. The ozone depletion effect was almost invisible for all three systems at all five locations. The status quo system had the highest global warming effect of the three systems, while the CBMeOH system generally had the lowest. With the exception of China, the CBMeOH system produced more smog effects than the status quo and CCPP systems at all locations. The status quo system had the largest acidification effects, while the CCPP had the lowest. Again, this held for all locations with the exception of China. The CCPP system had a negative eutrophication effect for all five locations; the CBMeOH system's eutrophication effect was unneglectable in the USA and Mexico. The CBMeOH and CCPP systems both had large carcinogenic effects. The CBMeOH system had a positive impact on carcinogenic effects for the locations in Mexico and the USA, but a negative impact for all of the other locations. In contrast, the CCPP system had a negative impact on carcinogenic effects for all locations. A similar trend was observed for non-carcinogenic effects. The impacts on respiratory effects were minimal for all five locations. Additionally, the CBMeOH process had a very large positive impact on eco-toxicity

for all locations (except for China), while the CCPP process had significant negative effect. Moreover, the CBMeOH system was the most effective at reducing fossil fuel depletion.

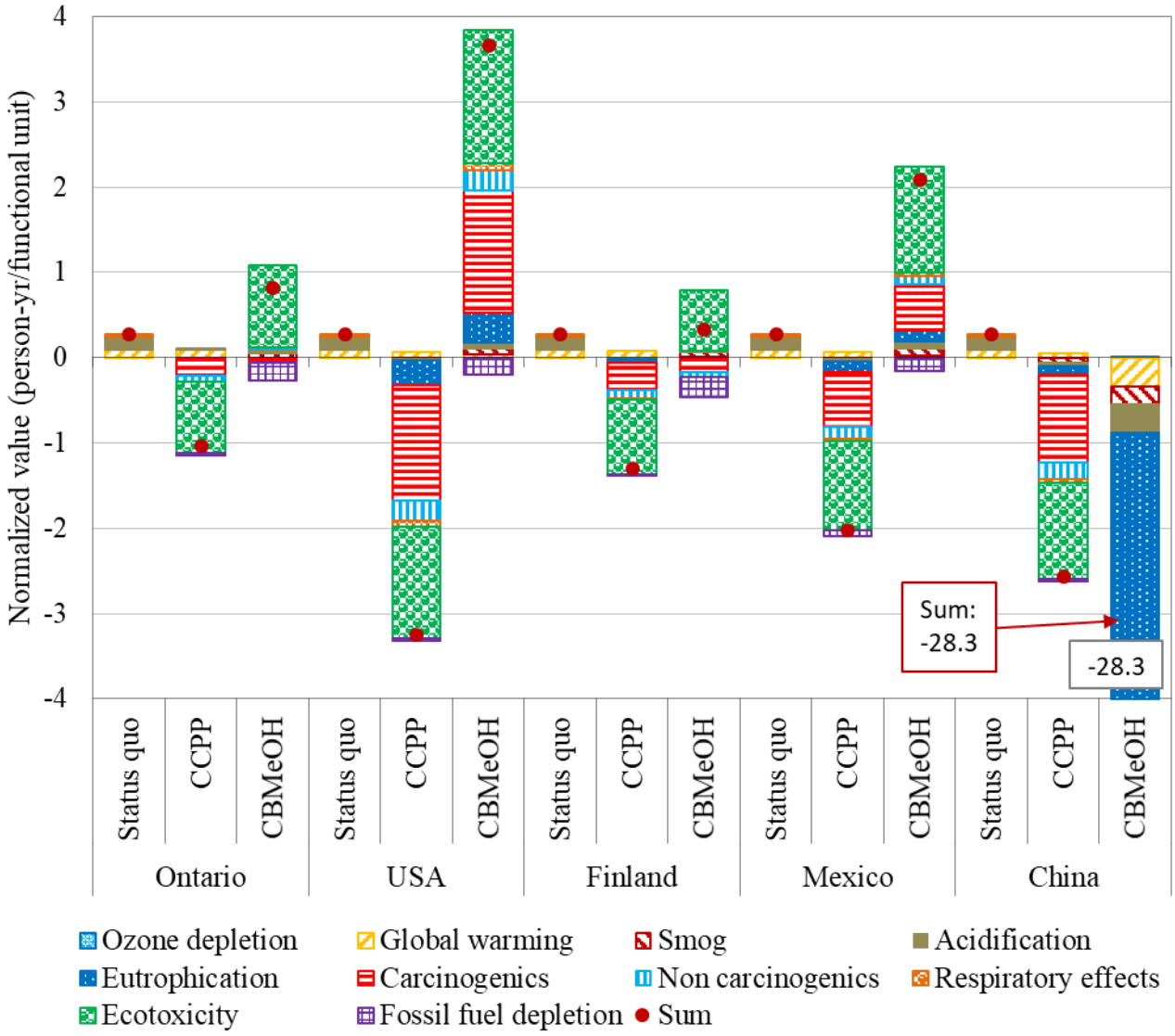

Figure 5. LCA of status quo, CCPP, and CBMeOH systems in five locations using the TRACI tool with normalization. The normalized value is equal to the number of equivalent persons affected during one year in the US-Canada region [25].

The sum data points in *Figure 5* indicate that, with the exception of China, the CCPP system yielded the lowest equivalent person affected per year for all studied locations. Conversely, the

CBMeOH system produced relatively higher effects for Ontario, the USA, Finland, and Mexico, but the lowest for China.

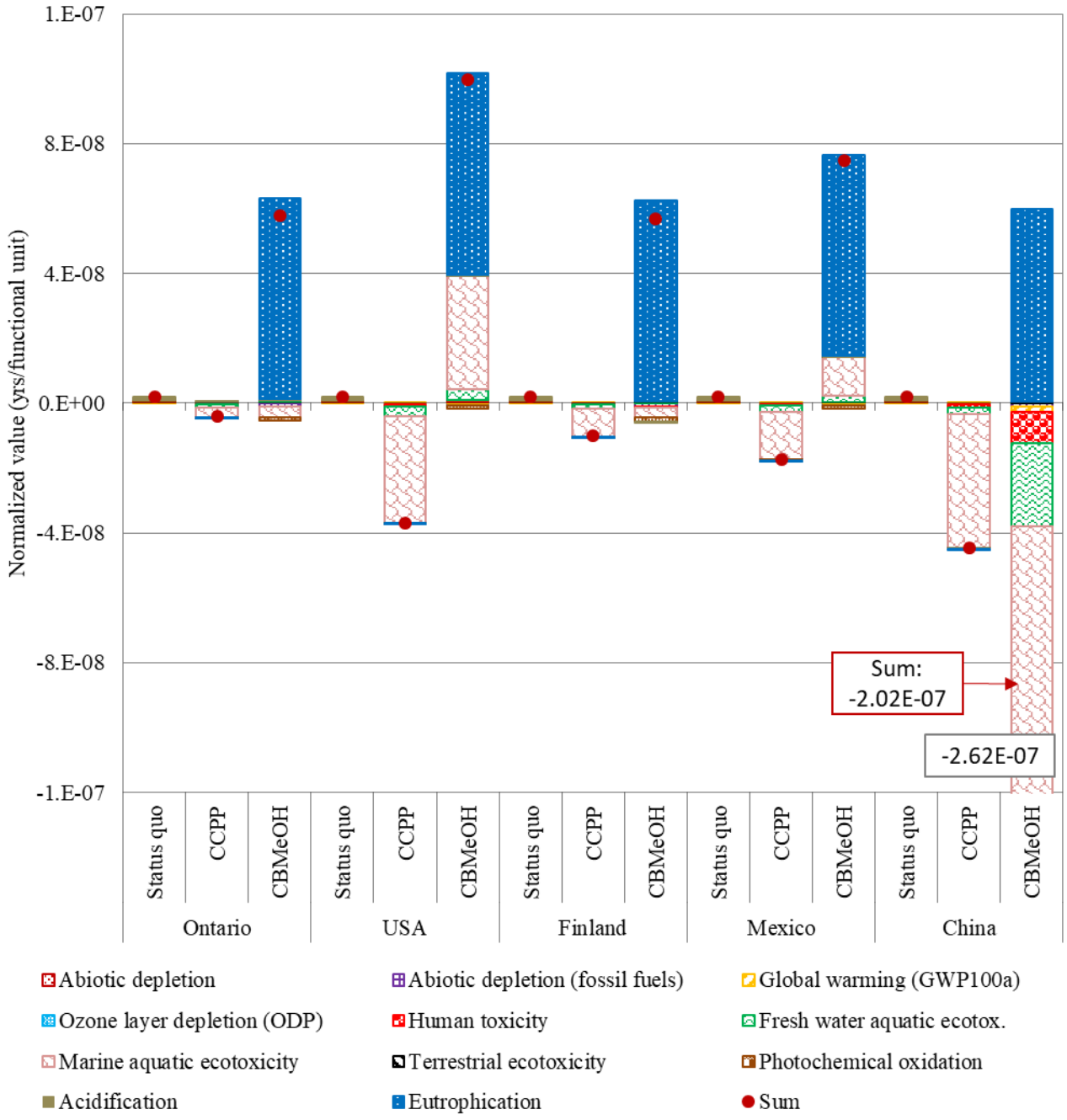

Figure 6. LCA of the status quo, CCPP, and CBMeOH systems in five locations using the CML tool with normalization. The normalized value is equivalent amount of emissions produced in the Europe in the span of one year [25].

The value of each category is seven or eight orders of magnitude smaller for CML than in TRACI (*Figure 6*). This difference is due to the fact that CML uses the total amount of emissions in Europe in one year as its normalization reference, while TRACI uses the total emissions in the US-Canada area in one year per person [Roland Hischier, 2010]. The CBMeOH system had a very large positive effect on eutrophication, while the CCPP system had almost none. Amonia is an important factor to account for with regards to eutrophication. Amonia's effect in the CML analysis was more than three times greater than its effect in TRACI. In addition, the eutrophication impact related to Methanol Avoided was very large due to the amount of electricity required in the methanol production process. As discussed earlier, cut-off methanol production data from the USLCI database was used for the Ontario, USA, and Mexico locations. Consequently, these locations all had very high eutrophication effects.

In the USA and Mexico, the CBMeOH system yielded increased marine aquatic ecotoxicity effects. In contrast, the use of this sytem in China resulted in significant negative effects on marine aquatic ecotoxicity. The status quo system had the highest impact on acidification across all five locations, while the CBMeOH system was most effective at reducing fossil fuel depletion. These two results are consistent those obtained using the TRACI tool. The sum of each system's normalized value with the CML method indicates that the CCPP system produced the lowest emissions in Ontario, the USA, Finland, and Mexico, while the CBMeOH system produced the lowest emissions in China.

Although the normalized values obtained using TRACI and CML are able to indicate each category's relative emissions, these tools are unable to capture each category's ability to cause damage and their total damage to human health, ecosystems, and resources. Hence, it is necessary to convert these emission categories into damage categories. For this reason, ReCiPe2016 and IMPACT2002+ are used.

In ReCiPe2016, all midpoint emissions are converted to three damage categories, which were discribed Section 2.3. However, the conversion equations and methods are outside the scope of this

work. In SimaPro, the conversion equations are embeded, and the endpoint method can be used to obtain a triangle for each location, thus enabling the comparison of two systems at a time. For such analyses, the system with the lower impact will show on the figure, while the system with higher impact will not. The results indicated that the staus quo system was the most environmental unfriendly system for all five locations. Thus, the area representing the status quo system will never show up in the triangle. As shown in *Figure 7*, the sum of the weighting factors (i.e., human health, ecosystems, and resource damages) will be 100% at any point of the triangle, with each weighting factor varing from 0% to 100%. For Ontario, Finland, and China, the CBMeOH system had a clear environmental advantage over the status quo and CCPP systems. In contrast, the CCPP system provided greater environmental benefits than the status quo and CBMeOH systems for the locations in the USA and Mexico. Hence from an environmental perspective, it is recommended that Ontario, Finland, and China utilize CBMeOH systems, and that the USA and Mexico pursue the use of CCPP systems.

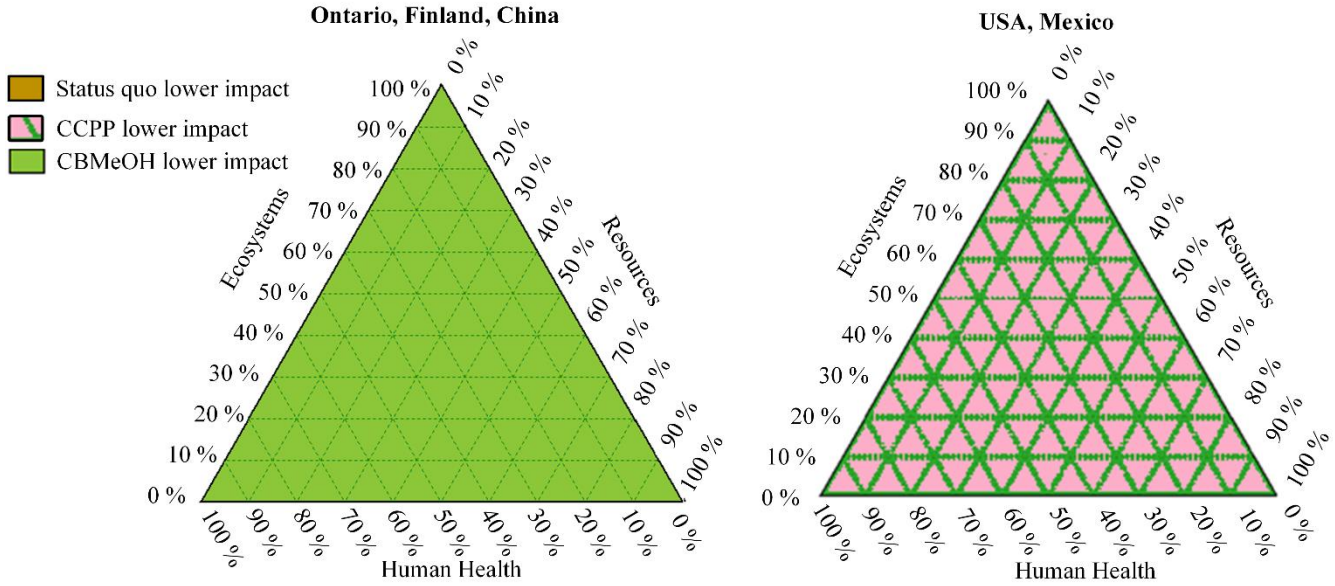

Figure 7. System comparison among five locations using ReCiPe2016.

IMPACT2002+ offers another useful tool for converting emissions categories into damage groups, as it summarizes all 17 impact categories into four damage categories: human health, ecosystem quality, climate change, and resources. Each category is assigned a weighting factor of 1

and is then summarized into a total number. As shown in Figure 8, the analysis using IMPACT2002+ returned similar results to those obtained using ReCiPe2016. That is, the CBMeOH system was the most environmentally friendly for the locations in Ontario, Finland, and China, while the CCPP system was most environmentally friendly for the locations in the USA and Mexico. *Figure 8* also shows that the CBMeOH system produced the most environmental damage for the US location, which means that, from an environmental perspective, under no circumstances should steel plants in the USA use CBMeOH systems. Furthermore, the status quo had the highest impact for the other four locations, and still far worse than the CCPP system in the US location. Thus, from an environmental perspective, the status quo system is not recommended.

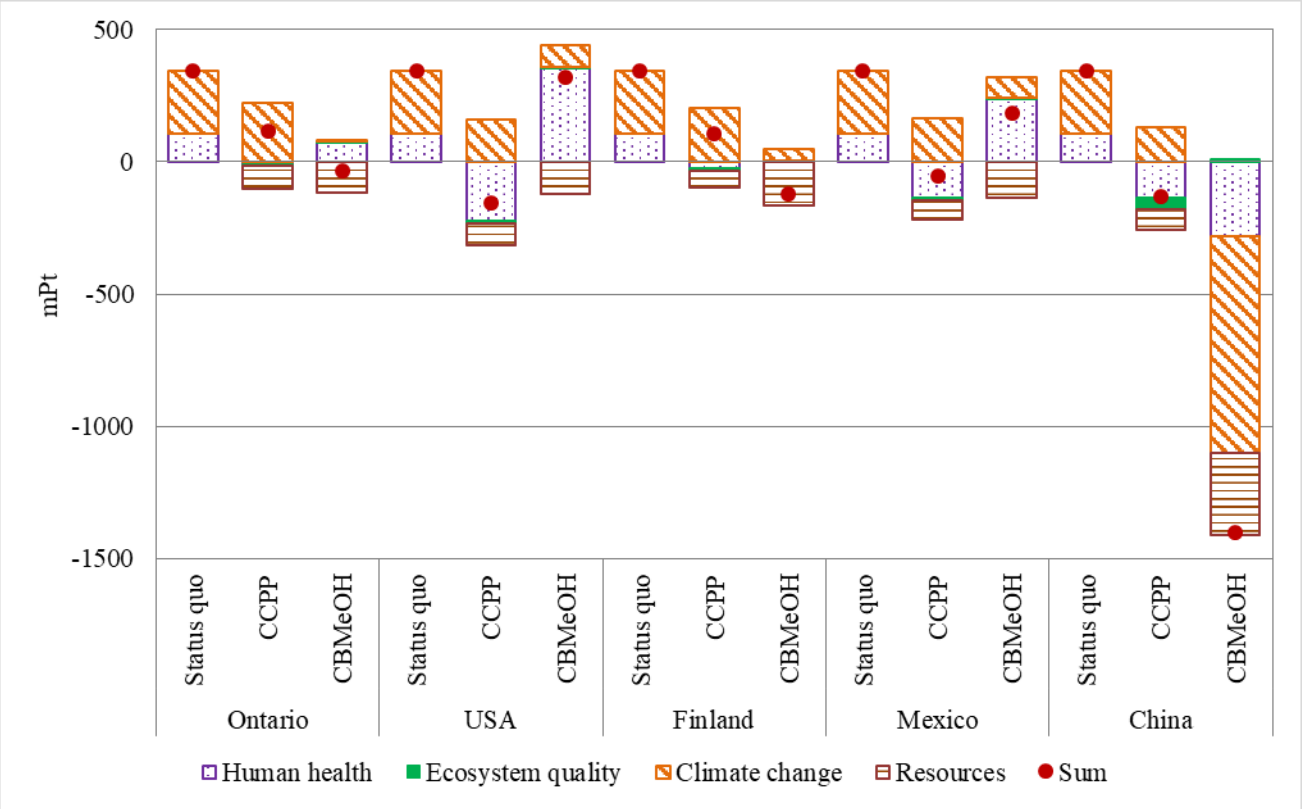

Figure 8. System comparison at five locations with IMPACT 2002+. The weighting factor for each damage category is 1.

Taken in conjunction with our earlier economic analysis [3], these results indicate that it would be profitable to build CBMeOH plants at the Ontario, USA, Mexico, and China locations. While the

construction of a CCPP plant in the USA would result in a negative NPV with no carbon tax, it would produce a positive NPV if the carbon tax was increased to $50/tonne when accounting for the benefit of avoided CO_2 taxes from the status quo [3]. In Finland, CCPP is expected to have a positive NPV in just 6 years over past 13 years studied. For China and Mexico, both CCPP and CBMeOH plants can produce NPVs of more than $190 million. However, it would be even more profitable to build CBMeOH palnts in Mexico and China. Hence, CBMeOH plants offer more overal environmental and economic benefits for locations such as Ontario, and China, while locations in the USA would see the biggest benefits form building CCPP plants once the carbon tax is increased to $50/tonne. For Mexico, CCPP plants are the best option in terms of environmental impact, but CBMeOH plants are the best choice in terms of economics. Overall, the results show that it is not recommended that more status quo systems are built in Mexico or China in any circumstance.

4. Improvement and Limitations

The biggest limitation of this work is region-specific data availability and accuracy. The same products are likely to have significantly different environmental impacts at each of the locations due to a variety of factors, such as how electricity is produced in that country. However, data on NG and MeOH production is not yet available for all of the locations examined in this study. Future work on this subject may have the benefit of more complete databases, or it could focus on developing our own database in order to obtain results that are more representative. In addition, it is always very difficult to estimate transportation distances, especially when considering systems as a concept rather than a specific case study. However this variable has a relatively insignificant impact on the overall system.

Another limitation to this work is that each method used different impact factors. For example, most of the chemical compounds considered in the environmental categories had different factors, and some of the tools took more components into consideration than others. Furthermore, most of the analytical tools were developed for European and North America contexts, which means they are not very representative when applied to Asian countries, especially considering huge differences in the

normalization reference among locations. The development of a tool that is more specific to an Asian context would be immensely helpful in producing more representative LCA results.

5. Conclusions

In conclusion, from both economic and environmental analysis, the overall results could be represented in the following table.

Table 3. Conclusion from both environmental and economic aspect

	Ontario	USA	Finland	Mexico	China
Environmentally	CBMeOH	CCPP	CBMeOH	CCPP	CBMeOH
Economically (In recent 13 years)	CBMeOH	CBMeOH	CCPP	CBMeOH	CBMeOH

Under no circumstances was the status quo system the best option in terms of environmental impact. When considered in terms of both economic benefit and environmental effects, it is clear that the CBMeOH plant is the best option for Ontario, and China, while the CCPP plant is the best option for the USA provided the carbon tax is increased to 50$/tonne. Mexico could realize big economic gains from building either CCPP or CBMeOH plant. On the one hand, a CBMeOH plant would result in higher NPV, but on the other hand it would have a more negative environmental impact than a CCPP plant. Thus, the system that is ultimately chosen will depend on the shareholders' preferences.

Acknowledgment

This research was funded through the Ontario Research Fund-Research Excellence Project [RE09-058] and the McMaster Advanced Control Consortium, of which AMD is a contributing member. We are grateful for their funding. The collaborations and data from Ian Shaw and David Meredith (AMD) are also gratefully acknowledged.

References

[1] T. Li, P. M. Castro, Z. M. Lv. Life cycle assessment and optimization of an iron making system with a combined cycle power plant: a case study from China. Clean Technologies and Environmental Policy 19.4 (2017): 1133-1145.

[2] L.Y. Deng, T.A. Adams II. Optimization of Coke Oven Gas Desulphurization and Combined Cycle Power Plant Electricity Generation. Industrial and Engineering Chemistry Research. (2018). DOI: 10.1021/acs.iecr.8b00246.

[3] L.Y. Deng, T.A. Adams II. Techno-economic analysis of coke oven gas and blast furnace gas to methanol process with carbon dioxide capture and utilization. Energy Conversion and Management 204 (2020): 112315. https://doi.org/10.1016/j.enconman.2019.112315.

[4] J.Y. Lee, X.X. Ma, H. Liu, X.Y. Zhang. Life cycle assessment and economic analysis of methanol production from coke oven gas compared with coal and natural gas routes. Journal of cleaner production 185 (2018): 299-308.

[5] C.H. Li, H. T. Bai, Y.Y. Lu, J.H. Bian, Y. Dong, H. Xu. Life-cycle assessment for coal-based methanol production in China. Journal of Cleaner Production 188 (2018): 1004-1017.

[6] Z. Chen, Q. Shen, N. N. Sun, W. Wei. Life cycle assessment of typical methanol production routes: The environmental impacts analysis and power optimization. Journal of Cleaner Production 220 (2019): 408-416.

[7] X. Ou, X. Zhang, Q. Zhang, X. L. Zhang. Life-cycle analysis of energy use and greenhouse gas emissions of gas-to-liquid fuel pathway from steel mill off-gas in China by the LanzaTech process. Front. Energy 7, 263–270 (2013) DOI:10.1007/s11708-013-0263-9

[8] ISO 14040: Environmental Management –Life Cycle Assessment-Principles and Framework.

[9] L. Sun, R. Smith. Rectisol wash process simulation and analysis. Journal of Cleaner Production 39 (2013): 321-328.

[10] Y.K. Salkuyeh, and T.A. Adams II. Combining coal gasification, natural gas reforming, and external carbonless heat for efficient production of gasoline and diesel with CO2 capture and sequestration. Energy Conversion and Management 74 (2013): 492-504.

[11] L.Hocine, D.Yacine, B. Kamel, K.M. Samira. Improvement of electrical arc furnace operation with an appropriate model. Energy 34.9 (2009): 1207-1214.

[12] IKE. Chinese life cycle database, http://www.ike-global.com/products-2/chinese-lca-database-clcd; [accessed Dec. 13th, 2019].

[13] L.W. Su, X.R. Li, Z.Y. Sun. The consumption, production and transportation of methanol in China: A review. Energy Policy 63 (2013): 130-138.

[14] Q. J. Li, Y. L. Zhong, Z. Q. Gu, Z. F. Liao. Developing strategy for joint production of methanol fuel in existing ammonia plants 6 (2001): 5-7, http://www.cqvip.com/Main/Detail.aspx?id=5956865.

[15] W.X. Zhang. Progress of process for combined methanol production in synthetic ammonia plant. Modern chemical industry. 23(2004): 23-28.

[16] M.A.J. Huijbregts, Z.J.N. Steinmann, P.M.F. Elshout, G. Stam, F. Verones, M. Vieira, M. Zijp, A. Hollander, R.V. Zelm. ReCiPe2016: a harmonized life cycle impact assessment method at midpoint and endpoint level Report I: Characterization. RIVM Report 2016-0104. National Institute for Public Health and the Environment (2016):1-159.

[17] S. Humbert, A.D. Schryver, X. Bengoa, M. Margni, O. Jolliet. IMPACT 2002+_UserGuide_for_vQ2.21, 2014.

[18] Ryberg, Morten, et al. Updated US and Canadian normalization factors for TRACI 2.1. Clean Technologies and Environmental Policy 16.2 (2014): 329-339.

[19] IAGS. Methanol, http://www.iags.org/methanol.htm; [accessed Dec. 4th, 2019].

[20] EIA. Electricity Power Annual. 2018, https://www.eia.gov/electricity/annual/; [accessed July 10th, 2019].

[21] F.M. Segundo. Country Nuclear Power Profiles. IAEA, 2018, https://www-pub.iaea.org/MTCD/Publications/PDF/cnpp2018/countryprofiles/Mexico/Mexico.htm; [accessed July 10th, 2019].

[22] Ontario Energy Board. Ontario's system-wide electricity supply mix: 2018 data, https://www.oeb.ca/sites/default/files/2018-supply-mix-data-update.pdf; [accessed Dec. 4th, 2019].

[23] Statista. Share of electricity produced from fossil fuel and peat consumed in Finland from 2008 to 2018, https://www.statista.com/statistics/536058/finland-share-of-electricity-produced-from-fossil-fuel/; [accessed Dec. 4th, 2019].

[24] Statista. Electric power generation in China in 2018, by source (in TWh), https://www.statista.com/statistics/302233/china-power-generation-by-source/; [accessed July 10th, 2019].

[25] R. Hischier, B. Weidema, H.-J. Althaus, C. Bauer, G. Doka, R. Dones, R. Frischknecht, S. Hellweg, S. Humbert, N. Jungbluth, T. Köllner, Y. Loerincik, M. Margni, T. Nemecek. Implementation of Life Cycle Impact Assessment Methods; Swiss Centre for Life Cycle Inventories: Dübendorf, Switzerland, 2010.

Chapter 5 Conclusions and Recommended Future Works

1. Conclusions

The work presented in this thesis examined the upgrading of two most widely commercialized steel manufacturing off-gas valorization systems: the electricity generating system (CCPP) and methanol generation system (CBMeOH). ProMax v4.0 was used to study the CCPP system, which uses MDEA solvent and high pressures (16 bar) to enable the detailed desulphurization of COG. To maximize profitability, a CCPP system with a fixed design was optimized via GAMS. In general, the results of the CCPP study indicated that CCPP systems are most profitable in places with higher electricity carbon intensity. However, the NPV of such systems might change based on the carbon tax, the electricity price, and the power purchasing parity. Furthermore, locations with lower fixed capital investment were found to be more likely to gain significantly more profit than locations with higher fixed capital investment. For example, Mexico and China are overwhelmingly better off building either CCPP or CBMeOH plants compared to Ontario and the USA. While Finland's fixed capital investment was the highest of the five locations, it also had the highest carbon tax, which made the construction of a CCPP plant at this location even more profitable than in other locations with relatively lower fixed capital investment, such as Ontario and the USA.

The proposed CBMeOH system not only included the novel idea of using BFG as a free available additional carbon source, but, more importantly, it features a much shorter methanol production process from COG compared to the commercialized process. Additionally, the CBMeOH system eliminates the two-stage hydrodesulfurization process required in the commercialized method by incorporating a CSR unit that can perform three roles simultaneously: methane reformation, organic sulfur conversion, and $(H_2\text{-}CO_2)/(CO+CO_2)$ molar ratio adjustment. Unlike the CCPP system, the CBMeOH system was not optimized; however, the economic analyses were performed in the same manner as those conducted for the CCPP system. The results of the economic analyses showed that the CBMeOH plant is much more expensive to build and has higher operating costs than the CCPP system. Notably, the profitability of the CBMeOH plant changed significantly as the methanol price

increased from $200/tonne to $600/tonne. Based on historical electricity prices and a methanol history price map, it would be highly profitable to build either a CCPP or CBMeOH plant in Mexico and China. In contrast, the USA's electricity prices have historically been fairly stable, which means that it makes sense to build a CCPP plant up to a certain carbon tax rate. Ultimately, however, both the CCPP and CBMeOH plants offer a greater chance of realizing a positive NPV than the status quo system.

With respect to environmental impact, the CBMeOH process could potentially be a viable solution to reducing carbon emissions for all five locations. The CBMeOH system had the lowest environmental impact for Ontario, Finland, and China, while CCPP system proved to be the most environmentally friendly option for the USA and Mexico. In general, locations with low electricity carbon intensity are ideal locations for building CBMeOH plants; in contrast CCPP is the best option for locations with higher electricity carbon intensity. Furthermore, the construction of CBMeOH plants will cause more environmental damage in locations where methanol is mainly produced via the cleanest routes (NG to methanol). Therefore, it is always recommended that new steel plants build either a CCPP or CBMeOH plant for on-site off-gas utilization, rather than a status quo system.

In the long-term, I would suggest that researchers find innovative steel manufacturing technologies to reduce CO_2 emissions. The off-gas utilization methods are not able to reduce more than 5% of total CO_2 emission (5 million tonnes) in steel manufacturing plants. Nowadays the steel making process is not able to further bring down the CO_2 emission. New reduction agents associated with fewer carbon emissions, and/or new iron reduction methods should be developed. For example, the most CO_2 neutral methods electrowinning and MOE should be the next generation of study focus. However, we should also take into consideration that the production of steel from EAF is ever-increasing form 287,255 thousand tonnes to 523,918 thousand tonnes from 2000 to 2018, and the increasing slop of steel from EAF is getting steeper since 2016 while the increasing of steel from BF is slower [25]. These indicate

that more and more recycled steel is available. Technology development shift toward a cleaner iron scrap reduction process might be the case in the near future.

2. Recommended Future Works

Throughout the course of this research, a number of questions arose that would provide fruitful ground for future research:

(1) What would an efficient system that uses both COG and BFG as input look like? Would it be more profitable? How much BFG would need to be added? Would it be better to blend COG and BFG together, or would it be more effective to burn them separately?

(2) What are the optimized operation parameters for the CBMeOH system? What flow rate of additional CO_2, purge ratio of the unconverted syngas, pressure of methanol synthesis, flash pressure and temperature, and steam flow rate is best for methane reforming?

(3) The CSR unit in the proposed CBMeOH system has three major roles: methane reformation, organic sulfur conversion, and $(H_2+CO_2)/(CO+CO_2)$ mole ratio adjustment. Though the results of different groups' research has confirmed that the CSR possesses these abilities, would this unit function the same in reality as it did in the simulations performed for this work? Furthermore, what steps could be taken to improve the function of the CRS unit? Since experimental tests are the next step in the commercialization of the CSR unit, it would be worthwhile to examine its performance via experimental studies.

(4) I was aware of a lack of cradle-to-gate data relating to NG and methanol during the LCA studies. This lack of data is significant, as these utilities have a big effect on the results and could change the investment decision. Further work could focus on developing a more location-based database. Furthermore, many important chemical production processes—for example, methanol production from coal and COG—have yet to be documented in the Ecoinvent database, which otherwise, creates difficulties when conducting studies related to such processes. Moreover, the LCA database could also be further expanded.

(5) What would the CBMeOH system production cost change considering various uncertainties for example equipment cost estimation off? What if the real application of the system is different from the estimation?

(6) How will the LCA decision change if the electricity grid changes? Or what is the threshold that one system (for example CCPP) would be better than the other (for example CBMeOH)? A sensitivity analysis and uncertainty analysis might be of great interest.

(7) Technological innovation in the steel manufacturing process remains an interesting and promising avenue for reducing CO_2 emissions. As such, further studies on technologies such as electrowinning and molten oxide electrolysis are encouraged, as these technologies possess great potential for reducing CO_2 emissions.

(8) As discussed in the introduction, the planning and scheduling of off-gas utilization is one of four methods for increasing energy efficiency and reducing CO_2 emissions. Therefore, it is well worth studying the effects of time-of-use power prices in different locations with respect to optimizing the decision to consume or store off-gas. Such a study could also be extended to investigate the optimal local market conditions for utilizing the off-gas on-site to provide heat during the steel refining process, storing it for future power plant consumption, or using it to produce chemical products, such as methanol.

References

[1] Hannah Ritchie and Max Roser. CO_2 and Greenhouse gas emissions. Our World in Data, 2019: https://ourworldindata.org/co2-and-other-greenhouse-gas-emissions. [Accessed Feb. 5th, 2020].

[2] World steel in figures 2019: https://www.worldsteel.org/steel-by-topic/statistics/steel-statistical-yearbook/World-Steel-in-Figures.html. [Accessed Feb. 5th, 2020].

[3] Technical Paper on the Federal Carbon Pricing Backstop; Environment and Climate Change, Canada, 2017: https://www.canada.ca/en/services/environment/weather/climatechange/technical-paper-federal-carbon-pricing-backstop.html. [Accessed Feb. 5th, 2019].

[4] About steel: https://www.worldsteel.org/about-steel.html. [Accessed Feb. 5th, 2020].

[5] Quader, M. Abdul, et al. A comprehensive review on energy efficient CO_2 breakthrough technologies for sustainable green iron and steel manufacturing. Renewable and Sustainable Energy Reviews 50 (2015): 594-614.

[6] Donald R. Sadoway and Gerbrand Ceder. A Feasibility Study of Steelmaking by Molten Oxide Electrolysis (TRP9956). United States: N. p., 2009. Web. doi:10.2172/974198.

[7] Allanore, Antoine, L. Ortiz, and D. Sadoway. Molten oxide electrolysis for iron production: Identification of key process parameters for large-scale development. Energy Technology 2011: Carbon Dioxide and Other Greenhouse Gas Reduction Metallurgy and Waste Heat Recovery (2011): 121.

[8] Hasanbeigi, Ali, Marlene Arens, and Lynn Price. Alternative emerging ironmaking technologies for energy-efficiency and carbon dioxide emissions reduction: a technical review. Renewable and Sustainable Energy Reviews 33 (2014): 645-658.

[9] Mousa, Elsayed, et al. Biomass applications in iron and steel industry: an overview of challenges and opportunities. Renewable and sustainable energy reviews 65 (2016): 1247-1266.

[10] Sohn, H. Y. Suspension Hydrogen Reduction of Iron Oxide Concentrates. University of Utah, 135 S 1460 E, Salt Lake City, UT, 2008.

[11] Nogami, Hiroshi, Yoshiaki Kashiwaya, and Daisuke Yamada. Simulation of blast furnace operation with intensive hydrogen injection. ISIJ international 52.8 (2012): 1523-1527.

[12] Zhao, Xiancong, Hao Bai, and Juxian Hao. A review on the optimal scheduling of byproduct gases in steel making industry. Energy Procedia 142 (2017): 2852-2857.

[13] Zhao, Xiancong, et al. Optimal scheduling of a byproduct gas system in a steel plant considering time-of-use electricity pricing. Applied Energy 195 (2017): 100-113.

[14] Deng, Lingyan, and Thomas A. Adams II. Techno-economic analysis of coke oven gas and blast furnace gas to methanol process with carbon dioxide capture and utilization. Energy Conversion and Management (2019): 112315.

[15] Razzaq, Rauf, Chunshan Li, and Suojiang Zhang. Coke oven gas: availability, properties, purification, and utilization in China. Fuel 113 (2013): 287-299.

[16] 卓创资讯能源观察. 焦炉煤气制 LNG 项目投资热度消退: http://gas.in-en.com/html/gas-2631405.shtml. [Accessed Feb. 10th, 2020].

[17] Iliev, Simeon. Comparison of Ethanol and Methanol Blending with Gasoline Using Engine Simulation. Biofuels-Challenges and opportunities. IntechOpen, 2018.

[18] 2019 Ethanol industry outlook, Renewable fuels association: https://ethanolrfa.org/wp-content/uploads/2019/02/RFA2019Outlook.pdf. [Accessed Feb. 5th, 2020].

[19] Ethanol's global growth, 2018: http://www.ethanolproducer.com/articles/15955/ethanolundefineds-global-growth. [Accessed Feb. 5th, 2020].

[20] Bromberg, Leslie, and Wai K. Cheng. Methanol as an alternative transportation fuel in the US: Options for sustainable and/or energy-secure transportation. Cambridge, MA: Sloan Automotive Laboratory, Massachusetts Institute of Technology (2010).

[21] Cindy Zimmerman. Ethanol VS. Methanol, 2006: http://energy.agwired.com/2006/02/13/ethanol-vs-methanol/. [Accessed Feb. 7th, 2020].

[22] Robert Zubrin. The methanol alternative, 2006: https://www.thenewatlantis.com/publications/the-methanol-alternative. [Accessed Feb. 5th, 2020].

[23] HIS Markit, 2017: https://news.ihsmarkit.com/prviewer/release_only/slug/country-industry-forecasting-media-global-methanol-demand-growth-driven-methanol-olefi. [Accessed Mar. 5th, 2020]

[24] M. McNeil. Province give $40 million to ArcelorMittal Dofasco energy-saving efforts. The Hamilton Spectator 2016: https://www.thespec.com/news-story/6965067-province-gives-40-million-to-arcelormittal-dofasco-energy-saving-efforts/. [Accessed Feb. 7th, 2020].

[25] Production of crude steel in electric arc furnaces: https://www.worldsteel.org/internet-2017/steel-by-topic/statistics/steel-data-viewer/P1_crude_steel_EF/IND/AUS/BRA/IRN/RUS/WORLD_ALL. [Accessed Mar. 5th, 2020].